Chapter

5

Results and Discussion

5. RESULTS AND DISCUSSION

5.1. SERIES-1: Schiff bases of 2-(4-aminophenyl)benzothiazole i.e., 4-arylidine/cycloalkylidine-benzenamine benzothiazole

5.1.1. BACKGROUND

Research and development of new antimicrobial and anticancer therapeutic agents are of paramount importance because of the innate ability of pathogen and tumor cells to develop resistance to existing therapies. The progression of multiple drug resistance to antimicrobial and anticancer agents in human cells has been recognized as major impediment to unbeaten microbial and cancer chemotherapy. Thus, studies for the identification of novel drugs and targets for the management of these diseases are at the cutting edge.

Schiff bases, characterized by the presence of azomethine group (–C=N–) have also achieved significance due to the array of pharmacological activities viz. anti-bacterial, antifungal, anti- inflammatory, anti-cancer and anti-viral [Wang *et al.*, 2001; Yadav and Singh, 2001]. These are generally synthesized by the condensation of primary amines with active carbonyl groups.

Various schiff bases were found to have anticancer activity [Sharma *et al.,* 1998; Pathak *et al.*, 2000; Vicini *et al.,* 2003) and a large number of benzothiazole also exhibited remarkable antimicrobial and anticancer activity [Beneteau *et al.,* 1999; Latrofa *et al.,* 2005; Mortimer *et al.,* 2006; Yalcin *et al.*, 1992]. These above-mentioned results prompted us to continue our investigation towards synthesis of schiff bases having benzothiazole ring system in order to achieve new lead compounds for future development as antimicrobial and anticancer agents. In this context, new series of N-(arylidene)-4-(benzo[d] thiazol-2-yl)benzenamines **(S01-17)** and 4-(benzo[d]thiazol-2-yl)-N-cyclopentylidene/ cyclohexylidene/ cycloheptylidene benzenamines **(S18-20)** were synthesized and their biological activities were evaluated.

5.1.2. CHEMISTRY

The compounds were rationally designed after analysis and comprehensive of literature review for antimicrobial and anticancer activity and were prepared by coupling of 2-(4'-aminophenyl) benzothiazole with substituted aryl aldehydes/cyclic ketones, refluxed in appropriate solvent (methanol/ethanol) in the presence of few drops of glacial acetic acid/conc.H_2SO_4 as catalyst. All the characterization data of the synthesized compounds

(**S01-20**) were in accordance with the proposed molecular structures. The purity assessment of the synthesized compounds was analysed by TLC and established by elemental analysis (Table 5.1).

The structure of Schiff bases of 2-(4'-aminophenyl) benzothiazole was confirmed by the comprehensive spectral data. The FT-IR spectra showed absorption bands at 3039 and 3183 cm^{-1} for aromatic C–H and at 1591 and 1691 cm^{-1} for azomethine group (–CH=N–). Formation of Schiff bases were confirmed by the absence of characteristic IR absorption peak (3140–3400 cm^{-1}) of N–H stretching, due to conversion of $–NH_2$ group to –CH=N– group. The ^1H NMR showed sharp singlet peak in the range of δ 8.23–8.84 ppm indicating the presence of azomethine proton (–CH=N–). The multiplet at δ 6.31–8.65 ppm was due to aromatic protons. The ^{13}C NMR spectra revealed all the corresponding peaks in the range of δ 140.12–151.22 ppm and δ 110.29–155.39 ppm which were due to azomethine (–CH=N–) carbon and aryl carbon respectively. The peak appearing in the range of δ 165.01–166.83 ppm corresponds to C2 of the benzothiazole ring. Phenolic-OH proton and methoxy protons of compound **S13** exhibited singlet at δ 10.36 and δ 3.80 ppm respectively. Methoxy protons of compounds **S01** and **S15** exhibited singlet at δ 3.82 and δ 3.88 ppm respectively. The phenolic-OH groups of compound **S05** showed broad singlet for *o*–OH proton at about δ 10.69 and singlet for *p*–OH proton at δ 9.92. The phenolic-OH proton for compound **S07** showed singlet at δ 9.72 ppm. Further, ESI-MS spectra gave all the (M+1) peaks related to molecular weight of the compounds. Compound **S05** showed peak at m/z 347(M+1,100%), which is in compliance with the molecular formula $C_{20}H_{14}N_2O_2S$.

5.1.3. PHYSICOCHEMICAL AND SPECTRAL CHARACTERIZATION DATA

Table 5.1 Physicochemical data of the benzothiazole Schiff base hybrids **(S01-S20)**

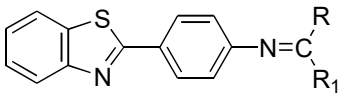

S01-17

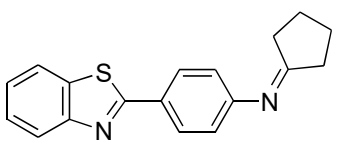

S18

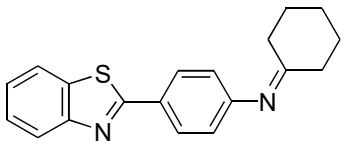

S19

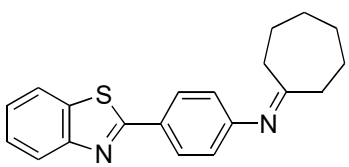

S20

Compound code	R	MW	Melting point (℃)	Yield (%)	R_f (solvent system)	Solubility
S01	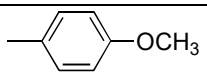	344.43	181-183	84	0.62 (A)	$CHCl_3$, MeOH,
S02	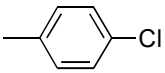	348.85	171-173	68	0.67 (A)	$CHCl_3$
S03	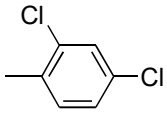	383.29	157-159	56	0.70 (A)	$CHCl_3$, MeOH
S04	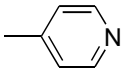	315.39	146-147	65	0.73 (B)	$CHCl_3$, MeOH
S05	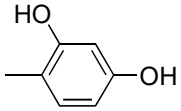	346.40	125-127	73	0.57 (B)	$CHCl_3$, MeOH
S06	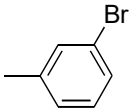	393.30	199-201	51	0.61 (B)	$CHCl_3$, MeOH
S07	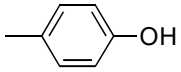	330.40	138-140	75	0.60 (A)	MeOH
S08	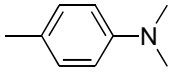	357.47	176-178	81	0.68 (A)	$CHCl_3$
S09	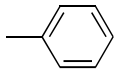	314.40	188-190	70	0.71 (B)	$CHCl_3$, MeOH
S10	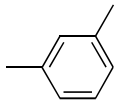	328.43	194-196	66	0.69 (B)	$CHCl_3$, MeOH
S11	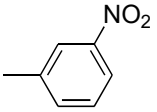	359.40	168-170	43	0.57 (B)	$CHCl_3$, MeOH
S12	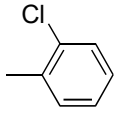	348.85	175-177	61	0.49 (B)	$CHCl_3$, MeOH
S13	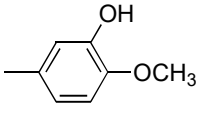	360.43	196-198	78	0.52 (B)	$CHCl_3$, MeOH
S14	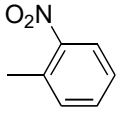	359.40	134-136	49	0.65 (B)	$CHCl_3$, MeOH
S15	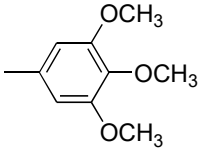	404.48	222-224	82	0.69 (B)	$CHCl_3$, MeOH

S16	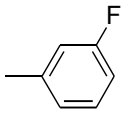	332.39	155-157	59	0.71 (B)	$CHCl_3$, MeOH
S17	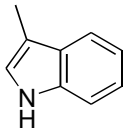	353.44	208-210	64	0.68 (B)	$CHCl_3$, MeOH
S18	-	292.40	165-166	60	0.51 (C)	$CHCl_3$, MeOH
S19	-	306.42	178-180	56	0.62 (C)	$CHCl_3$, MeOH
S20	-	320.45	191-192	52	0.57 (C)	$CHCl_3$, MeOH

Solvent system: (A) Methanol: Chloroform, 2:8, (B) Methanol: Chloroform, 1:9, (C) Ethylacetate: Hexane, 7:3

Spectral data for benzothiazole Schiff base hybrids

Compound S01: *N-(4-methoxybenzylidene)-4-(benzo[d]thiazol-2-yl)benzenamine*

IR (KBr, υmax cm^{-1}): 3081 (Aromatic C–H str.), 2850 (C–H str., O–CH_3 group), 1591 (C=N str., azomethine), 2924, 2853 (C–H str., N=CH group)

^{1}H NMR (DMSO-d_6, 300 MHz) δ (ppm): 3.82 (s, 3H, OCH_3), 6.60–7.89 (m, 12H, Ar–H), 8.47 (s, 1H, –N=CH)

^{13}C NMR (DMSO-d_6) δ (ppm): 55.69 (OCH_3), 141.33 (C=N–), 165.51 (benzothiazole–C–2), 164.24 (Ar–C–OCH_3), 129.67–140.05 (Aromatic–C, C_4–C_9 $C_{1'}$–$C_{6'}$ $C_{1''}$–$C_{6''}$)

MS (m/z, %): 345 (M + 1, 100).

Anal $C_{21}H_{16}N_2OS$. Calc. for: C, 73.23; H, 4.68; N, 8.13. Found: C, 73.21; H, 4.62; N, 8.09%.

Compound S02: *N-(4-chlorobenzylidene)-4-(benzo[d]thiazol-2-yl)benzenamine*

IR (KBr, υmax cm^{-1}): 3127, 3087 (Aromatic C–H str.), 1065 (C–Cl str.), 1621 (C=N str., azomethine), 2926, 2846 (C–H str., N=CH group)

^{1}H NMR (DMSO-d6, 300 MHz) δ (ppm): 7.26–8.28 (m, 12H, Ar–H), 8.52 (s, 1H, –N=CH)

^{13}C NMR (DMSO-d_6) δ (ppm): 149.62 (C=N–), 166.35 (benzothiazole–C–2), 121.34–146.73 (Aromatic–C, C4–C9 C1'–C6' C1"–C6")

MS (m/z, %): 349 (M + 1, 100).

Anal $C_{20}H_{13}ClN_2S$. Calc. for: C, 68.86; H, 3.76; N, 8.03. Found: C, 68.85; H, 3.74; N, 8.04%.

Compound S03: *N-(2,4-dichlorobenzylidene)-4-(benzo[d]thiazol-2-yl)benzenamine*

IR (KBr, υmax cm^{-1}): 3118, 3083 (Aromatic C–H str.), 1108, 1065 (C–Cl str.), 1627 (C=N str., azomethine), 2919, 2841 (C–H str., N=CH group)

^{1}H NMR (DMSO-d_6, 300 MHz) δ (ppm): 7.34–8.25 (m, 11H, Ar–H), 8.83 (s, 1H, –N=CH)

^{13}C NMR (DMSO-d_6) δ (ppm): 151.22 (C=N–), 165.15 (benzothiazole–C–2), 123.39–145.73 (Aromatic–C, C_4–C_9 $C_{1'}$–$C_{6'}$, $C_{1''}$–$C_{6''}$)

MS (m/z, %): 384 (M + 1, 100).

Anal $C_{20}H_{12}Cl_2N_2S$. Calc. for: C, 62.37; H, 3.16; N, 7.31. Found: C, 62.35; H, 3.18; N, 7.29%.

Compound S04: *4-(benzo[d]thiazol-2-yl)-N-(pyridin-4-ylmethylene)benzenamine)*

IR (KBr, υmax cm^{-1}): 3112, 3089 (Aromatic C–H str.), 1632 (C=N str., azomethine), 2929, 2854 (C–H str., N=CH group)

^{1}H NMR (DMSO-d_6, 300 MHz) δ (ppm): 7.23–8.65 (m, 12H, Ar–H), 8.26 (s, 1H, –N=CH)

^{13}C NMR (DMSO-d_6) δ (ppm): 151.22 (C=N–), 166.51 (benzothiazole–C–2), 124.19–155.39 (Aromatic–C, C_4–C_9 $C_{1'}$–$C_{6'}$, $C_{1''}$–$C_{6''}$)

MS (m/z, %): 316 (M + 1, 100).

Anal $C_{19}H_{13}N_3S$. Calc. for: C, 72.36; H, 4.15; N, 13.32. Found: C, 72.35; H, 4.12; N, 13.36%.

Compound S05: *N-(2, 4-dihydroxybenzylidene)-4-(benzo[d]thiazol-2-yl)benzenamine*

IR (KBr, υmax cm^{-1}): 3102 (Aromatic C–H str.), 3126 (O–H str., br.), 1631 (C=N str., azomethine), 2924, 2852 (C–H str., N=CH group)

^{1}H NMR (DMSO-d_6, 300 MHz) δ (ppm): 10.69 (br, s, 1H, *o*–OH group), 9.92 (s, 1H, *p*–OH group), 6.31–7.54 (m, 11H, Ar–H), 8.35 (s, 1H, –N=CH)

^{13}C NMR (DMSO-d_6) δ (ppm): 163.27 (Ar–C–OH), 143.20 (C=N–), 165.23 (benzothiazole–C–2), 110.29–132.99 (Aromatic–C, C_4–C_9 $C_{1'}$–$C_{6'}$, $C_{1''}$–$C_{6''}$)

MS (m/z, %): 347 (M + 1, 100).

Anal $C_{20}H_{14}N_2O_2S$. Calc. for: C, 69.35; H, 4.07; N, 8.09. Found: C, 69.35; H, 4.08; N, 8.07%.

Compound S06: *N-(3-bromobenzylidene)-4-(benzo[d]thiazol-2-yl)benzenamine*

IR (KBr, υmax cm^{-1}): 3107 (Aromatic C–H str.), 765 (C–Br str.), 1636 (C=N str., azomethine), 2931, 2835 (C–H str., N=CH group)

^{1}H NMR (DMSO-d_6, 300 MHz) δ (ppm): 7.21–8.18 (m, 12H, Ar–H), 8.82 (s, 1H, –N=CH)

^{13}C NMR (DMSO-d_6) δ (ppm): 148.42 (C=N–), 165.32 (benzothiazole–C–2), 123.48–145.73 (Aromatic–C, C_4–C_9 $C_{1'}$–$C_{6'}$, $C_{1''}$–$C_{6''}$)

MS (m/z, %): 394 (M + 1, 100).

Anal $C_{20}H_{13}BrN_2S$. Calc. for: C, 61.08; H, 3.33; N, 7.12. Found: C, 61.05; H, 3.31; N, 7.10%.

Compound S07: *N-(4-hydroxybenzylidene)-4-(benzo[d]thiazol-2-yl)benzenamine*

IR (KBr, υmax cm^{-1}): 3132 (Aromatic C–H str.), 3426 (O–H str.), 1634 (C=N str., azomethine), 2924, 2813 (C–H str., N=CH group)

^{1}H NMR (DMSO-d_6, 300 MHz) δ (ppm): 9.72 (s, 1H, –OH), 7.11–7.94 (m, 12H, Ar–H), 8.32 (s, 1H, –N=CH)

^{13}C NMR (DMSO-d_6) δ (ppm): 160.17 (Ar–C–OH), 141.20 (C=N–), 166.83 (benzothiazole–C–2), 112.79–138.91 (Aromatic–C, C_4–C_9 $C_{1'}$–$C_{6'}$, $C_{1''}$–$C_{6''}$)

MS (m/z, %): 331 (M + 1, 100).

Anal $C_{20}H_{14}N_2OS$. Calc. for: C, 72.70; H, 4.27; N, 8.48. Found: C, 72.71; H, 4.25; N, 8.46%.

Compound S08: *4-((4-(benzo[d]thiazol-2-yl)phenylimino)methyl)-N,N-dimethyl benzenamine*

IR (KBr, υmax cm^{-1}): 3067 (Aromatic C–H str.), 1336 (–C–N str.), 2878 (C–H str., -CH_3 group), 1621 (C=N str., azomethine), 2921, 2827 (C–H str., N=CH group)

^{1}H NMR (DMSO-d_6, 300 MHz) δ (ppm): 3.23 (s, 6H, -CH_3), 7.06–8.28 (m, 12H, Ar–H), 8.61 (s, 1H, –N=CH)

^{13}C NMR (DMSO-d_6) δ (ppm): 44.21, 45.65 ($2CH_3$–), 144.52 (C=N–), 166.10 (benzothiazole–C–2), 112.37–140.73 (Aromatic–C, C_4–C_9 $C_{1'}$–$C_{6'}$, $C_{1''}$–$C_{6''}$)

MS (m/z, %): 358 (M + 1, 100).

Anal $C_{22}H_{19}N_3S$. Calc. for: C, 73.92; H, 5.36; N, 11.75. Found: C, 73.90; H, 5.35; N, 11.74%.

Compound S09: *4-(benzo[d]thiazol-2-yl)-N-benzylidenebenzenamine)*

IR (KBr, υmax cm^{-1}): 3147 (Aromatic C–H str.), 1630 (C=N str., azomethine), 2938, 2815 (C–H str., N=CH group)

^1H NMR (DMSO-d_6, 300 MHz) δ (ppm): 7.22–7.98 (m, 13H, Ar–H), 8.48 (s, 1H, –N=CH)

^{13}C NMR (DMSO-d_6) δ (ppm): 142.34 (C=N–), 165.09 (benzothiazole–C–2), 124.98–139.17 (Aromatic–C, C_4–C_9 $C_{1'}$–$C_{6'}$, $C_{1''}$–$C_{6''}$)

MS (m/z, %): 315 (M + 1, 100).

Anal $C_{20}H_{14}N_2S$. Calc. for: C, 76.40; H, 4.49; N, 8.91. Found: C, 76.38; H, 4.49; N, 8.90%.

Compound S10: *N-(4-methylbenzylidene)-4-(benzo[d]thiazol-2-yl)benzenamine*

IR (KBr, υmax cm^{-1}): 3068 (Aromatic C–H str.), 2892 (C–H str., $–CH_3$ group), 1691 (C=N str., azomethine), 2936, 2829 (C–H str., N=CH group)

^1H NMR (DMSO-d_6, 300 MHz) δ (ppm): 2.82 (s, 3H, $–CH_3$), 7.06–7.82 (m, 12H, Ar–H), 8.28 (s, 1H, –N=CH)

^{13}C NMR (DMSO-d_6) δ (ppm): 22.36 ($–CH_3$), 140.12 (C=N–), 166.15 (benzothiazole–C–2), 112.46–139.03 (Aromatic–C, C_4–C_9 $C_{1'}$–$C_{6'}$, $C_{1''}$–$C_{6''}$)

MS (m/z, %): 329 (M + 1, 100).

Anal $C_{21}H_{16}N_2S$. Calc. for: C, 76.80; H, 4.91; N, 8.53. Found: C, 76.78; H, 4.50; N, 8.53%.

Compound S11: *N-(3-nitrobenzylidene)-4-(benzo[d]thiazol-2-yl)benzenamine*

IR (KBr, υmax cm^{-1}): 3127 (Aromatic C–H str.), 1351 (N=O str.), 1632 (C=N str., azomethine), 2939, 2831 (C–H str., N=CH group)

^1H NMR (DMSO-d_6, 300 MHz) δ (ppm): 7.12–8.10 (m, 12H, Ar–H), 8.74 (s, 1H, –N=CH)

^{13}C NMR (DMSO-d_6) δ (ppm): 149.40 (C=N–), 165.02 (benzothiazole–C–2), 121.98–147.73 (Aromatic–C, C_4–C_9 $C_{1'}$–$C_{6'}$, $C_{1''}$–$C_{6''}$)

MS (m/z, %): 360 (M + 1, 100).

Anal $C_{20}H_{13}N_3O_2S$. Calc. for: C, 66.84; H, 3.65; N, 11.69. Found: C, 66.85; H, 3.63; N, 11.68%.

Compound S12: *N-(2-chlorobenzylidene)-4-(benzo[d]thiazol-2-yl)benzenamine*

IR (KBr, υmax cm^{-1}): 3116 (Aromatic C–H str.), 1061 (C–Cl str.), 1646 (C=N str., azomethine), 2942, 2844 (C–H str., N=CH group)

^{1}H NMR (DMSO-d_6, 300 MHz) δ (ppm): 7.06–8.26 (m, 12H, Ar–H), 8.69 (s, 1H, –N=CH)

^{13}C NMR (DMSO-d_6) δ (ppm): 148.02 (C=N–), 166.05 (benzothiazole–C–2), 122.84–148.33 (Aromatic–C, C_4–C_9 $C_{1'}$–$C_{6'}$ $C_{1''}$–$C_{6''}$)

MS (m/z, %): 349 (M + 1, 100).

Anal $C_{20}H_{13}ClN_2S$. Calc. for: C, 68.86; H, 3.76; N, 8.03. Found: C, 68.85; H, 3.74; N, 8.02%.

Compound S13: *5-((4-(benzo[d]thiazol-2-yl)phenylimino)methyl)-2-methoxyphenol*

IR (KBr, υmax cm^{-1}): 3088, 3054 (Aromatic C–H str.), 3458 (O–H str.), 2885 (C–H str., O–CH_3 group), 1641 (C=N str., azomethine), 2930, 2843 (C–H str., N=CH group)

^{1}H NMR (DMSO-d_6, 300 MHz) δ (ppm): 10.36 (br, s, 1H, –OH group), 3.80 (s, 3H, OCH_3), 6.96–7.70 (m, 11H, Ar–H), 8.34 (s, 1H, –N=CH)

^{13}C NMR (DMSO-d_6) δ (ppm): 56.06 (OCH_3), 145.33 (C=N–), 165.01 (benzothiazole–C–2), 124.67–144.15 (Aromatic–C, C_4–C_9 $C_{1'}$–$C_{6'}$ $C_{1''}$–$C_{6''}$)

MS (m/z, %): 361 (M + 1, 100).

Anal $C_{21}H_{16}N_2O_2S$. Calc. for: C, 69.98; H, 4.97; N, 7.77. Found: C, 69.95; H, 4.95; N, 7.75%.

Compound S14: *N-(2-nitrobenzylidene)-4-(benzo[d]thiazol-2-yl)benzenamine*

IR (KBr, υmax cm^{-1}): 3169 (Aromatic C–H str.), 1365 (N=O str.), 1643 (C=N str., azomethine), 2973, 2845 (C–H str., N=CH group)

^{1}H NMR (DMSO-d_6, 300 MHz) δ (ppm): 7.11–8.46 (m, 12H, Ar–H), 8.84 (s, 1H, –N=CH)

^{13}C NMR (DMSO-d_6) δ (ppm): 150.94 (C=N–), 164.70 (benzothiazole–C–2), 126.08–143.27 (Aromatic–C, C_4–C_9 $C_{1'}$–$C_{6'}$ $C_{1''}$–$C_{6''}$)

MS (m/z, %): 360 (M + 1, 100).

Anal $C_{20}H_{13}N_3O_2S$. Calc. for: C, 66.84; H, 3.65; N, 11.69. Found: C, 66.84; H, 3.63; N, 11.66%.

Compound S15: *N-(3,4,5-trimethoxybenzylidene)-4-(benzo[d]thiazol-2-yl)benzenamine*

IR (KBr, υmax cm^{-1}): 3146, 3120, 3068 (Aromatic C–H str.), 2915, 2835, 2812 (C–H str., O–CH_3 group), 1634 (C=N str., azomethine), 2924, 2854 (C–H str., N=CH group)

^{1}H NMR (DMSO-d_6, 300 MHz) δ (ppm): 3.72 (s, 3H, OCH_3), 3.87 (s, 6H, OCH_3), 6.96–7.90 (m, 10H, Ar–H), 8.23 (s, 1H, –N=CH)

^{13}C NMR (DMSO-d_6) δ (ppm): 57.83, 56.85, 56.20 (OCH_3), 142.03 (C=N–), 165.66 (benzothiazole–C–2), 114.67–134.85 (Aromatic–C, C_4–C_9 $C_{1'}$–$C_{6'}$ $C_{1''}$–$C_{6''}$)

MS (m/z, %): 405 (M + 1, 100).

Anal $C_{23}H_{20}N_2O_3S$. Calc. for: C, 68.30; H, 4.98; N, 6.93. Found: C, 68.29; H, 4.96; N, 6.91%.

Compound S16: *N-(3-fluorobenzylidene)-4-(benzo[d]thiazol-2-yl)benzenamine*

IR (KBr, υmax cm^{-1}): 3183 (Aromatic C–H str.), 1653 (C=N str., azomethine), 2933, 2821(C–H str., N=CH group)

^{1}H NMR (DMSO-d_6, 300 MHz) δ (ppm): 7.14–8.55 (m, 12H, Ar–H), 8.75 (s, 1H, –N=CH)

^{13}C NMR (DMSO-d_6) δ (ppm): 149.02 (C=N–), 165.09 (benzothiazole–C–2), 118.34–139.13 (Aromatic–C, C_4–C_9 $C_{1'}$–$C_{6'}$ $C_{1''}$–$C_{6''}$)

MS (m/z, %): 333 (M + 1, 100).

Anal $C_{20}H_{13}FN_2S$. Calc. for: C, 72.27; H, 3.94; N, 8.43. Found: C, 72.25; H, 3.93; N, 8.40%.

Compound S17: *N-((1H-indol-3-yl)methylene)-4-(benzo[d]thiazol-2-yl)benzenamine*

IR (KBr, υmax cm^{-1}): 3095 (Aromatic C–H str.), 3276 (–N–H str.), 1614 (C=N str., azomethine), 2941, 2856 (C–H str., N=CH group)

^{1}H NMR (DMSO-d_6, 300 MHz) δ (ppm): 11.35 (s, 1H, Indole NH), 7.01–7.89 (m, 12H, Ar–H), 8.37 (s, 1H, –N=CH)

^{13}C NMR (DMSO-d_6) δ (ppm): 142.82 (C=N–), 165.41 (benzothiazole–C–2), 121.74–140.33 (Aromatic–C, C_4–C_9 $C_{1'}$–$C_{6'}$ $C_{1''}$–$C_{6''}$)

MS (m/z, %): 354 (M + 1, 100).

Anal $C_{22}H_{15}N_3S$. Calc. for: C, 74.76; H, 4.28; N, 11.89. Found: C, 74.75; H, 4.27; N, 11.90%.

Compound S18: *4-(benzo[d]thiazol-2-yl)-N-cyclopentylidenebenzenamine*

IR (KBr, υmax cm^{-1}): 3071-3039 (Aromatic C–H str.), 2920–2825 (C–H str. of cylopentyl group), 1647 (C=N str., azomethine)

^{1}H NMR (DMSO-d_6, 300 MHz) δ (ppm): 1.41–1.85 (m, 8H, cyclopentylidene–H), 7.31–8.58 (m, 8H, Ar–H)

^{13}C NMR (DMSO-d_6) δ (ppm): 22.03–34.38 (cyclopentyl-C), 141.53 (C=N–), 165.41 (benzothiazole–C–2), 121.34–134.38 (Aromatic–C, C_4–C_9 $C_{1'}$–$C_{6'}$ $C_{1''}$–$C_{6''}$)

MS (m/z, %): 293 (M + 1, 100).

Anal $C_{18}H_{16}N_2S$. Calc. for: C, 73.94; H, 5.52; N, 9.58. Found: C, 73.92; H, 5.50; N, 9.56%.

Compound S19: *4-(benzo[d]thiazol-2-yl)-N-cyclohexylidenebenzenamine*

IR (KBr, υmax cm^{-1}): 3118-3049 (Aromatic C–H str.), 2923–2834 (C–H str. of cylohexyl group), 1618 (C=N str., azomethine)

^{1}H NMR (DMSO-d_6, 300 MHz) δ (ppm): 1.78–2.35 (m, 10H, cyclohexylidene–H), 7.34–8.18 (m, 8H, Ar–H)

^{13}C NMR (DMSO-d_6) δ (ppm): 24.37–36.58 (cyclohexyl-C), 146.42 (C=N–), 166.01 (benzothiazole–C–2), 123.94–140.28 (Aromatic–C, C_4–C_9 $C_{1'}$–$C_{6'}$ $C_{1''}$–$C_{6''}$)

MS (m/z, %): 307 (M + 1, 100).

Anal $C_{19}H_{18}N_2S$. Calc. for: C, 74.47; H, 5.92; N, 9.14. Found: C, 74.45; H, 5.91; N, 9.13%.

Compound S20: *4-(benzo[d]thiazol-2-yl)-N-cycloheptylidenebenzenamine*

IR (KBr, υmax cm^{-1}): 3131-3058 (Aromatic C–H str.), 2933–2854 (C–H str. of cyloheptyl group), 1637 (C=N str., azomethine)

^{1}H NMR (DMSO-d_6, 300 MHz) δ (ppm): 1.86–2.63 (m, 12H, cycloheptylidene–H), 7.31–8.25 (m, 8H, Ar–H)

^{13}C NMR (DMSO-d_6) δ (ppm): 27.17–38.98 (cyloheptyl-C), 148.22 (C=N–), 165.72 (benzothiazole–C–2), 124.94–143.18 (Aromatic–C, C_4–C_9 $C_{1'}$–$C_{6'}$ $C_{1''}$–$C_{6''}$)

MS (m/z, %): 321 (M + 1, 100).

Anal $C_{20}H_{20}N_2S$. Calc. for: C, 74.96; H, 6.29; N, 8.74. Found: C, 74.95; H, 6.29; N, 8.72%.

5.1.4. *IN-VITRO* ANTIMICROBIAL ACTIVITY

The results of anti-microbial studies of all the novel compounds against bacteria and fungi are presented in Table 5.2 and 5.3, respectively. Some of them inhibited the growth of bacteria with good to excellent MIC values ranging between 1 and 100 µg/mL while few of them showed moderate to good anti-fungal activity with MICs between 15 and 65 µg/mL. According to the antimicrobial studies, all the compounds showed better activity in comparison to their anti-fungal one. Almost all the compounds showed activity against *E.coli* and *S.typhi* and only some of them showed activity on rest of the bacterial strains. In

addition, compound **S05** showed moderate activity against all bacterial strains while compound **S06** showed activity against *E.coli* only. Compounds **S02**, **S08**, **S13**, **S15** and **S19** showed good activity against all the bacterial strains.

Table 5.2 Antibacterial activity (MIC µg/mL) of the synthesized benzothiazole Schiff base hybrids **(S01-20)**

Compound code	Bacteria					
	Gram positive bacteria		Gram negative bacteria			
	S. aureus **(ATCC 25323)**	***E. faecalis*** **(Clinical isolate)**	***E. coli*** **(ATCC 35218)**	***S. typhi*** **(MTCC 3216)**	***K. pneumonia*** **(ATCC 31488)**	***P. aeruginosa*** **(ATCC 27893)**
S01	31.2	31.2	15.6	31.2	-	-
S02	31.2	7.81	15.6	31.2	15.6	15.6
S03	62.5	15.6	31.2	-	-	-
S04	-	15.6	62.5	15.6	-	7.81
S05	31.2	62.5	62.5	15.6	31.2	31.2
S06	-	-	62.5	-	-	-
S07	-	-	31.2	31.2	-	-
S08	15.6	15.6	3.91	7.81	31.2	7.81
S09	31.2	-	62.5	31.2	-	-
S10	-	31.2	31.2	15.6	62.5	-
S11	>100	-	62.5	-	>100	>100
S12	31.2	-	31.2	-	62.5	31.2
S13	7.81	31.2	15.6	15.6	15.6	15.6
S14	>100	>100	>100	>100	>100	>100
S15	3.91	7.81	7.81	7.81	15.6	3.91
S16	-	-	7.81	62.5	31.2	62.5
S17	31.2	62.5	62.5	62.5	31.2	62.5
S18	-	31.2	15.6	31.2	31.2	15.6
S19	7.81	31.2	15.6	15.6	15.6	3.91
S20	15.6	31.2	15.6	31.2	-	15.6
CIP	≥6.25	≥6.25	≥6.25	≥6.25	≥6.25	≥3.12

The comparative zone of inhibition of compounds **S02**, **S08**, **S13**, **S15** and **S19** against all the bacterial strains is represented in Fig. 5.1. Particularly, compound 4-((4-(benzo[d]thiazol-2-yl) phenylimino)methyl)-N,N-dimethylbenzenamine (**S08**) showed maximum activity (zone of inhibition up to 30–32 mm at concentration of 3.91 µg/mL) against *E.coli*. Compounds N-(3,4,5-trimethoxybenzylidene)-4-(benzo[d]thiazol-2-yl)benzenamine (**S15**) and 4-(benzo[d]thiazol-2-yl)-N-cyclohexylidenebenzenamine (**S19**) showed excellent activity (zone of inhibition up to 30–32 mm at concentration range of 3.91-7.81 µg/mL) against *S. aureus* and *P. aeruginosa.* Also compounds **S11** and **S14** have activity at higher concentration. In context to the anti-fungal screening, compounds **S15** and **S19** yielded good activity at concentration of 15.6 µg/mL, against *C. krusei* and *C. albicans* respectively. Compounds **S01, S02, S05, S06, S08, S11, S14, S15, S18, S19** and **S20** showed moderate activity against few fungal strains.

Structure–activity relationship (SAR) studies from the results of the antimicrobial activity revealed that conversion of amino group to azomethine group via Schiff base formation may contribute for enhanced activity. The greater antimicrobial activity of **S02**, **S08**, **S13**, **S15** and **S19** may be attributed to the presence of electron donating substituents such as methoxy, hydroxyl on phenyl ring. Schiff bases of cyclic ketones were found to have more antibacterial action as compared to antifungal action. The presence of electronegative atom such as chloro group at para position also enhanced the antimicrobial effect.

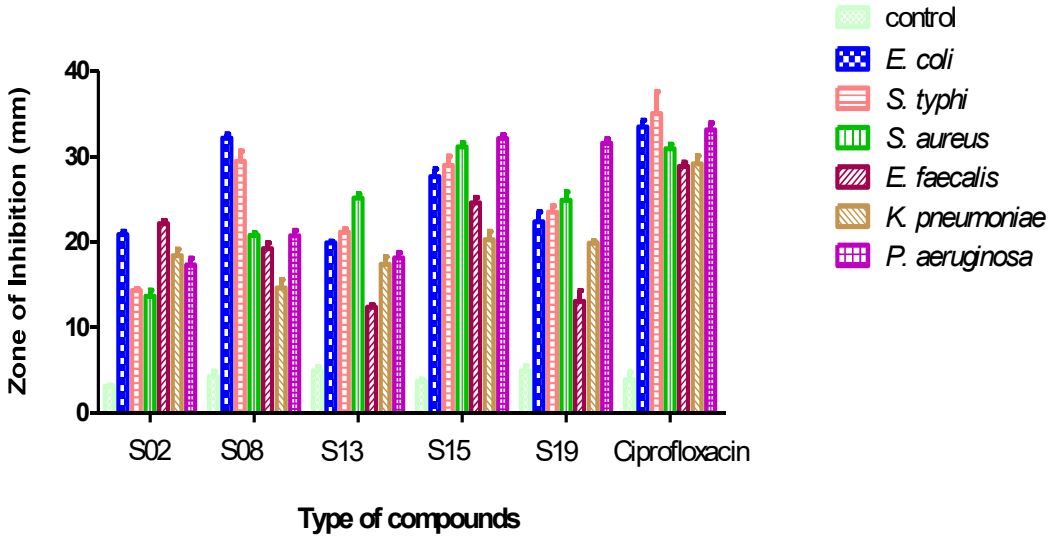

Fig 5.1 Comparative zone of inhibition of compounds **S02, S08, S13, S15** and **S19** against all the bacterial strains.

Table 5.3 Antifungal activity (MIC µg/mL) of the synthesized benzothiazole Schiff base hybrids **(S01-20)**

Compound code	*C. albicans* (ATCC 90028)	*C. tropicalis* (ATCC 750)	*C. krusei* (ATCC 6268)
S01	62.5	62.5	-
S02	-	62.5	-
S03	-	-	-
S04	-	-	-
S05	31.2	-	-
S06	-	62.5	-
S07	-	-	-
S08	31.2	-	62.5
S09	-	-	-
S10	-	-	-
S11	-	62.5	62.5
S12	-	-	-
S13	-	-	-
S14	62.5	-	-
S15	31.2	31.2	15.6
S16	-	-	-
S17	-	-	-
S18	-	31.2	
S19	15.6	31.2	-
S20	-	-	62.5
Fluconazole	≥6.25	≥6.25	≥6.25

5.1.4.1. Mechanism of action study

Bactericidal kinetics

The bactericidal activity of lead compounds **S08** and **S15** were carried out toward the specific *S. aureus* and *E. coli* strains in order to confirm the potency. It was determined at fixed time intervals to see the potential killing effects of bacterial cells at concentration fourfold MIC's (4 × MIC). Time-kill studies demonstrated that compounds **S08** and **S15**

were rapid with 90 to 99% lethality within 2 to 5 h (Fig. 5.2). The inhibition kinetics in *S. aureus* showed compound **S15** more effective than compound **S08** even up to 5 h and vice versa in *E. coli* strain. At concentration of 4 × MIC, both the compounds inhibited bacterial growth 2 h onwards until 5 h.

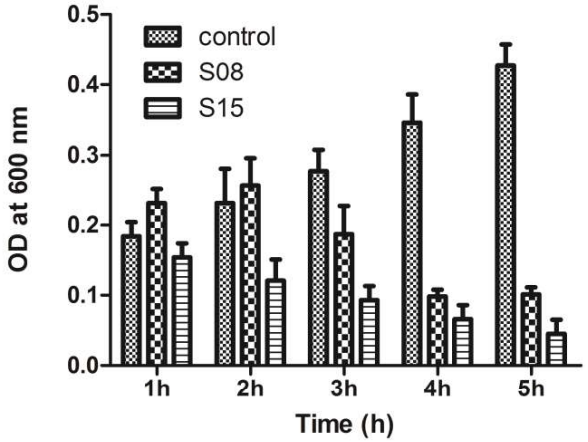

(A)

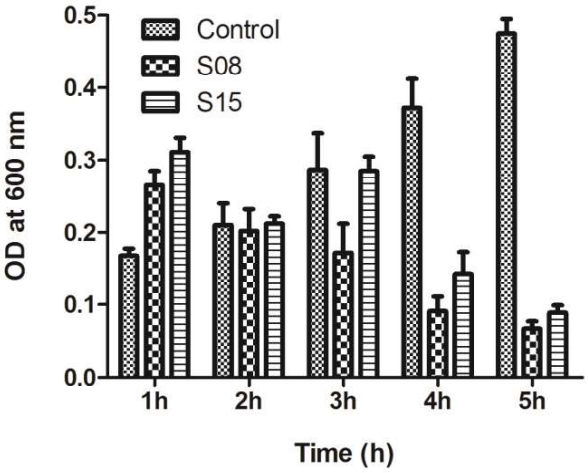

(B)

Fig. 5.2 Time dependent killing of (A) *S. aureus* (B) *E. coli* upon treatment with compounds **S08** and **S15** at 4 × MIC.

Membrane depolarization

To get approaching the mechanism of antimicrobial activity of designed analogues, compound-induced permeability of *S. aureus* and *E. coli* was examined by determining the membrane depolarization assay. Cationic membrane potential-sensitive cyanine dye [3, 3'-dipropyl- thiadicarbocyanine iodide $DiSC_3(5)$] was used to determine the depolarization

ability of cytoplasmic membrane. In this experiment, an increase in fluorescence intensity of dye is observed if any analogues alter the membrane potential due to pore formation/ membrane destabilization. This ultimately leads to the loss of the membrane potential gradient, causing the dye to be released into the medium resulting in membrane depolarization [Sims *et al.,* 1974]. Triton (2%) was found to depolarize the bacterial membrane and was used as a positive control. At the maximum concentration (i.e., 4 x MIC) of designed analogues **S08** and **S15** tested, the level of depolarization reached to saturation from about 2 to 5 mins of time. Compounds **S08** and **S15** have completely depolarized the membrane at concentrations lower than those other compounds. All compounds showed similar profile with respect to positive control (Fig. 5.3).

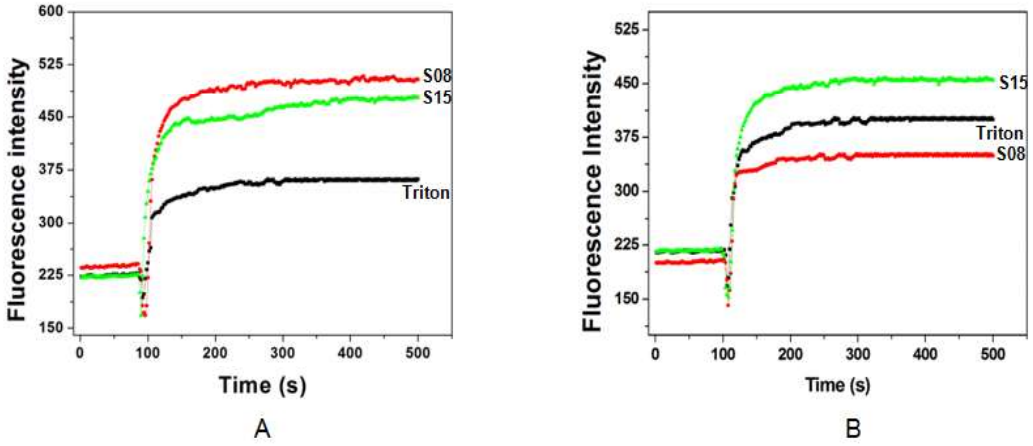

Fig. 5.3 Membrane depolarization ability of designed compounds on (A) *E.coli* and (B) *S.aureus* treated with 4xMIC concentration of compounds **S08** and **S15**.

Membrane permeability of viable bacteria

Cell viability was examined using FACS (Fuorescence assisted cell cytometer) by quantifying the amount of DNA released in terms of Propidium Iodide (PI) after the incubation of test compounds with *S. aureus* and *E. coli*. Consistent with the outer membrane depolarization assay of bacteria, designed analogue **S08** induced maximum damages to the membrane organization of *E. coli,* whereas compound **S15** leads to more pore formation in *S. aureus* as compared to *E. coli*, indicated by PI staining of the cells (Fig. 5.4). However, both compounds **S08** and **S15** induced reasonable damage of bacterial membrane in both strains.

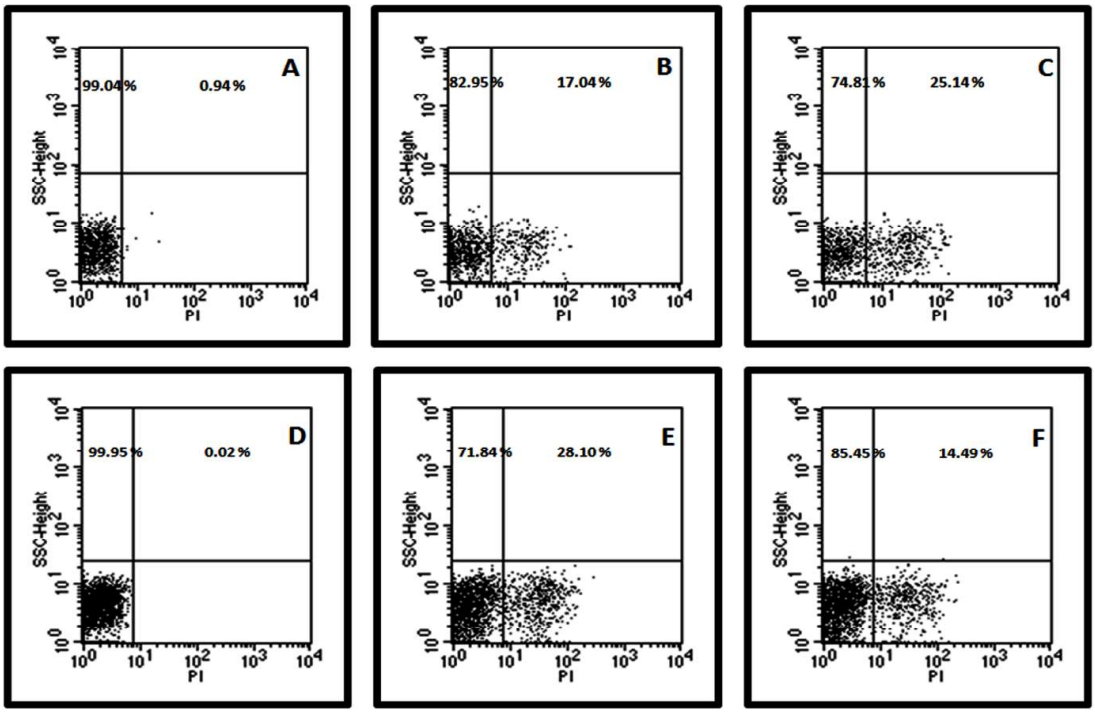

Fig. 5.4 Determination of compound-induced membrane damage of *S. aureus* and *E. coli* cells. (A–F) PI staining of *S. aureus* (A) control without PI treatment (B) **S08** (C) **S15** and on *E. coli* (D) control without PI treatment (E) **S08** (F) **S15** respectively.

DNA binding activity

Together interpreting the results of membrane permeabilization assay and FACS analysis, we found that series of Benzothiazole Schiff base hybrids could extricate the integrity of plasma membrane, leading to leakage of bacterial cell contents. Simultaneously, during the interface with membrane, test compounds unavoidably could enter into the cytoplasm, but the effect of these test compounds in the cytoplasm is absolutely unknown. Thus, we determined the DNA-binding propensity of test compounds **S08** and **S15** by analyzing the electrophoretic mobility of plasmid DNA at different concentration. Compound **S15** showed prominent binding with pUC19 plasmid DNA (200ng) causing retardation at 31.2 µg/mL, whereas in case of compound **S08**, no retardation was observed even at all concentration range used (Fig. 5.5). However it was interesting that DNA binding was predisposed with the whole structure of the compound, i.e. tri-methoxy containing compound **S15** showed most potent DNA binding ability in comparison with compound **S08**. Overall the study signifies lead compounds **S08** and **S15** and related compounds disrupts the membrane potential which was exploited for cellular energy production and membrane damage and, somehow showed binding interactions with plasmid DNA.

To explore the actual mechanism of preferential binding with major and minor groove regions of DNA, the MG/DAPI staining techniques were used. The DNA was treated with DAPI or MG prior to the addition of compounds. When DAPI (minor groove binder) was added to the reaction mixture containing compound **S15**, significant inhibition in the cleavage pattern was observed. But, in presence of methyl green (major groove binder), the cleavage was not suppressed (Fig. 5.6). Thus electrophoretic pattern demonstrated that compound **S15** showed specific binding affinity towards the major groove and partial affinity towards the minor groove.

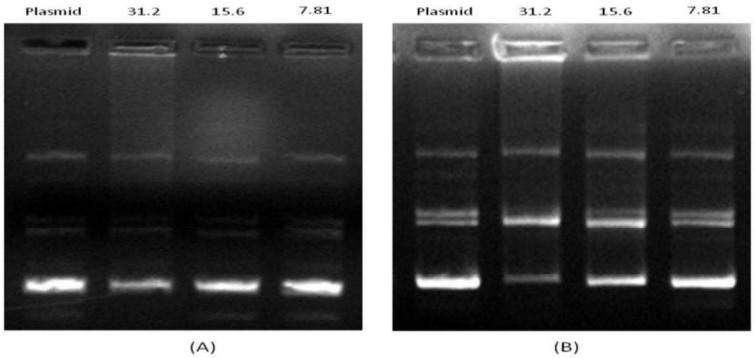

Fig. 5.5 Agarose gel electrophoresis patterns of pUC19 (200 ng) cleaved by (A) **S08** (31.2–7.81 µg/mL), after 1 h incubation time (concentration dependent) Lane 1: control; Lane 2: 31.2 µg/mL **S08** + DNA; Lane 3: 15.6 µg/mL **S08** + DNA; Lane 4: 7.81 µg/mL **S08** + DNA, and (B) **S15** (31.2–7.81 µg/mL), after 1 h incubation time (concentration dependent) Lane 1: control; Lane 2: 31.2 µg/mL **S15** + DNA; Lane 3: 15.6 µg/mL **S15** + DNA; Lane 4: 7.81 µg/mL **S15** + DNA, in buffer (5 mM Tris–HCl/50 mM NaCl, pH 7.2 at 25 °C).

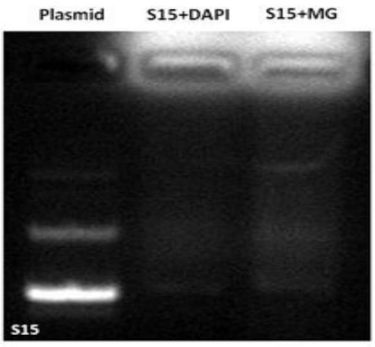

Fig. 5.6 Agarose gel electrophoresis pattern for the cleavage of supercoiled DNA (200 ng) by compound **S15** in the presence of DAPI and Methyl Green.

5.1.4.2. Docking study against Glc-6-PS

The active site of glucosamine-6-phosphate synthase (GlcN-6-P synthase) was used to determine the orientation of inhibitors. Thus, we studied the molecular basis of interaction and affinity of binding of all synthesized benzothiazole derivatives. All molecules were docked into the catalytic domain of GlcN-6-P synthase by molecular docking study using the Surflex dock program incorporated in Sybyl-X1.2. All the molecules showed very good binding energy ranging from 3-6 dock score. Docking score of the standard drugs Ciprofloxacin and Fluconazole were 6.06 and 6.4, respectively. Compounds S08, S13 and S15 showed good interaction with receptor as shown in Table 5.4. The ligand receptor interactions of compounds S13 and S19 and also of standard drugs are shown in Fig. 5.7. Compound S13 was found to have a score of 5.78 and formed 2 strong H-bonds with Ser401 and Ser604 group, whereas no binding was observed for compounds S18, S19 and S20. From the results, it was evident that the *in-silico* findings were well associated with the data obtained through *in-vitro* microbial assay.

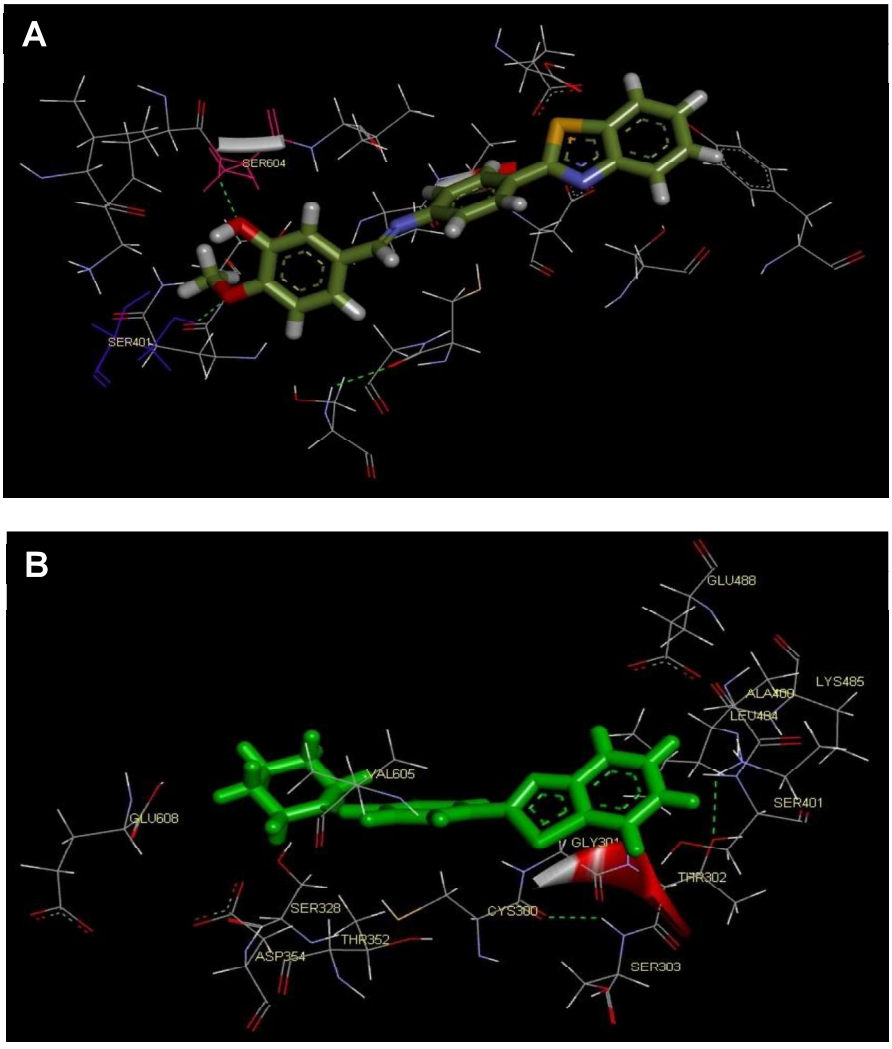

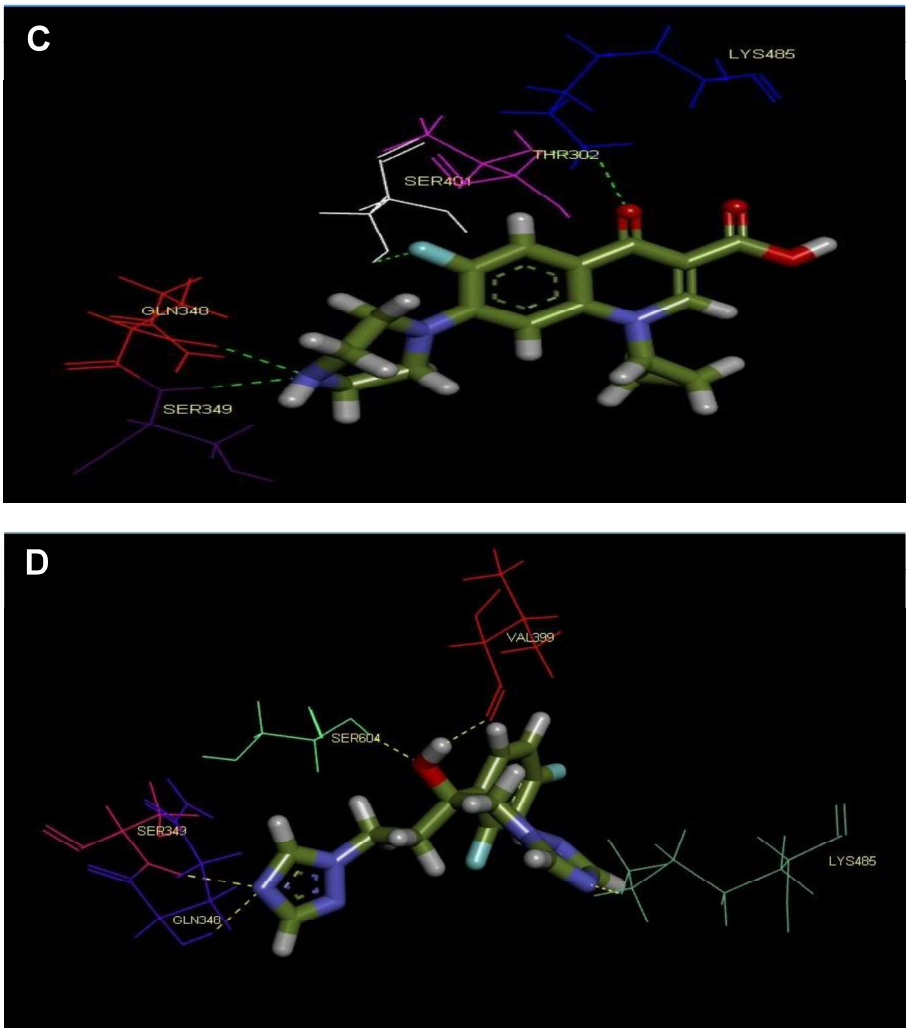

Fig. 5.7 Binding pose of compound (A) **S13**, (B) **S19**, (C) Ciprofloxacin and (D) Fluconazole with glucosamine-6-phosphate synthase. Hydrogen bonding interactions are displayed by green dotted lines.

Table 5.4 Molecular docking scores of Benzothiazole Schiff Base Hybrids with GlcN-6-P synthase.

Sr. No	Compound Id	Docking Score	Crash Value	Interacting amino acids
1	S01	4.7417	-0.6441	Lys485
2	S02	3.2966	-0.7941	Ser303, Ser349
3	S03	3.2587	-1.1262	Ser303
4	S04	4.6106	-0.8362	Thr302,Val605
5	S05	5.0385	-0.9887	Ser347, Cys300, Ser303, Gln348, Ser349

6	S06	3.746	-1.704	Ser303, Ser349
7	S07	4.7744	-1.2065	Val399,Cys300, Ser604
8	S08	5.3111	-1.0624	Ser303, Thr302, Gln348, Ser349
9	S09	3.4731	-0.8192	Lys485
10	S10	4.2495	-0.9508	Ser347, Cys300, Ser303, Gln348, Ser349
11	S11	3.3111	-1.0624	Ser303, Ser349
12	S12	2.9272	-0.6629	Ser 349
13	S13	5.7852	-1.0256	Ser401, Ser604
14	S14	3.3218	-1.2011	Ser 349
15	S15	5.3219	-0.9636	Ser604, Val605
16	S16	3.8616	-1.0495	Lys485, Ser 349
17	S17	4.052	-0.8571	Ser401
18	S18	3.4554	-0.5121	No Binding
19	S19	3.4554	-0.4323	No Binding
20	S20	4.366	-0.6673	No Binding
21	Ciprofloxacin	6.0614	2.0428	Ser347, Gln348, Ser349, Ser401, Lys485
22	Fluconazole	6.4092	-1.4344	Val399, Gln348, Ser349, Lys485, Ser604

5.1.4.3. *In-Silico* Pharmacokinetic Predictions

Predicting ADME properties at an early stage of drug discovery and development process is very important to remove compounds with poor pharmacokinetic properties and minimize extremely expensive and time-consuming steps. In the present study the best-fit ligands i.e. **S01**, **S05, S07, S13** and **S15** were subjected to preADMET server to predict the *in-silico* pharmacokinetic properties. The molecular descriptors have been employed to predict various human ADMET processes and other pharmacokinetic parameters such as log P analysis, drug-likeliness, human intestinal absorption, *in-vitro* plasma protein binding and water solubility in buffer system. The predicted drug likelinesss of the synthesized compounds follows the Lipinski‘‘Rule of Five’’. All the four parameters for a compound, i.e. Log P <5, H-bond donors <5, H-bond acceptors <10 and molecular weight <500 suggested that the compounds might have good

absorption or permeability properties. The results are summarized in Table 5.5 and description of descriptors is given in Table 5.6.

Table 5.5 Theoretical prediction of different properties of novel Schiff base benzothiazole hybrids using PreADMET Server

Comp No.	Log p	$LogS_b$ (mg/L)	HIA (%)	*In-vitro* PPB (%)	HB-donors	HB-acceptors
S01	5.5	117.01	100	91.08	0	4
S05	4.7	0.262	92.72	96.65	0	3
S07	3.6	56.84	98.46	89.51	2	3
S13	4.9	5.08	96.76	90.12	0	4
S15	5.3	20.33	99.42	83.27	1	4

Table 5.6 PreADMET Server properties and descriptors

Sr. No.	Descriptor	Description	Recommended range
1	Log P	physicochemcal descriptor	-2 to 8
2	Log S_b	physicochemcal descriptor	broad range
3	HIA (%)	It predicts human intestinal absorption on 0–100 % scale.	Poorly absorbed: 0 to 20%, moderately absorbed: 20-70% and well absorbed compounds: 70-100%.
4	*In-vitro* PPB (%)	In-vitro plasma protein binding prediction tool predicts percent drug bound in plasma protein as *In-vitro* data on human.	Strongly bound chemicals >90% Weakly bound chemicals <90%
5	HB-donors	Estimated number of hydrogen bonds that would be donated by the solute to water molecules in an aqueous solution.	0.0–6.0
6	HB-acceptors	Estimated number of hydrogen bonds that would be accepted by the solute from water molecules in an aqueous solution.	2–20

5.1.5. *IN-VITRO* ANTICANCER ACTIVITY

The compounds **S01-20** were subjected to MTT assay against human ovarian sensitive (A2780 and SKOV3) and resistant (A2780-CR and A2780-PR) cell lines in order to determine growth inhibitory/cytotoxic capability. The IC_{50} values derived from *In-vitro* screening revealed that compounds **S02** and **S05** possess significant cytotoxicity against A2780 and SKOV3 and compound **S05** also showed significant cytotoxicity against A2780-CR cell line. However, no cytotoxicity was observed against A2780-PR cell line for all the compounds. Statistical analysis was performed by using non-linear regression analysis on Graph Pad prism 5.0. IC_{50} values were calculated from each set of triplicate wells. The synthesized compounds **S01**, **S11** and **S13** showed cytotoxic activity with IC_{50} values over 100 μg/mL on A2780 and SKOV3 and compound **S13** also displayed same cytotoxicity on A2780-CR. Rest of the compounds did not display any cytotoxicity on all the cell lines used in the study (Table 5.7).

5.1.5.1. Cytotoxicity study against ovarian cancer cell lines

To understand the cytotoxic potential of the Schiff base benzothiazole hybrids, both A2780 and SKOV3 cell lines were treated with the S-series compounds for 48 hrs and analyzed by MTT assay. As represented in Fig. 5.8, both compounds **S02** and **S05** exhibited low cell killing effect at lower concentration (91% cell survival at 4.9 and 3.4μg/mL, respectively) compared to significantly high cell killing effect at highest concentration (21% cell survival at 490 and 340 μg/mL, respectively) in A2780 cells. Similar effects were also observed in SKOV3 cell line except for compound **S02** that showed reactivity with McCoy's medium at higher concentration. For both cell lines, IC_{50} values of compounds **S02** and **S05** were found to be 49 μg/mL and 34μg/mL. The rest three compounds did not show any growth inhibitory effect and therefore compound **S05** was used for further evaluation (Fig. 5.8). IC_{50} values of synthesized compounds, Cisplatin and Paclitaxel in sensitive (SKOV3, A2780-S) and resistant (A2780-CR and A2780-PR) cells are mentioned in Table 5.7. The detailed % cell viability results of compounds **S02** and **S05** in A2780, SKOV3 and A2780-CR cell lines are represented graphically in Figs. 5.9, 5.10 and 5.11.

In-vitro growth inhibitory effect of compound **S05** against A2780-CR and A2780-PR cells was assessed using MTT reduction assay as shown Fig. 5.12. Interestingly, A2780-CR showed similar response as its sensitive counterpart A2780-S (IC_{50} at 34μg/mL, Fig.

5.12A) on treatment with compound **S05**. However, in paclitaxel resistant cells (A2780-PR) compound **S05** showed inhibitory effect only at higher dosage (~20% at 340µg/mL) compared to intermediate and lower dosage (~80% for both 34 µg/mL and 3.4 µg/mL) (Fig. 5.12B).

Table 5.7 IC_{50} (µg/mL) of compounds **S02**, **S05**, Cisplatin and Paclitaxel in SKOV3, A2780-S, A2780-CR and A2780-PR cell lines.

Comp Code	SKOV3	A2780-S	A2780-CR	A2780-PR
S01	>100	>100	-	-
S02	49	49	-	-
S03	-	-	-	-
S04	>100	>100	-	-
S05	34	34	34	-
S06	-	-	-	-
S07	-	-	-	-
S08	-	-	-	-
S09	-	-	-	-
S10	-	-	-	-
S11	>100	>100	-	-
S12	-	-	-	-
S13	>100	>100	>100	-
S14	-	-	-	-
S15	-	-	-	-
S16	-	-	-	-
S17	-	-	-	-
S18	-	-	-	-
S19	-	-	-	-
S20	-	-	-	-
Cisplatin	-	500ng/mL	5µg/mL	NA
Paclitaxel	-	4.3ng/mL	NA	21.3ng/mL

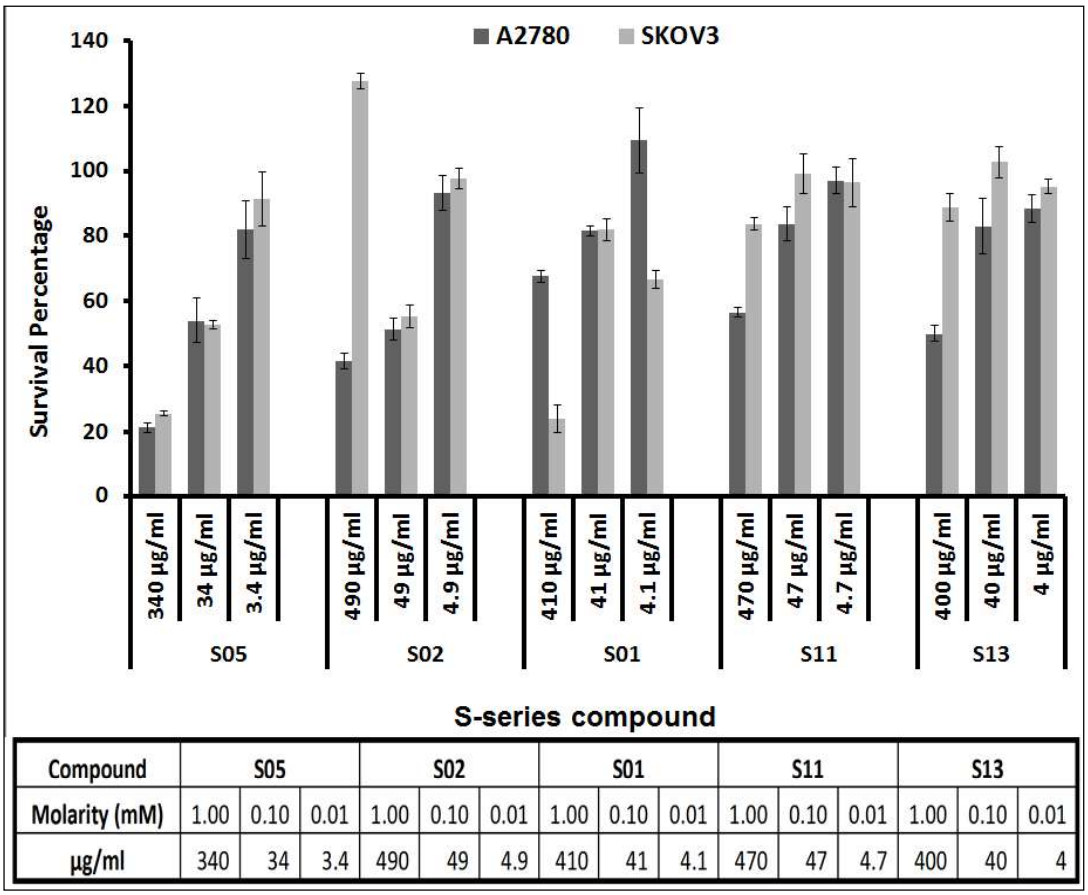

Compound	S05			S02			S01			S11			S13		
Molarity (mM)	1.00	0.10	0.01	1.00	0.10	0.01	1.00	0.10	0.01	1.00	0.10	0.01	1.00	0.10	0.01
µg/ml	340	34	3.4	490	49	4.9	410	41	4.1	470	47	4.7	400	40	4

Fig. 5.8 Effect of different concentrations (1mM, 0.1mM and 0.01mM) of compounds **S05, S02, S01, S11** and **S13** on viability of ovarian cancer cell lines (A2780 and SKOV3)

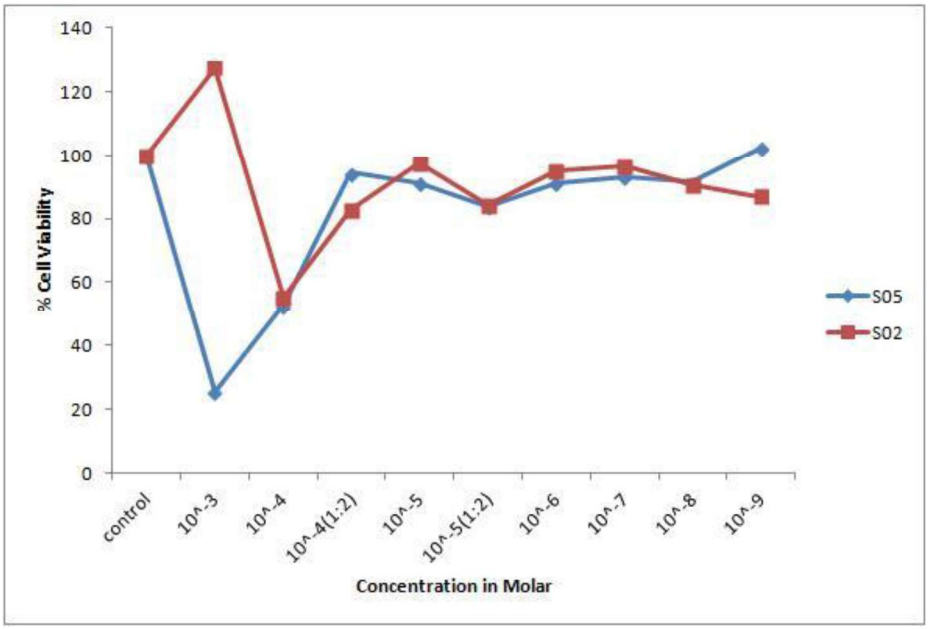

Fig. 5.9 Effect of concentration (1mM – 1nM) of compounds **S05** and **S02** on viability of human ovarian cancer SKOV3 cell line.

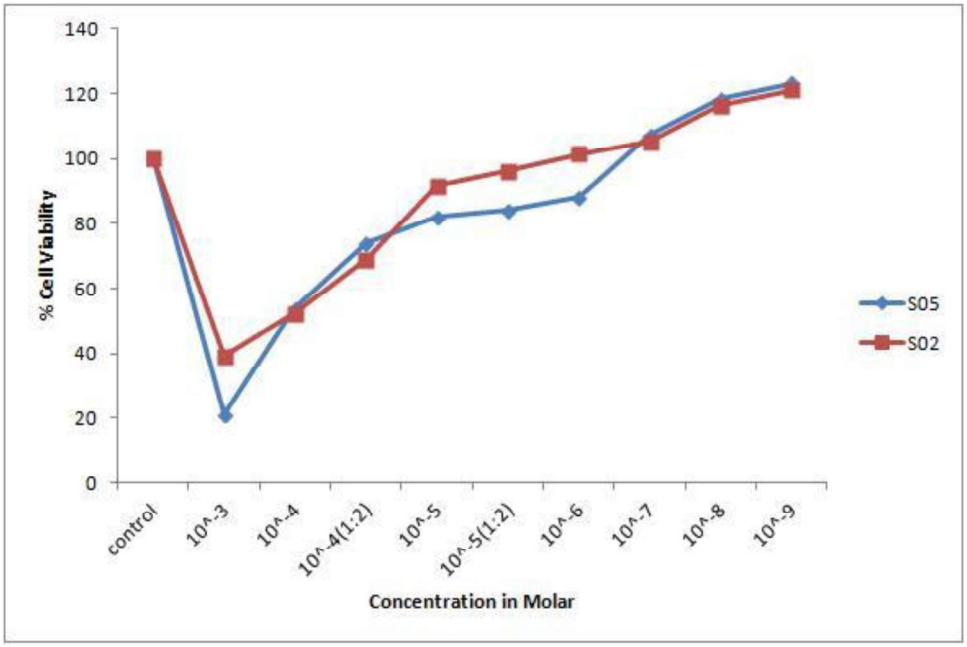

Fig. 5.10 Effect of concentration (1mM – 1nM) of compounds **S05** and **S02** on viability of human ovarian cancer A2780 cell line.

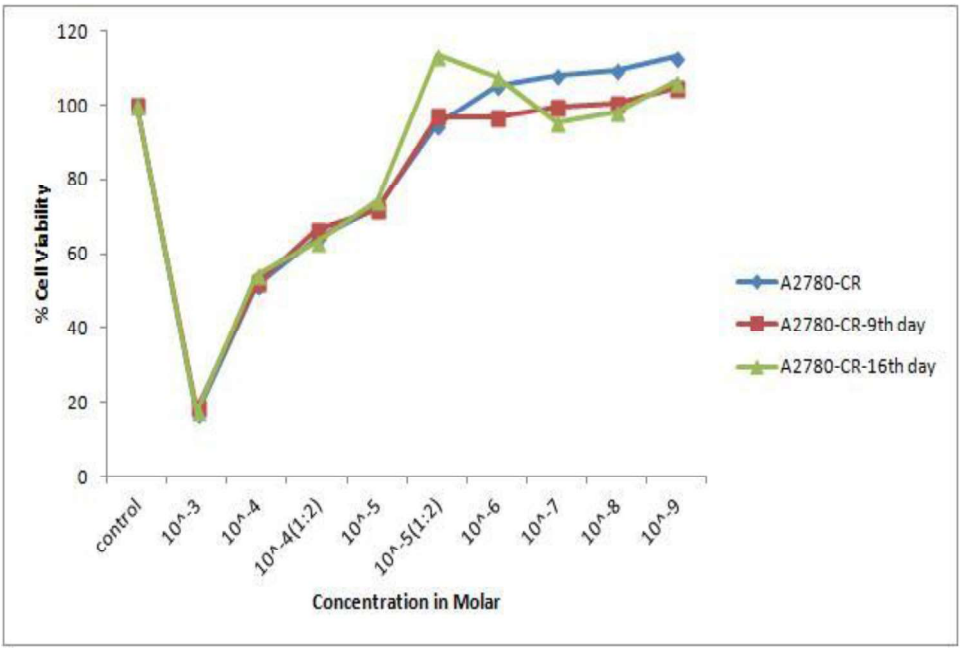

Fig. 5.11 Effect of concentration (1mM – 1nM) of compound **S05** on viability of human ovarian cancer A2780-CR cell line.

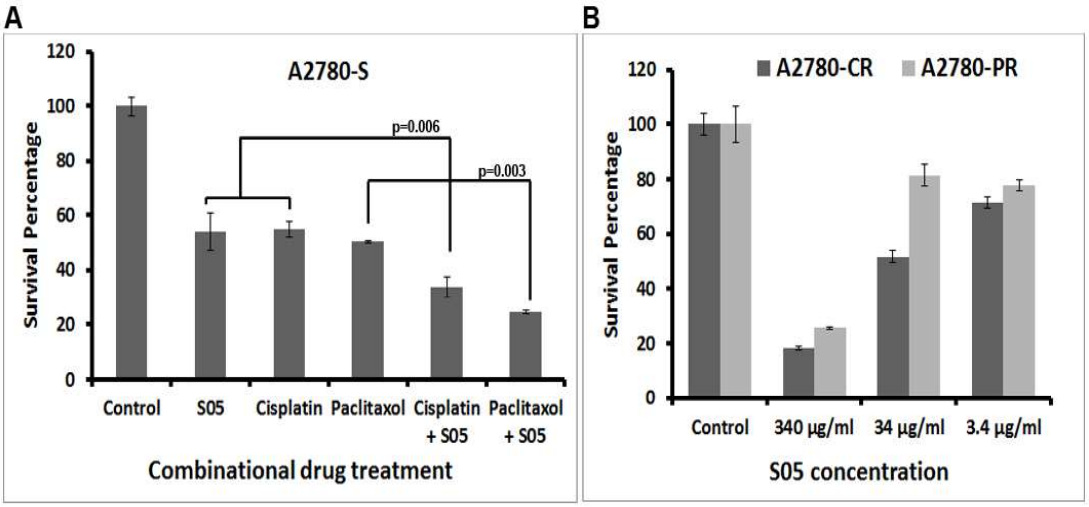

Fig. 5.12 Growth inhibitory effect of compound **S05** on (A) A2780-S (B) A2780-CR and A2780-PR cell lines.

5.1.5.2. Cytotoxicity assessment on the basis of selectivity index

To establish the specificity of compound **S05** towards cancer cells, normal ovarian surface cell line IOSE 364 was incubated with different concentration of **S05**. As represented in Fig. 5.13, only ~20% reduction in cell viability was seen at 34 µg/mL of **S05**, which was found to induce 50% lethality in other two cancer cell lines (A2780 & SKOV3) indicating the specificity of the compound.

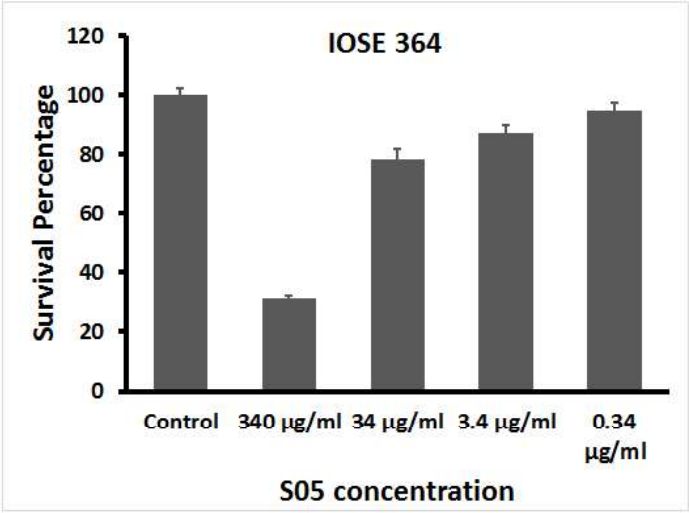

Fig. 5.13 Growth inhibitory effect of compound **S05** on viability of normal ovarian cancer surface epithelial cell line (IOSE 364)

5.1.5.3. Combinatorial treatment approach

To evaluate influence of compound **S05** as a combinatorial therapeutic agent with cisplatin or paclitaxel, A2780-S cells were treated with IC_{50} dosage of each drug alone and/or in combination. Compound **S05** along with cisplatin and paclitaxel showed significant growth inhibition (50% to 20%) (p= 0.006 and p= 0.003 respectively) compared to individual drug treatments indicating a synergistic effects.

Further, this synergistic effect of compound **S05** was studied in the cisplatin and paclitaxel resistant models. When cisplatin resistant cells were treated with compound **S05** alone and **S05** with cisplatin (at IC_{50} dose for A2780-CR cells), a significant growth inhibition (40%, p=0.02) was observed in combinatorial treatment. The synergistic effect of compound **S05** was also observed with lower concentration of cisplatin (IC_{50} dose for A2780-S) in A2780-CR cells. When A2780-CR was treated with cisplatin (500ng/mL) and compound **S05** together, significant growth inhibition (39%) compared to individual drugs (50% for **S05** and 90% cisplatin, p=0.0245 & p=0.0009) treatments was found (Fig. 5.14A). The paclitaxel resistance cells (A2780-PR) were also used to study the similar synergistic effect of **S05** with paclitaxel. However, no significant growth inhibition was observed with combination treatment of **S05** and paclitaxel compared to individual treatments (Fig. 5.14B).

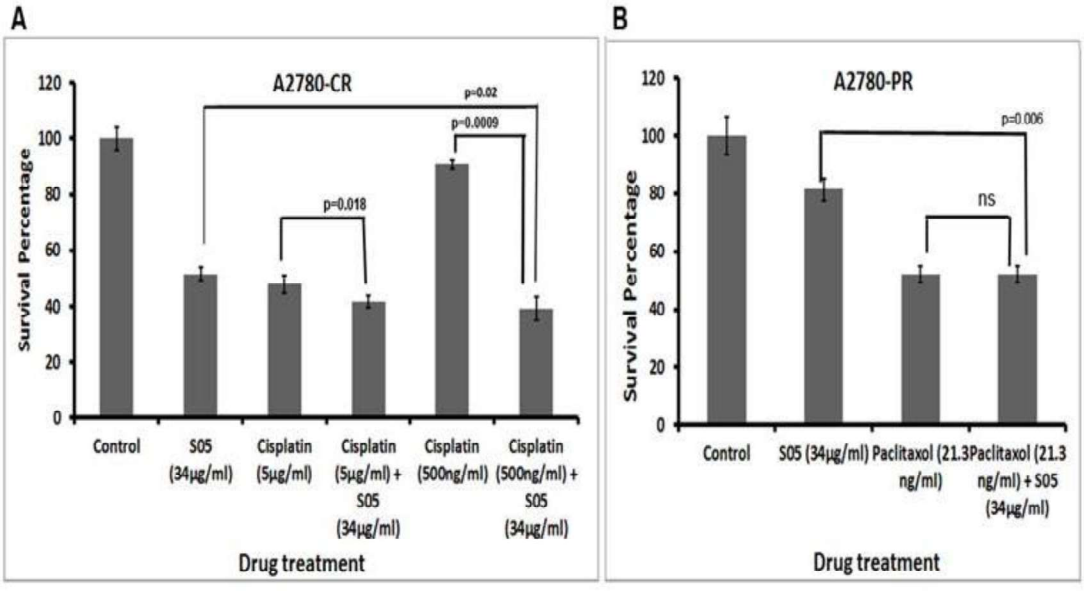

Fig. 5.14 Growth inhibitory effect of compound **S05** as a combinatorial treatment on (A) A2780-CR (B) A2780-PR cell lines.

Platinum/taxane based chemotherapy serves as excellent first line treatment for ovarian cancer, but majority of these tumors recur due to acquirement of resistance to chemotherapy. Herein, we investigated novel EGFR ligand inhibitor as a therapeutic agent for ovarian cancer. When all newly synthesized derivatives were tested for their cytotoxic activities in two different ovarian cancer cells, compound **S05** showed the maximal effect in both. In combination with cisplatin and paclitaxel, compound **S05** significantly decreased the viability by 33% & 24% in A2780 sensitive cells. We have also evaluated the efficacy of compound **S05** against chemoresistant cellular model for cisplatin and paclitaxel. Interestingly, when tested against cisplatin resistant cells, compound **S05** significantly decreased the viability with IC_{50} value determined at 34μg/mL. However, in paclitaxel resistant cells decreased viability was only observed at very high concentration indicating that level of IGFR/EGFR probably varies with drug dependent resistance which in turn determines the effect of these compounds.

Further, we assessed the influence of compound **S05** as a combinatorial drug with platinum or taxane based drugs. We observed that compound **S05** is more effective cytotoxic agent in combination with chemotherapeutic drugs than alone in both sensitive and resistant model. The compound **S05** makes cisplatin treatment even more effective against resistant cellular models, indicating a synergistic effect. In fact, even at lower dosage of cisplatin, compound **S05** was found to be more effective than cisplatin or **S05** alone. Combinatorial treatment of compound **S05** with paclitaxel was effective only in sensitive model but no significant effect was observed in resistance model, indicating the least influence of EGFR-driven pathways in paclitaxel resistance.

5.1.5.4. Docking study against EGFR-TK

The molecular docking software, Autodock 4.0 was used to study the binding behaviour of the ligands onto receptor binding pockets. The association of EGFR family of tyrosine kinases in cancer proliferation suggests ligands which block the kinase activity of the entire EGFR family and may have profound therapeutic potential. Benzothiazoles act via challenging with ATP intended for binding at the catalytic domain of tyrosine kinase. The ATP binding site has the following features: Adenine region – plays an important role in hydrogen bonding; Sugar region – a hydrophilic region; Hydrophobic pocket – though not used by ATP but plays an imperative role in inhibitor selectivity; Hydrophobic channels – even if not used by ATP but may be exploited for inhibitor specificity; and Phosphate binding region – precisely used for improving inhibitor

selectivity [Fabbro *et al.,* 2002]. Thus, we selected EGFR target to carry out the docking study of synthesized compounds and delineate their best possible mechanism of action. The proposed hypothetical model of the highly active N-(2,4-dihydroxybenzylidene)-4-(benzo[d]thiazol-2-yl)benzenamine (S05) bound to ATP binding site of EGFR tyrosine kinase is shown in Fig. 5.15.

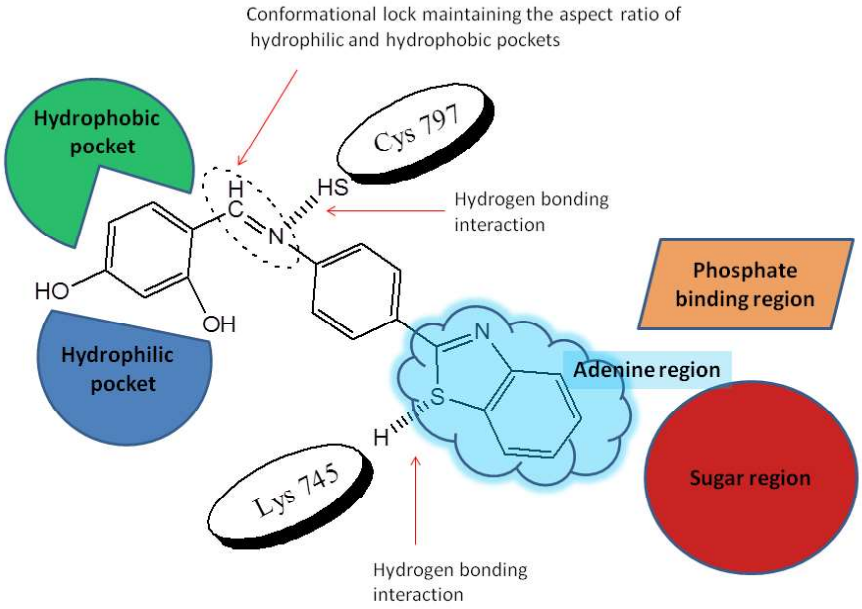

Fig. 5.15 Proposed hypothetical model of the highly active N-(2, 4-dihydroxybenzylidene)-4-(benzo[d]thiazol-2-yl)benzenamine (**S05**) bound to ATP binding site of EGFR Protein tyrosine kinase

Molecular docking studies of the target compounds were performed to explore the possible interaction between target (ATPase domain of tyrosine kinase) and synthesised compounds. A number of general residues involved in this type of interaction are LYS745, VAL726, MET766, ASP800, and MET793. Almost all the compounds were found to reveal hydrogen bonding with wide range of residues. LYS745 was found to be the common residue involved in the docking of maximum number of ligands. Although, MET793 contributes the hinge binding with the ligands but it is not necessary that all ligands exhibit such an interaction. Due to different conformational changes and orientation behaviour of the ligands in the amino acid pool of receptor, only 'O' atom of methoxy group contributes hinge binding with the residues MET793 as found in compound S01 and S13. Despite tri-methoxy substitution in compound S15, this interaction was absent due to bulkiness of compound resulting in altered conformational position. Binding

pose of compound S01 in the ATP binding site of EGFR-TK showing hinge binding, is shown in Fig. 5.16.

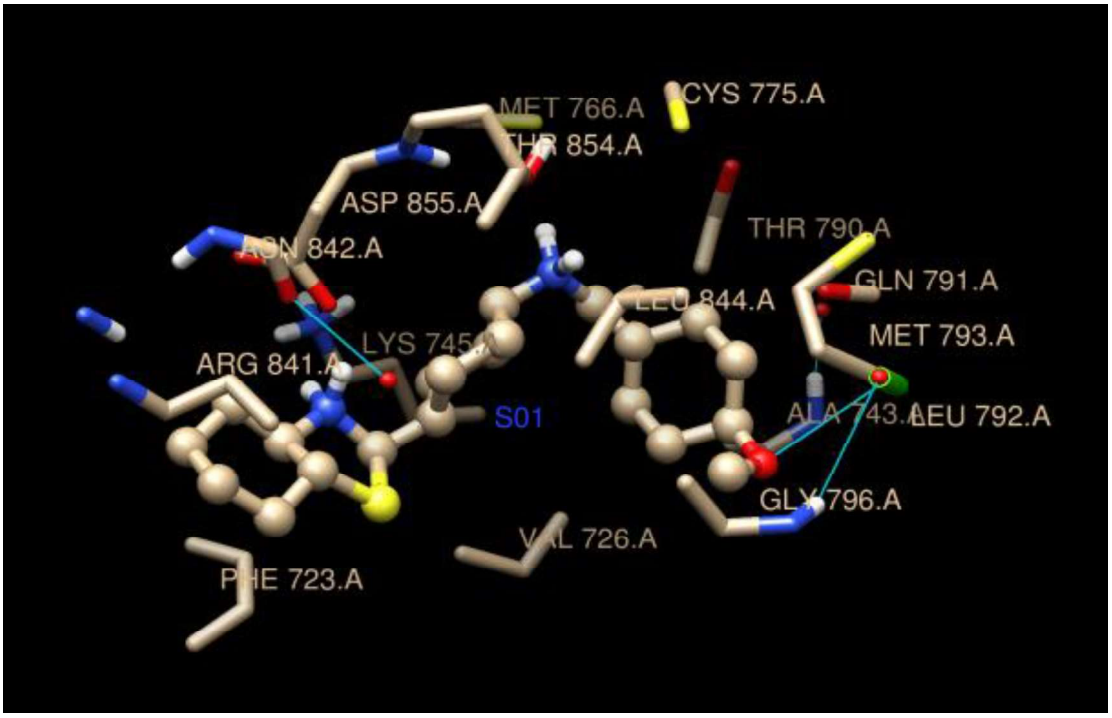

Fig. 5.16 Predicted binding pose of compound **S01** at the ATP-binding site of EGFR-TK.

The compounds S01, S02, S05, S11 and S13 were found to have high negative docking energy or score ranging from -8.94 to -9.85 kcal/mol (Table 5.8) indicating, these compounds formed most stable drug-receptor complexes. The minimum docking energy was found for compound S05 (-9.85 kcal/mol) with an estimated inhibition constant of 36.75μM and RMSD 0.89. Fig. 5.17(a) demonstrates binding mode of compound S05 in the ATP binding site of EGFR-TK. The sulphur atom of benzothiazole ring system in compound S05 is involved in hydrogen bond formation with LYS-745 and nitrogen of azomethine linkage of Schiff base shows hydrogen bond interaction with CYS-797. The azomethine linkage at 4th position of 2-phenyl substituted benzothiazoles is behaving as a conformational lock and extending substituted -CH=N- portion into the lipophillic pockets of EGFR tyrosine kinase, making it predominantly hydrophobic/lipophillic. Residues within 5 Å area of compound S05 is shown in Fig. 5.17(b). Fig. 5.17(c) depicts the color-coded visualization of electrostatic potential surface owing to the charge density of the compound. The color scale of the electrostatic potential shows red for the highest magnitude, blue for the lowest magnitude and white for neutral.

The aforesaid-findings confirm that the experimental results of wet lab are in good agreement with the predicted ones as observed from the dock scores. However, compounds S01, S11 and S13 exhibited good docking scores but did not show significant activities. It is possible that these compounds might have some permeability problems, and further studies are required to elucidate this.

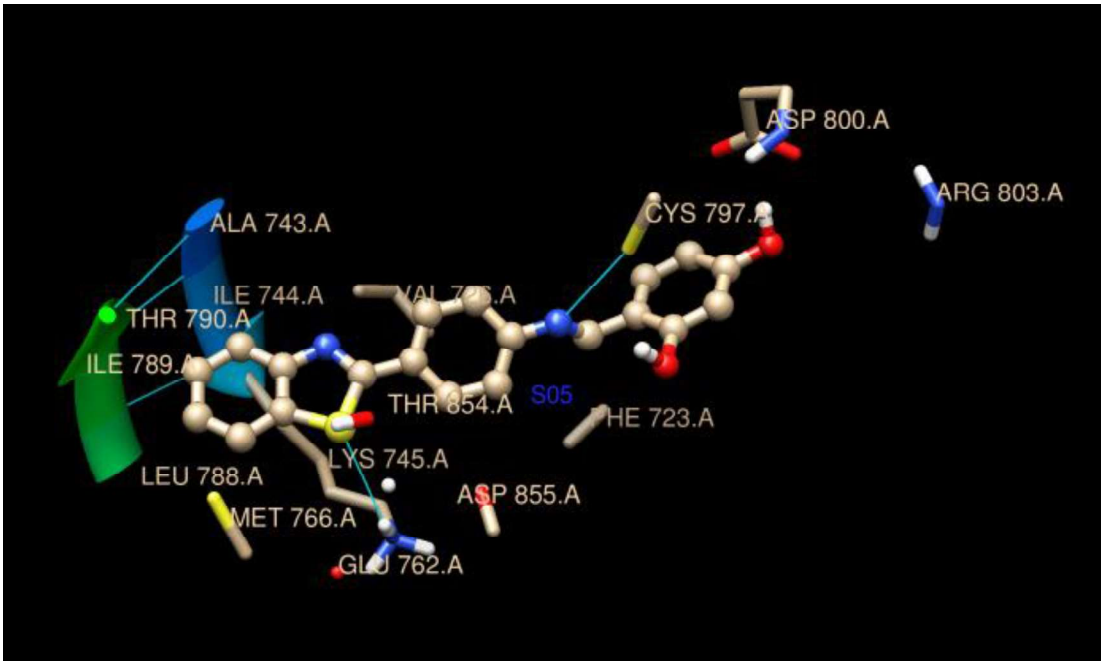

(A)

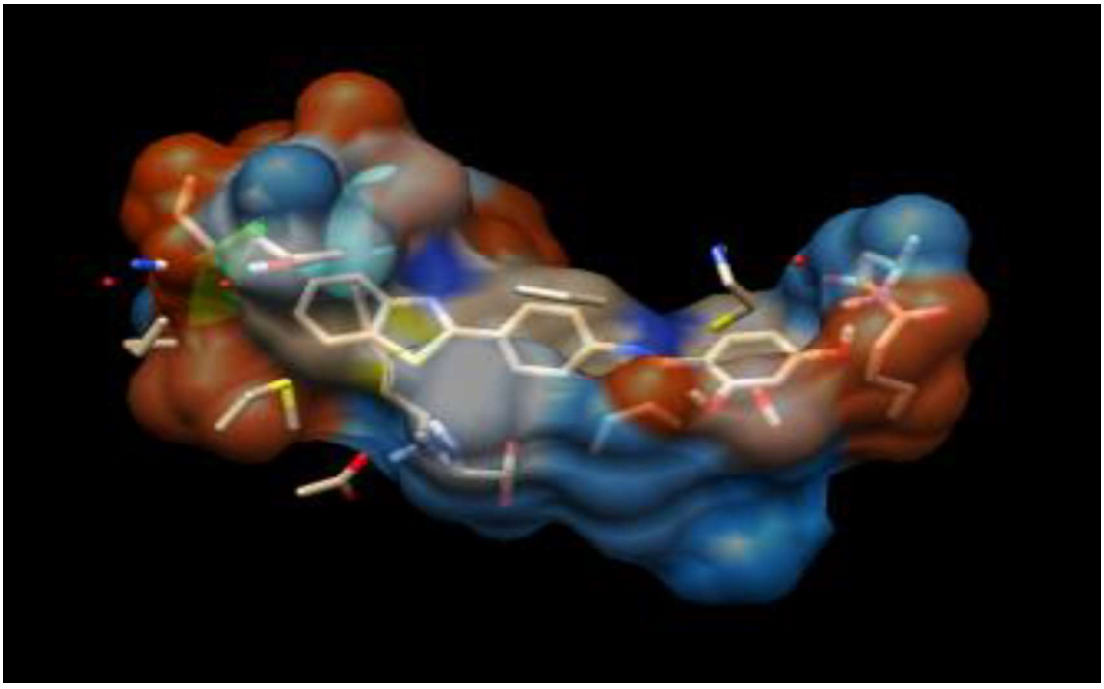

(B)

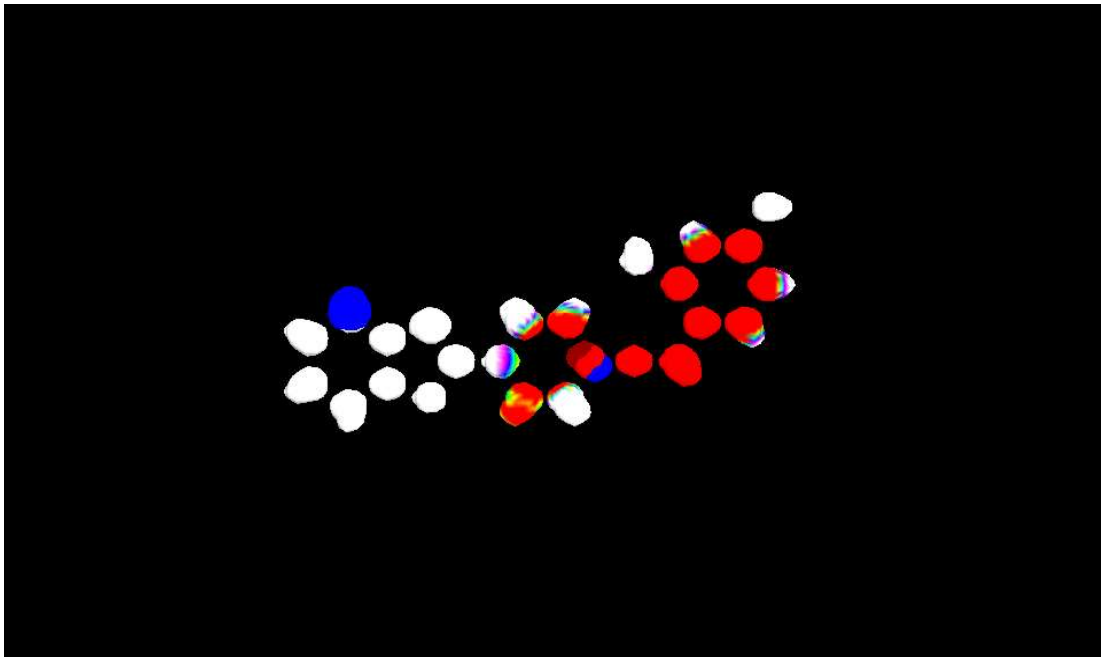

(C)

Fig. 5.17 (A) Predicted binding pose of compound **S05** at the ATP-binding site of EGFR (B) Hydrophobic surface regions of EGFR kinase domain. (C) Electrostatic potential regions over molecule **S05**, The coloring for regions is described as follows: red, negative electricity region; blue, positive electricity region; white, neutral region.

Table 5.8 Docking results based on hydrophobic interaction, hydrogen bonding interaction, docking energy/ score, inhibition constant, bond length and RMSD

Comp No.	Hydrophobic interaction (within 5 Å)	H-bond interaction	Docking energy/score [kcal/mol]	Inhibition constant [µM]	Bond length [A^0]	RMSD
S01	LYS745, ALA743, VAL726, PHE723, THR790, GLN791, MET793, ASP855, THR855, ARG841, LEU844.	O- of OCH3 group and H atom of amino acid backbone of MET-793	-9.17	1.44	1.75	0.83
S02	LYS745, VAL726, THR790, THR855, ARG841, LEU844, ASP 800, CYS797, MET766, LEU788, ILE789.	S- of benzothiazole and H atom of amino acid backbone of LYS-745	-9.45	22.44	2.61	0.39

		=N- of azomethine linkage and S atom of amino acid backbone of CYS-797			2.28	
S03	LYS745, ALA743, VAL726, PHE723, MET793, ASP855, THR855, ARG841, LEU788, CYS79, LYS797.	S- of benzothiazole and H atom of amino acid backbone of LYS-745	-6.98	12.29	2.75	0.68
S04	ALA743, VAL726, PHE723, MET793, ASP855, CYS797, ILE789, MET766, GLU762, LYS797, LEU792, ILE 744.	No H-bonds	-6.47	16.85	----	1.08
S05	LYS745, ALA743, VAL726, THR790, MET766, ASP855, ARG841, LEU788, ASP 800, CYS797, ILE789, ILE 744.	S- of benzothiazole and H atom of amino acid backbone of LYS-745	-9.85	36.75	2.79	0.89
		=N- of azomethine linkage and S atom of amino acid backbone of CYS-797			2.24	
S06	LYS745, ALA743, VAL726, PHE723, THR790, ASP855, ASP 800, CYS797, ILE789, MET766, GLU762, LYS797.	No H-bonds	-6.90	13.96	----	0.83
S07	LYS745, ALA743, VAL726, PHE723, GLN791, MET793, ASP855, LEU844, ASP 800, MET766, GLU762, LYS797.	S- of benzothiazole and H atom of amino acid backbone of LYS-745	-7.28	23.11	2.63	1.26

S08	LYS745, ALA743, THR790, GLN791, MET793, LEU844, ASP 800, CYS797, MET766, GLU762, LYS797, ILE 744.	S- of benzothiazole and H atom of amino acid backbone of LYS-745	-7.17	5.34	2.55	1.11
S09	LYS745, VAL726, PHE723, THR790, GLN791, ASP855, LEU844, LEU788, ASP 800, CYS797, LYS797, ILE744.	S- of benzothiazole and H atom of amino acid backbone of LYS-745	-6.13	19.89	2.67	0.76
S10	LYS745, ALA743, VAL726, PHE723, THR790, MET793, ASP855, LEU844, LEU788, ASP 800, CYS797, ILE789, MET766.	S- of benzothiazole and H atom of amino acid backbone of LYS-745	-6.65	28.74	2.60	0.66
S11	LYS745, ALA743, VAL726, PHE723, THR790, MET793, ASP855 LEU788, ASP 800, CYS797, LYS797, LEU792, ILE 744.	O- of nitro group and H atom of amino acid backbone of ASP-855	-9.32	58.74	1.09	0.58
		=N- of azomethine linkage and O- atom of amino acid backbone of ASP-855			1.72	
S12	LYS745, VAL726, THR790, THR855, ARG841, LEU844, ASP 800, CYS797, MET766, LEU788, ILE789, MET793.	S- of benzothiazole and H atom of amino acid backbone of LYS-745	-6.74	26.43	2.70	0.55
S13	LYS745, ALA743, VAL726, PHE723, THR790, MET793, ASP855, LEU844, LEU788, ASP 800, CYS797, ILE789, MET766, LEU792.	S- of benzothiazole and H atom of amino acid backbone of LYS-745	-8.94	67.14	2.42	0.94

		O- of OCH_3 group and H atom of amino acid backbone of MET-793			1.09	
S14	LYS745, ALA743, VAL726, PHE723, THR790, MET793, ASP855 LEU788, ASP 800, CYS797, LYS797, LEU792, ILE 744, LEU844.	=N- of azomethine linkage and O- atom of amino acid backbone of ASP-855	-6.82	41.69	1.89	1.05
S15	LYS745, ALA743, VAL726, THR790, MET793, ASP855, ARG841, LEU844, ASP 800, CYS797, GLU762, LEU792, ILE 744.	S- of benzothiazole and H atom of amino acid backbone of LYS-745	-7.08	96.74	2.44	0.99
S16	LYS745, ALA743, VAL726, PHE723, THR790, MET793, ARG841, CYS797, GLU762, LYS797, LEU792.	S- of benzothiazole and H atom of amino acid backbone of LYS-745	-6.78	24.96	2.63	0.78
S17	LYS745, ALA743, VAL726, PHE723, THR790, GLN791, MET793, ASP855, THR855, ARG841, LEU844, ILE 744.	No H-bonds	-6.41	13.96	----	0.71
S18	LYS745, ALA743, VAL726, MET793, ASP855, THR855, ARG841, LEU844, ASP 800, MET766, GLU762, LYS797.	S- of benzothiazole and H atom of amino acid backbone of LYS-745	-6.32	84.32	2.34	0.96
S19	LYS745, ALA743, VAL726, MET793, ASP855, THR855, LEU844, LEU788, ASP 800, CYS797, GLU762, LYS797.	S- of benzothiazole and H atom of amino acid backbone of LYS-745	-6.73	76.63	2.45	0.87

S20	LYS745, ALA743, VAL726, MET793, ASP855, THR855, ARG841, ASP 800, CYS797, GLU762, LYS797, ILE 744.	S- of benzothiazole and H atom of amino acid backbone of LYS-745	-6.96	79.12	2.77	0.99

5.1.5.5. Immunoblot analysis

The *in-silico* studies and anti-proliferative assay suggested that synthesized benzothiazole derivatives bind to EGFR-TK and showed significant cytotoxicity. Concomitantly, we carried out immunoblotting by using specific antibody of phosphorylated EGFR to unravel the mechanism of targeted inhibition. The synthesized Schiff base derivatives **S01-S20** were evaluated for their ability to inhibit the autophosphorylation of EGFR-TK. EGFR is a 170 kDa transmembrane glycoprotein, contains an external membrane binding and intracellular tyrosine kinase domain. Gefitinib was employed as the positive control which mimics the ATP competitive binding regions of EGFR tyrosine kinase. Densitometric analysis of the western blots was quantified in order to translate biochemical results into statistical values. Figure 5.18 shows the results of immunoblotting for phosphorylated EGFR after exposure to compounds **S11, S13, S02**, **S05** and gefitinib for 48 hours. Gefitinib completely inhibit phosphorylated EGFR (~100% inhibition) and exhibited lethal effects at a single dose (10 μM) against the EGFR expressing cell lines SKOV3, A2780-S and A2780-CR. The results are summarized in Table 5.9. It was observed that Schiff base-benzothiazole hybrid **S05** containing dihydroxy substituents showed fairly good inhibitory activity against EGFR-TK with percentage enzyme inhibition value of 69.71, 67.80 and 75.36 against SKOV3, A2780-S and A2780-CR respectively, as compared to that of gefitinib. Subsequently, SAR studies were performed by modification of the parent compound to determine how the different substituents of the subunits affect the EGFR inhibitory activity. The introduction of more electron releasing substituents in phenyl ring resulted in dramatic decrease in activity. For instance, compound **S13** bearing hydroxy and methoxy substituents, demonstrated only 10.52, 11.07 and 25.37 percentage EGFR inhibition against SKOV3, A2780-S and A2780-CR respectively, in comparison to gefitinib. Compound **S02** with electronegative group 'Cl' in phenyl ring demonstrated favorable inhibitory activity with 33.66 and 46.93 percentage EGFR inhibition against SKOV3 and A2780-S respectively. However, compound **S11** possessing electron withdrawing ($-NO_2$) group showed 40.63 and 12.48 percentage EGFR inhibition on SKOV3 and A2780-S

respectively. Overall, this indicated that less bulky electron releasing moiety suitably adapted the hydrophobic and hydrophilic pocket of EGFR kinase domain. Thus, four compounds **S02**, **S05**, **S11** and **S13** exhibited EGFR tyrosine kinase inhibition, while rest of the compounds of the S-series were not active to this target. In cisplatin resistant cells i.e. A2780-CR**,** phosphorylated EGFR expression was decreased significantly for compounds **S05** and **S13,** suggesting that the maximum inhibition of overexpression was in resistant cells. The high selectivity of compound **S05** towards EGFR tyrosine kinase might be attributed to difference in the geometry of the binding pocket of this enzyme which enables its fitting and interaction.

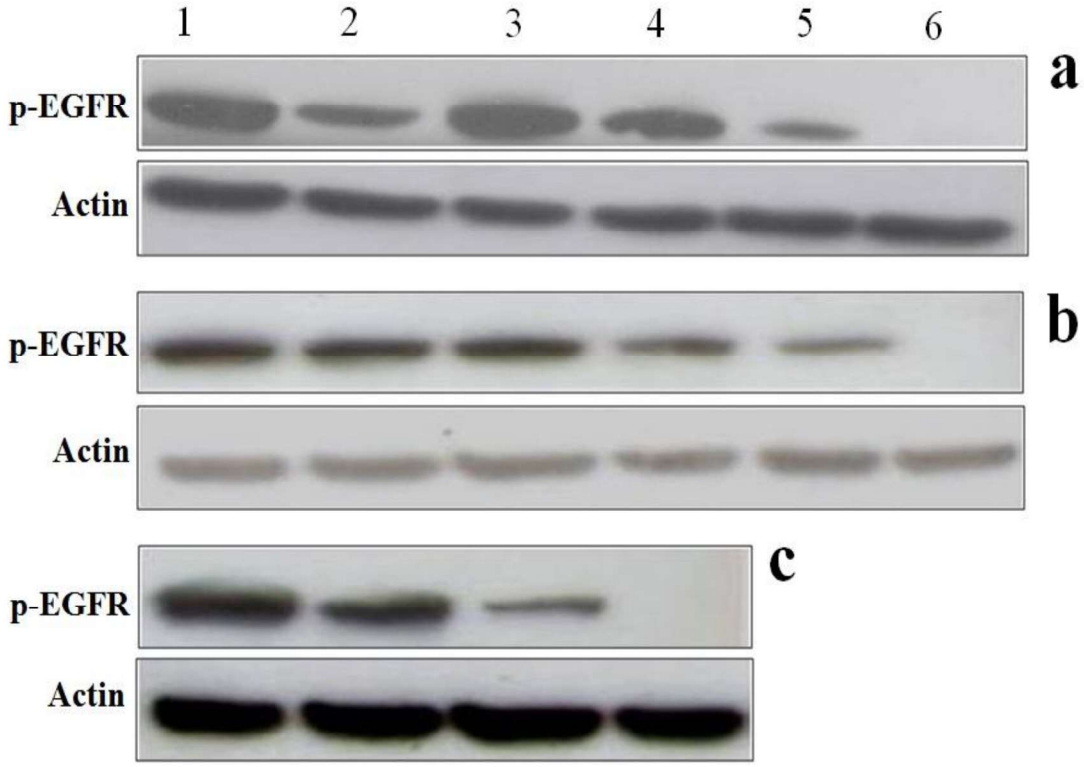

Fig. 5.18 Immunoblot analysis of the EGFR in ovarian cancer cell lines. The (a) SKOV3 and (b) A2780-S ovarian cancer cell lysates were prepared from cells treated for 48 hr without chemical treatment, Lane 1: phosphorylated EGFR and with chemical treatment, Lane 2: **S11**, Lane 3: **S13,** Lane 4: **S02**, Lane 5: **S05**, Lane 6: **Gefitinib**, in normal growth medium. The (c) A2780-CR ovarian cancer cell lysates was prepared from cells treated for 48 hr without chemical treatment, Lane 1: phosphorylated EGFR and with chemical treatment, Lane 2: **S13**, Lane 3: **S05**, Lane 4: Gefitinib, in normal growth medium. EGFR was immunoprecipitated and probed with antiphosphotyrosine antibodies, as described in Material and Methods. Another blot represents the Actin to ensure equal loading in all the cell lines described in the figure.

Table 5.9 Percentage EGFR-TK inhibitory activity of synthesized Schiff bases **(S01-S20)**

Compound code	% EGFR-TK Inhibition of SKOV3[a]	% EGFR-TK Inhibition of A2780-S[a]	% EGFR-TK Inhibition of A2780-CR[a]
S01	-	-	-
S02	33.66± 0.52	46.93± 0.12	-
S03	-	-	-
S04	-	-	-
S05	69.71± 0.07	67.80± 0.16	75.36± 0.15
S06	-	-	-
S07	-	-	-
S08	-	-	-
S09	-	-	-
S10	-	-	-
S11	40.63± 0.22	12.48± 0.68	-
S12	-	-	-
S13	10.52± 0.10	11.07± 0.17	25.37± 0.34
S14	-	-	-
S15	-	-	-
S16	-	-	-
S17	-	-	-
S18	-	-	-
S19	-	-	-
S20	-	-	-
Gefitinib	~100*	~100*	~100*

[a] The data were means from at least three independent experiments at a single dose of 100 μM.

[b] Gefitinib was used as a reference compound tested at 10 μM concentration.

*Absence of immunoblot in Lane 6 of SKOV3 and A2780 and in Lane 4 of A2780-CR, showed complete inhibition of EGFR phosphorylation.

5.2. SERIES-2: Amide derivatives of 2-(4-aminophenyl) benzothiazole i.e., Benzamide analogues

5.2.1. BACKGROUND

The growing prevalence of multidrug resistance to therapeutic antibiotics poses a challenge to the identification of novel targets and drugs for the treatment of infectious disease. Cancer is an enormous global health burden, touching every geographical regions and socioeconomic levels of people. Cervical cancer, one of the most common type in women worldwide. Human papillomavirus (HPV) represents a group of widely diversified viruses, detectable in nearly all types of cervical cancers. Two prophylactic HPV vaccines i.e., Gardasil and Cervarix are commercially available since 2006. Thus, the discovery and development of drugs, possessing least cytotoxicity and capable of effectively triggering apoptosis in tumour cells, have been receiving considerable attention.

Amides, RCONHR' moiety are known to play a pivotal role in selective binding with anion substrates such as DNA. Many investigations indicated that the presence of hydrogen bonding domain e.g., amide (–CONH) seems to be valuable in the structures of antimicrobials [Jagessar and Rampersaud, 2007]. Further, various amide derivatives of benzothiazole also possess potent anticancer properties [Kamal *et al.,* 2015]. These findings pave a way for research to be carried out in this area and prompted us to continue our investigation towards synthesis of amide bearing benzothiazole ring system. In this context, new series of N-(4-(benzo[d]thiazol-2-yl)phenyl)-substituted benzamides **(A01-10)** was synthesized and their biological activity was evaluated.

5.2.2. CHEMISTRY

The synthesis of compounds (**A01–A10**) outlined in two steps. Firstly, key intermediate from 2-amino thiophenol and para amino benzoic acid (PABA) was synthesized in a satisfactory yield. Then, to a solution of key intermediate i.e., 2-(4'-aminophenyl) benzothiazole in acetonotrile, different benzoic acid derivatives were added, together with double equivalent of N,N'-Dicyclohexylcarbodiimide (DCC). The reaction mixtures were refluxed with stirring for 4-10 h to obtain the desired compounds (**A01–A10**). All the IR, Mass, ^{1}H-NMR, ^{13}C-NMR spectral data of compounds (**A01–A10**) were in accordance with the proposed molecular structures. The purity of the synthesized compounds was monitored by TLC and ascertained by elemental analysis (Table 5.10).

The structure of amide derivatives of 2-(4'-aminophenyl) benzothiazole was confirmed by the comprehensive spectral data. The FT-IR spectra showed absorption bands at 3037 and

3109 cm^{-1} for aromatic C–H, and at range of 3309-3353 cm^{-1} for (–NH str). Formation of amide derivatives were confirmed by the presence of carbonyl stretching at 1627 and 1681 cm^{-1}, due to conversion of $–NH_2$ group to –CONH group. The ^1H NMR showed sharp singlet peak in the range of δ 9.13–9.58 ppm indicating the presence of amide proton (–CONH). The multiplet at δ 7.11–7.91 ppm was due to aromatic protons. The ^{13}C NMR spectra revealed all the corresponding peaks in the range of δ 162.12–164.18 ppm and δ 110.28–148.07 ppm which were due to –CONH carbon and aryl carbon respectively. Methoxy carbon of compound **A07** exhibited a peak at δ 58.11. Styrene moiety (–CH=CH) of compounds **A10** exhibited doublet of doublet at δ 6.72, 6.77.

5.2.3. PHYSICOCHEMICAL AND SPECTRAL CHARACTERIZATION DATA

Table 5.10 Physicochemical data of the benzothiazole amide derivatives **(A01-A10)**

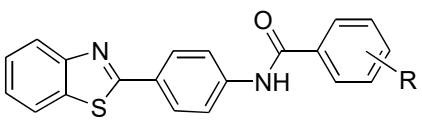

A01-09

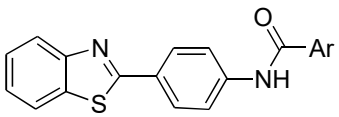

A10

Compound code	R, Ar	MW	Melting point (℃)	Yield (%)	R_f (solvent system)	Solubility
A01	H	330	126–128	91	0.71 (B)	$CHCl_3$, MeOH, EtAc
A02	3,5-di NO_2	420	122–124	90	0.59 (B)	$CHCl_3$, EtAc
A03	2-OH	346	132–134	94	0.76 (A)	$CHCl_3$, MeOH, EtAc
A04	3-NO_2	375	136–139	91	0.73 (B)	$CHCl_3$, MeOH
A05	2-Cl	364	136–139	92	0.62 (B)	$CHCl_3$, MeOH, EtAc
A06	2-F	348	140–143	90	0.69 (B)	$CHCl_3$, MeOH
A07	5-Cl, 2-OCH_3	378	150–143	96	0.71 (A)	$CHCl_3$
A08	2,4-diOH	362	150–143	96	0.60 (A)	$CHCl_3$, EtAc
A09	2-OCH_3	360	168–170	95	0.75 (A)	$CHCl_3$, MeOH, EtAc
A10		356	147–149	92	0.64 (B)	$CHCl_3$, MeOH, EtAc

Solvent system: (A) Methanol: Chloroform, 2:8, (B) Ethylacetate: Hexane, 7:3

Spectral data for benzothiazole amide derivatives

Compound A01: *N-(4-(benzo[d]thiazol-2-yl)phenyl)benzamides*

IR (KBr, υmax cm^{-1}): 3309.02 (–NH str.), 1668.12 (C=O str. of amide), 3048.14 (Ar–C–H str.)

^{1}H NMR ($CDCl_3$, 300 MHz) δ (ppm): 7.02–7.98 (m, 13H, Ar–H), 9.48 (s, 1H, –CONH)

^{13}C NMR (DMSO-d6) δ (ppm): 163.34 (C=O of amide), 155.09 (benzothiazole–C–2), 118.98–138.17 (Aromatic–C, C4–C9 C1'–C6' C1"–C6")

MS (m/z, %): 331 ($C_{20}H_{14}N_2OS$, $[M + H]^+$).

Anal $C_{20}H_{14}N_2OS$. Calc. for: C, 72.70; H, 4.27; N, 8.48. Found: C, 72.68; H, 4.25; N, 8.48%.

Compound A02: *N-(4-(benzo[d]thiazol-2-yl)phenyl)-3,5-dinitro-benzamides*

IR (KBr, υmax cm^{-1}): 3327.32 (–NH str.), 1627.92 (C=O str. of amide), 3066.92, 3109.35 (Ar–C–H str.) 1342.50 ($–NO_2$ str.)

^{1}H NMR ($CDCl_3$, 300 MHz) δ (ppm): 7.31–7.87 (m, 11H, Ar–H), 9.13 (s, 1H, –CONH)

^{13}C NMR (DMSO-d6) δ (ppm): 162.48 (C=O of amide), 156.42 (benzothiazole–C–2), 121.67–140.17 (Aromatic–C, C4–C9 C1'–C6' C1"–C6")

MS (m/z, %): 421 ($C_{20}H_{12}N_4O_5S$, $[M + H]^+$)

Anal $C_{20}H_{12}N_4O_5S$. Calc. for: C, 57.14; H, 2.88; N, 13.33. Found: C, 57.12; H, 2.85; N, 13.31%.

Compound A03: *N-(4-(benzo[d]thiazol-2-yl)phenyl)-2-hydroxy-benzamides*

IR (KBr, υmax cm^{-1}): 3312.68 (–NH str.), 1681.42 (C=O str. of amide), 3096.10 (Ar–C–H str.)

^{1}H NMR ($CDCl_3$, 300 MHz) δ (ppm): 7.18–7.79 (m, 12H, Ar–H), 9.32 (s, 1H, –CONH), 10.48 (br, s, 1H, –OH)

^{13}C NMR (DMSO-d6) δ (ppm): 163.90 (C=O of amide), 154.17 (benzothiazole–C–2), 110.28–135.46 (Aromatic–C, C4–C9 C1'–C6' C1"–C6")

MS (m/z, %): 347 ($C_{20}H_{14}N_2O_2S$, $[M + H]^+$)

Anal $C_{20}H_{14}N_2O_2S$. Calc. for: C, 69.35; H, 4.07; N, 8.09. Found: 69.33; H, 4.08; N, 8.10%.

Compound A04: *N-(4-(benzo[d]thiazol-2-yl)phenyl)-3-nitro-benzamides*

IR (KBr, υmax cm^{-1}): 3325.82 (–NH str.), 1648.12 (C=O str. of amide), 3037.77 (Ar–C–H str.) 1356.50 ($–NO_2$ str.)

^{1}H NMR ($CDCl_3$, 300 MHz) δ (ppm): 7.24–7.69 (m, 12H, Ar–H), 9.58 (s, 1H, –CONH)

^{13}C NMR (DMSO-d6) δ (ppm): 164.04 (C=O of amide), 157.23 (benzothiazole–C–2), 116.20–148.07 (Aromatic–C, C4–C9 C1'–C6' C1"–C6")

MS (m/z, %): 376 ($C_{20}H_{13}N_3O_3S$, $[M + H]^+$)

Anal $C_{20}H_{13}N_3O_3S$. Calc. for: C, 63.99; H, 3.49; N, 11.19. Found: 63.97; H, 3.47; N, 11.17%.

Compound A05: *N-(4-(benzo[d]thiazol-2-yl)phenyl)-2-chloro-benzamides*

IR (KBr, υmax cm^{-1}): 3333.10 (–NH str.), 1647.26 (C=O str. of amide), 3066.92 (Ar–C–H str.), 1070.63 (C–Cl str.)

^{1}H NMR ($CDCl_3$, 300 MHz) δ (ppm): 7.26–7.61 (m, 12H, Ar–H), 9.49 (s, 1H, –CONH)

^{13}C NMR (DMSO-d6) δ (ppm): 162.71 (C=O of amide), 156.57 (benzothiazole–C–2), 119.64–145.85 (Aromatic–C, C4–C9 C1'–C6' C1"–C6")

MS (m/z, %): 365 ($C_{20}H_{13}ClN_2OS$, $[M + H]^+$)

Anal $C_{20}H_{13}ClN_2OS$. Calc. for: C, 65.84; H, 3.59; N, 7.68. Found: C, 65.82; H, 3.60; N, 7.67%.

Compound A06: *N-(4-(benzo[d]thiazol-2-yl)phenyl)-2-fluro-benzamides*

IR (KBr, υmax cm^{-1}): 3309.96 (–NH str.), 1653.05 (C=O str. of amide), 3061.13 (Ar–C–H str.)

^{1}H NMR ($CDCl_3$, 300 MHz) δ (ppm): 7.08–7.42 (m, 12H, Ar–H), 9.18 (s, 1H, –CONH)

^{13}C NMR (DMSO-d6) δ (ppm): 162.88 (C=O of amide), 156.78 (benzothiazole–C–2), 115.83–143.86 (Aromatic–C, C4–C9 C1'–C6' C1"–C6")

MS (m/z, %): 349 ($C_{20}H_{13}FN_2OS$, $[M + H]^+$)

Anal $C_{20}H_{13}FN_2OS$. Calc. for: C, 68.95; H, 3.76; N, 8.04. Found: C, 68.93; H, 3.75; N, 8.05%.

Compound A07: *N-(4-(benzo[d]thiazol-2-yl)phenyl)-2-methoxy-5-chloro-benzamides*

IR (KBr, υmax cm^{-1}): 3319.60 (–NH str.), 1637.62 (C=O str. of amide), 3061.13 (Ar–C–H str.), 2852.81 (C–H str., OCH_3 group)

^{1}H NMR ($CDCl_3$, 300 MHz) δ (ppm): 7.11–7.78 (m, 11H, Ar–H), 9.39 (s, 1H, –CONH)

^{13}C NMR (DMSO-d6) δ (ppm): 162.49 (C=O of amide), 58.11 (OCH_3), 153.01 (benzothiazole–C–2), 122.36–136.75 (Aromatic–C, C4–C9 C1'–C6' C1"–C6")

MS (m/z, %): 379 ($C_{21}H_{15}ClN_2OS$, $[M + H]^+$).

Anal $C_{21}H_{15}ClN_2OS$. Calc. for: C, 66.57; H, 3.99; N, 7.39. Found: C, 66.54; H, 3.96; N, 7.37%.

Compound A08: *N-(4-(benzo[d]thiazol-2-yl)phenyl)-2,4-dihydroxy-benzamides*

IR (KBr, υmax cm^{-1}): 3353.18 (–NH str.), 1664.73 (C=O str. of amide), 3085.10 (Ar–C–H str.)

^1H NMR ($CDCl_3$, 300 MHz) δ (ppm): 7.22–7.86 (m, 11H, Ar–H), 9.56 (s, 1H, –CONH), 10.48, 9.86 (s, 2H, –OH)

^{13}C NMR (DMSO-d6) δ (ppm): 162.79 (C=O of amide), 155.44 (benzothiazole–C–2), 121.78–145.26 (Aromatic–C, C4–C9 C1'–C6' C1"–C6")

MS (m/z, %): 363 ($C_{20}H_{14}N_2O_3S$, $[M + H]^+$)

Anal $C_{20}H_{14}N_2O_3S$. Calc. for: C, 66.28; H, 3.89; N, 7.73. Found: C, 66.24; H, 3.86; N, 7.71%.

Compound A09: *N-(4-(benzo[d]thiazol-2-yl)phenyl)-2-methoxy-benzamides*

IR (KBr, υmax cm^{-1}): 3322.68 (–NH str.), 1647.23 (C=O str. of amide), 3054.13 (Ar–C–H str.), 2850.11 (C–H str., OCH_3 group)

^1H NMR ($CDCl_3$, 300 MHz) δ (ppm): 7.28–7.91 (m, 12H, Ar–H), 9.26 (s, 1H, –CONH)

^{13}C NMR (DMSO-d6) δ (ppm): 163.25 (C=O of amide), 56.15 (OCH_3), 156.23 (benzothiazole–C–2), 122.46–146.35 (Aromatic–C, C4–C9 C1'–C6' C1"–C6")

MS (m/z, %): 361 ($C_{21}H_{16}N_2O_2S$, $[M + H]^+$)

Anal $C_{21}H_{16}N_2O_2S$. Calc. for: C, 69.98; H, 4.47; N, 7.77. Found: C, 69.96; H, 4.46; N, 7.75%.

Compound A10: *N-(4-(benzo[d]thiazol-2-yl)phenyl)-styrene-amides*

IR (KBr, υmax cm^{-1}): 3317.40 (–NH str.), 1653.82 (C=O str. of amide), 3087.42 (Ar–C–H str.)

^1H NMR ($CDCl_3$, 300 MHz) δ (ppm): 7.26–7.71 (m, 14H, Ar–H), 9.58 (s, 1H, –CONH), 6.72, 6.77 (dd, –CH=CH)

^{13}C NMR (DMSO-d6) δ (ppm): 164.18 (C=O of amide), 156.30 (benzothiazole–C–2), 116.36–138.15 (Aromatic–C, C4–C9 C1'–C6' C1"–C6")

MS (m/z, %): 357 ($C_{22}H_{16}N_2OS$, $[M + H]^+$)

Anal $C_{22}H_{16}N_2OS$. Calc. for: C, 74.13; H, 4.52; N, 7.86. Found: C, 74.12; H, 4.50; N, 7.85%.

5.2.4. *IN-VITRO* ANTIMICROBIAL ACTIVITY

The antimicrobial results revealed that most of the compounds exhibited good to moderate antibacterial activity with MIC values ranging between 3.91 and 125 µg/mL. Out of the 10 benzothiazole derivatives, compound N-(4-(benzo[d]thiazol-2-yl)phenyl)-2-methoxy-5-chloro-benzamides (**A07)** which is carrying chloro and methoxy groups on aryl ring displayed broad-spectrum activity against all the tested bacterial strains with MIC values of 3.91–62.5 µg/mL. It also displayed the most potent activity with MIC values of 15.6, 7.81, 15.6, 3.91 µg/mL against *S. aureus*, *E. coli*, *S. typhi* and *K. pneumonia,* respectively which was comparable with penicillin and ciprofloxacin with corresponding MIC values of 3.12, 1.56, 1.56, 1.56 µg/mL and 6.25, 6.25, 6.25, 6.25 µg/mL, respectively. Compound N-(4-(benzo[d]thiazol-2-yl)phenyl)-styrene-amides (**A10)** appears to exhibit maximum antibacterial activity against *E. coli* and *P. aeruginosa* (zone of inhibition up to 16–19 mm at concentration of 15.6 µg/mL) while compounds **A01, A02, A03, A04, A05, A06, A08** and **A09** showed moderate activity against few bacterial strains. Among the potent compounds (**A07** and **A10**) against *S. aureus*, it can be clearly seen that the compound **A07** with optimum lipophilicity displayed higher activity. In addition, the above mentioned two derivatives were also found to contribute highest inhibition of *E. coli* at good MIC's. Some of synthesized benzamides inhibited the growth of fungi with good to excellent MIC values ranging between 3.91 and 15.6 µg/mL while rest of them showed moderate to good anti-fungal activity with MICs ranging 31.2 - 125 µg/mL. Compounds **A07** showed excellent activity at concentration of 3.91 and 7.81 µg/mL, against *C. tropicalis* and *C. albicans,* respectively. Compound **A10** exhibited good activity at 15.6 µg/mL against *C. albicans.* Compounds **A07** and **A10** exhibited the potent antibacterial and antifungal activity with MIC values of 3.91–31.25 µg/mL. The antibacterial and antifungal activity of benzothiazole amide derivatives are presented in Table 5.11 and 5.12, respectively.

Structure–activity relationship (SAR) studies were performed to determine how the substituents on the benzene ring affected the antimicrobial activity. Compounds **A02, A04, A05, A06** with electron withdrawing group (NO_2) and halogen substitutions (Cl, F) were found to be more active than the compounds with electron releasing (OH, OCH_3) groups **A03, A08, A09** against both the Gram positive and negative strains. In addition, compounds **A05** with chlorine and **A06** with fluorine on phenyl ring appeared with almost same potential inhibitory efficacy against *E. faecalis* and *E. coli* at 31.2 µg/mL of MIC.

Hence, it can be inferred that chloro, fluoro and methoxy substituents bearing derivatives are the most suitable compounds for achieving the best antimicrobial spectrum. The

results may be explained by electron density of the compounds. It has been reported that electron-donating groups increase the electron density which makes the compounds effective against microorganisms and enhances the antibacterial activity [Kumar *et al.,* 2009b]. However, high electron density causes more difficult diffusion through the bacteria cell and substantial activity loss may occur [Hania *et al.,* 2009]. Thus, for a compound an optimum electron density is inevitable to gain significant antimicrobial activity. Hence, the combined electron donating ability of chloro and methoxy groups contributes to the activity of compound **A07** and aryl group bearing compound **A10** reaches an optimum electron density which is important for its significant antimicrobial activity.

Table 5.11 Antibacterial activity (MIC µg/mL) of the benzothiazole amide derivatives (**A01-A10**)

Compound code	Bacteria					
	Gram positive bacteria		Gram negative bacteria			
	S. aureus **(ATCC 25323)**	***E. faecalis*** **(Clinical isolate)**	***E. coli*** **(ATCC 35218)**	***S. typhi*** **(MTCC 3216)**	***K. pneumonia*** **(ATCC 31488)**	***P. aeruginosa*** **(ATCC 27893)**
A01	12-14(62.5)	11-13(62.5)	-	-	10-12(62.5)	-
A02	11-14(62.5)	12-15(31.2)	11-13(62.5)	-	10-13(62.5)	-
A03	<10(125)	-	<10(125)	-	<10(125)	-
A04	11-13(62.5)	-	12-13(62.5)	12-15(31.2)	-	-
A05	-	12-15(31.2)	14-16(31.2)	-	-	-
A06	-	13-15(31.2)	13-15(31.2)	-	-	-
A07	17-19(15.6)	12-15(31.2)	24-25(7.81)	16-18(15.6)	28-31(3.91)	10-12(62.5)
A08	10-13(62.5)	-	11-13(62.5)	<10(125)	<10(125)	-
A09	<10(125)	11-13(62.5)	10-13(62.5)	-	-	-
A10	14-17(31.2)	-	16-19(15.6)	13-15(31.2)	13-15(31.2)	16-19(15.6)
Penicillin	33-35(3.12)	33-35(3.12)	36-40(1.56)	36-40(1.56)	36-40(1.56)	36-40(1.56)
CIP	30-32(6.25)	28-30(6.25)	33-35(6.25)	34-35(6.25)	29-30(6.25)	33-35(3.12)

Table 5.12 Antifungal activity (MIC µg/mL) of the benzothiazole amide derivatives (**A01-A10**).

Compound code	*C. albicans* (ATCC 90028)	*C. tropicalis* (ATCC 750)	*C. krusei* (ATCC 6268)
A01	11-14(62.5)	10-12(62.5)	-
A02	-	10-12(62.5)	13-15(31.2)
A03	16-19(15.6)	12-15(31.2)	-
A04	<10(125)	12-15(31.2)	16-19(15.6)
A05	16-19(15.6)	-	-
A06	-	12-15(31.2)	12-15(31.2)
A07	24-25(7.81)	28-31(3.91)	-
A08	12-16(31.2)	-	10-13(62.5)
A09	10-14(62.5)	-	-
A10	16-18(15.6)	-	<10(125)
Fluconazole	22-25(6.25)	24-27 (6.25)	20-24 (6.25)

The value of each compound consisted of 'zone of inhibition range (MIC)' of 03 replicates. Level of significance $p < 0.05$

5.2.4.1. Mechanism of action study

Bactericidal kinetics

The bactericidal activity of designed compounds was determined at regular time intervals so as to evaluate the potential killing effects of bacterial cells within minutes at concentrations higher than MIC. In order to monitor the rapidity of mode of action of designed compounds, we incubated compounds **A07** and **A10** with log-phase. Gram positive *S. aureus* and Gram negative *E. coli* at 37 °C and monitored the course of change in optical density (OD_{600}) at different time intervals. The results showed a significant reduction in numbers of gram positive and negative bacteria (90 to 99%) within the first hour after addition of the compound **A07** at 4 × MIC (Fig. 5.19). Compound **A10** was found to be less effective as compared to compound **A07** in *E. coli* and *S. aureus* even up to 5 h. At 4 × MIC both compounds inhibited bacterial growth from 2 h onwards keeping

growth arrested till 5 h. However, complete eradication of bacterial growth by any of the tested compounds was not observed up to 5 h. At 4 × MIC compound **A07** exhibited the most potent inhibition of growth compared to compound **A10** in both the strains. Thus the designed compounds are capable of inhibiting bacterial growth within hours of initial interactions.

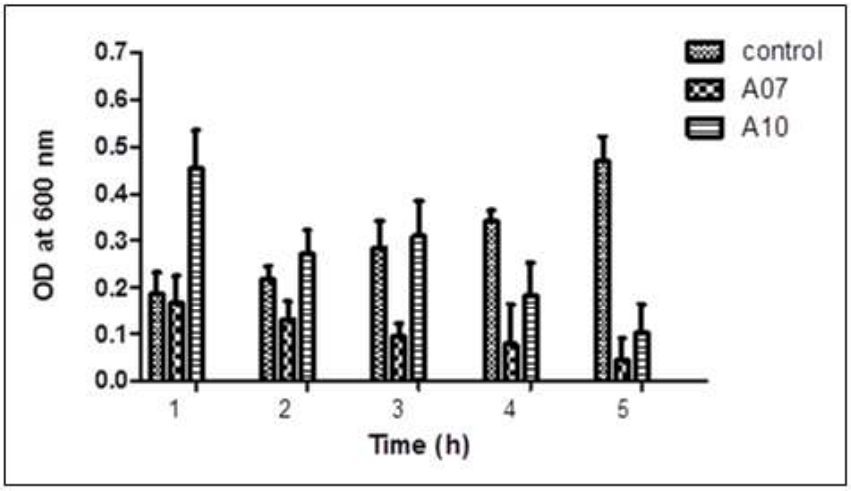

(A)

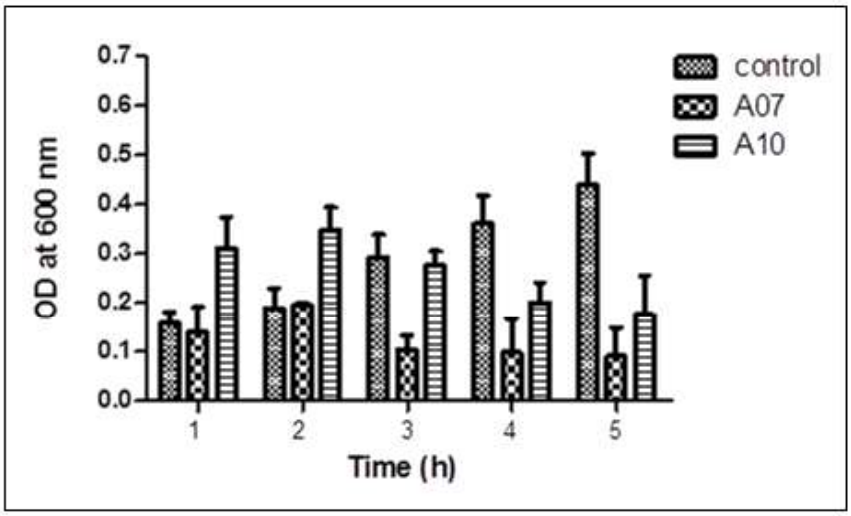

(B)

Fig. 5.19 Time dependent killing of (A) *S. aureus* (B) *E.coli* upon treatment with compounds **A07** and **A10** at 4 × MIC.

Cytoplasmic Membrane depolarization assay

To study the mode of action of designed analogs, the assay for depolarization of the cytoplasmic membrane was done with both Gram-positive (*S.aureus*) and Gram-negative (*E.coli*) bacteria. A family of fluorescent cyanine dyes has been developed that can be used to monitor membrane depolarization [Sun *et al.,* 2012]. These dyes lose fluorescence intensity in polarized membranes and become highly fluorescent once polarization is lost. Therefore, the effects of the designed analogs on the membrane of respective strains by using DiSC3(5) dye was determined. In this experiment, if the analogs alter the membrane potential as a result of pore formation/membrane destabilization, an increase in fluorescence intensity is observed. Figure 5.20 shows membrane depolarization, by an increase in fluorescence units, as a function of time. An increase of approximately 150 fluorescence unit was observed using triton 2% as a positive control. Compounds **A07** and **A10** showed similar profile with respect to positive control. At the highest concentration of designed analogs **A07** and **A10** tested (i.e., 4 x MIC), the level of depolarization appeared to reach a maximum at times from about 2 min to 5 min. All of the designed analogs studied here had the ability to depolarize the cytoplasmic membrane of *S.aureus* and *E.coli*; however, compounds with different structures had different concentration-activity profiles (data not shown here). Comparisons were made between the maximum levels of depolarization indicated by the fluorophore to levels of depolarization reached at various time points and concentrations of designed analogs. Compounds **A07** and **A10** completely depolarized the membrane at lower concentrations than those of the other compounds studied.

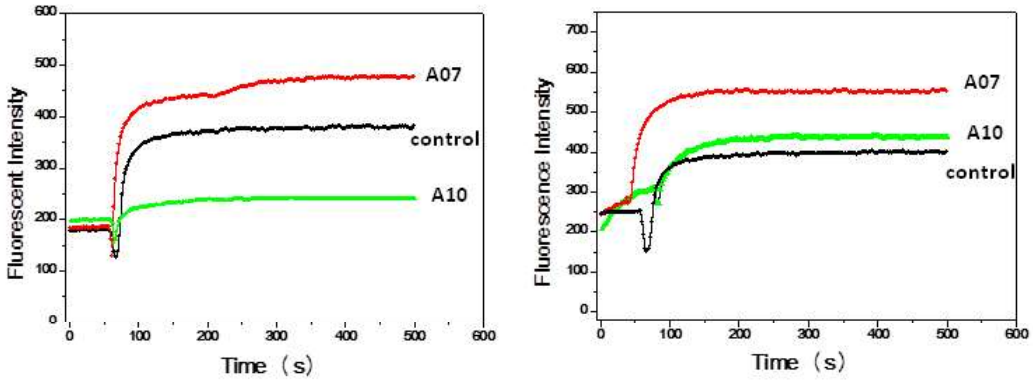

(A) (B)

Fig. 5.20 Membrane depolarization ability of designed compounds on (A) *E.coli* and (B) *S.aureus* treated with 4xMIC concentration of compounds **A07** and **A10**.

Flow Cytometry analysis

The change in membrane potential may leads to rupture of bacterial cells. So to further explore the permeabilization of the cytoplasmic membrane responsible for cell killing, we monitored cell viability via FACS (fluorescence assisted cell cytometer) analysis by quantifying the amount of DNA released using propidium iodide (PI) as DNA probe. Similar to the fluorometric analysis, flow cytometric assays were performed concurrently with cell viability measurements. Consistent with the permeabilization of bacteria, designed analogs **A07** and **A10** induced damages to the membrane organization of *S. aureus* but induced significantly lesser damage to the membrane organization of *E. coli* as indicated by PI staining of the cells following the treatments of these compounds (Fig. 5.21). However, the number of PI-stained cells in both strains decreased significantly in **A10** analogs. Overall this suggests that the mode of action of designed analogs **A07** and **A10** and related compounds might result from disruption of the membrane potential that is utilized for cellular energy production. However, this is unlikely to be the sole mechanism, since compound **A10** was slightly less active than **A07**. The results further indicated that the ability of **A10** analog to damage the organization of both bacterial cell membranes decreased appreciably due its aryl-substitution. Thus the results showed that the **A10** analog exhibited contrasting lytic activity towards the bacterial cells.

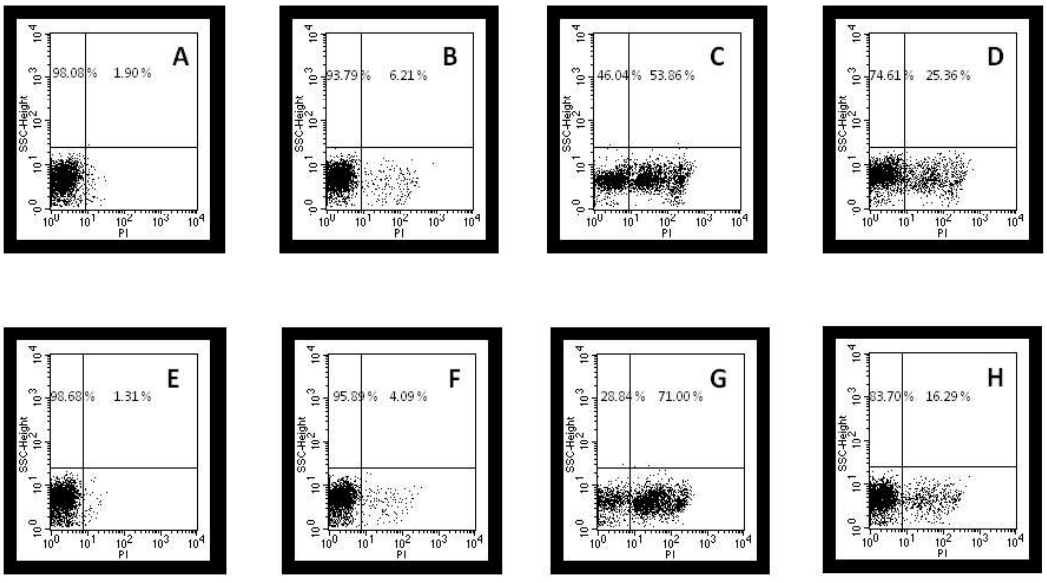

Fig. 5.21 Determination of compound-induced membrane damage of *E. coli* and *S.aureus* cells by flow cytometric studies. (A–H) PI staining of *E. coli* (A) control without PI treatment (B) control with PI treatment (C) **A07** (D) **A10** and on *S.aureus* (E) control without PI treatment (F) control with PI treatment (G) **A07** (H) **A10** respectively.

DNA binding

Compound **A07** showed excellent binding with DNA (200 ng) causing retardation at 31.2 µg/mL whereas for **A10** no retardation was observed at all the concentrations (Fig. 5.22). However it was intriguing that DNA binding was influenced by overall structure of the compounds as chloro and methoxy containing compound **A07** showed the most potent DNA retardation ability as compared to styrene analog **A10**.

Regardless to the actual mechanism of staining, the MG/DAPI technique is of great value to both research cytogenetics and clinical investigators in the identification of major and minor groove regions of DNA. To probe the interacting site of **A07** with pUC19, the plasmid DNA was treated with DAPI or MG (methyl green) [Tabassum *et al.,* 2011] prior to the addition of **A07**. DAPI (minor groove binder) was added to the reaction mixture, no significant inhibition was observed in the cleavage pattern. Whereas in presence of methyl green (major groove binder), the cleavage pattern was also not affected (Fig. 5.23). The electrophoretic pattern demonstrates that compound **A07** shows non-specific affinity towards both the major and the minor grooves, and this is only possible if the compound extend through the DNA double helix, as seen from an intercalation binding mode. Thus, in the present study upon comparing DNA binding and antimicrobial potency (compound **A10** showed no DNA binding though was equipotent as **A07**) it was evident that there were no direct correlations between DNA retardation and antimicrobial mode of action.

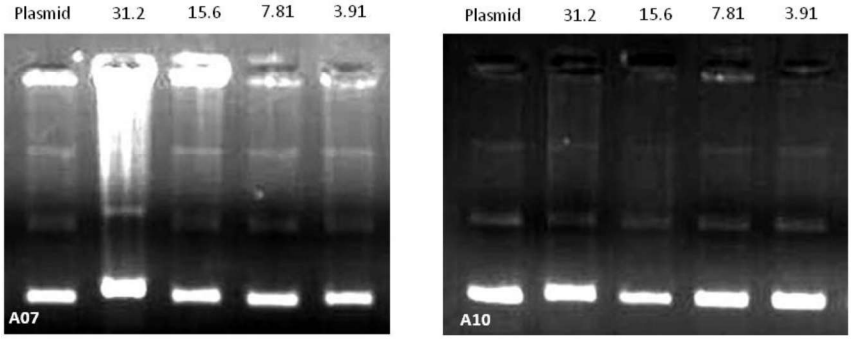

(A) (B)

Fig. 5.22. Agarose gel electrophoresis patterns of pUC19 (200 ng) cleaved by (A) **A07** (31.2–3.91 µg/mL), after 1 h incubation time (concentration dependent) Lane 1: control; Lane 2: 31.2 µg/mL **A07** + DNA; Lane 3: 15.6 µg/mL **A07** + DNA; Lane 4: 7.81 µg/mL **A07** + DNA; Lane 5: 3.91 µg/mL **A07** + DNA, and (B) **A10** (31.2–3.91 µg/mL), after 1 h incubation time (concentration dependent) Lane 1: control; Lane 2: 31.2 µg/mL **A10** + DNA; Lane 3: 15.6 µg/mL **A10** + DNA; Lane 4: 7.81 µg/mL **A10** + DNA; Lane 5: 3.91 µg/mL **A10** + DNA, in buffer (5 mM Tris–HCl/50 mM NaCl, pH 7.2 at 25 °C).

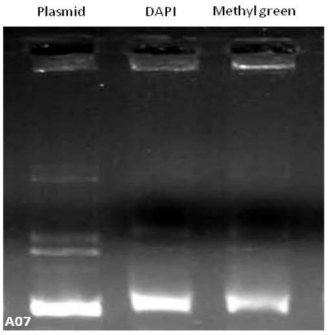

Fig. 5.23 Agarose gel electrophoresis pattern for the cleavage of supercoiled DNA (200 ng) by **A07** in presence of DAPI and methyl green.

5.2.4.2. Docking study against Glc-6-PS

The active site of glucosamine-6-phosphate synthase (GlcN-6-P synthase) was used to study the molecular basis of interaction and affinity of binding of the synthesized benzothiazole amide derivatives using the Surflex dock program incorporated in Sybyl-X1.2. All the molecules showed very good binding energy ranging from 4-6 dock score which was comparable with the standard drugs used. Compounds **A02, A04, A07** and **A10** showed good docking score with receptor as shown in Table 5.13. Compound **A10** was found to have a score of 6.12 forming a strong H-bond with Ala602. The ligand receptor interactions of compound **A10** is shown in Fig. 5.24. From the results, it was evident that the *in-silico* findings were in accordance with *in-vitro* antimicrobial assay.

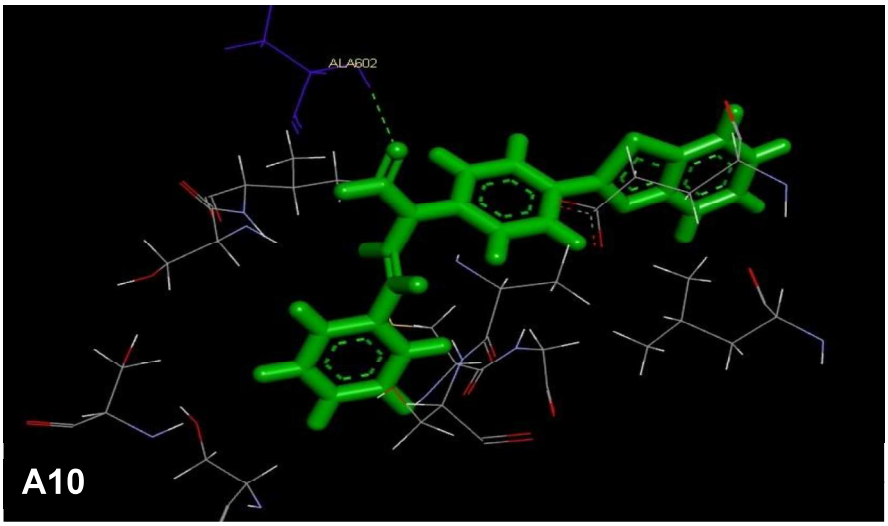

Fig. 5.24 Binding pose of compound **A10** with glucosamine-6-phosphate synthase. Hydrogen bonding interactions are displayed by green dotted lines.

Table 5.13 Molecular docking scores of Benzothiazole amide derivatives with GlcN-6-P synthase.

Sr. No	Compound code	Docking Score	Crash Value	Interacting amino acids
1	A01	4.2152	-0.6812	Ser604
2	A02	5.7655	-2.0208	Thr355, Cys300, Thr302, Ser303, Gln348, Ser349, Thr352
3	A03	4.6833	-0.7397	Val399,Ala602,Ser604
4	A04	5.5733	-1.3145	GLn348, Ser349, Ser604
5	A05	4.5162	-0.7286	Thr352,Ser604
6	A06	4.11	-1.1887	ser303
7	A07	5.7744	-1.2065	Val399,Ala602, Thr302, Ser401
8	A08	5.1596	-0.6388	Val399, Gln348, Ser349, Ser604
9	A09	4.8254	-0.7711	Ser604
10	A10	6.1268	-1.5639	Ala602
11	Ciprofloxacin	6.0614	2.0428	Ser347, Gln348, Ser349, Ser401, Lys485
12	Fluconazole	6.4092	-1.4344	Val399, Gln348, Ser349, Lys485, Ser604

5.2.4.3. *In-Silico* Pharmacokinetic Predictions

In-silico pharmacokinetic properties prediction is one of the important areas in drug discovery process. Compounds **A02, A04, A07, A08 and A10** with significant antimicrobial activity and good docking score were checked for their ADME properties by using preADMET server to predict the *in-silico* pharmacokinetic properties. The predicted drug likelinesss of the synthesized compounds follows the Lipinski''Rule of Five''. The results are summarized in Table 5.14.

Table 5.14. Theoretical prediction of different properties of Benzothiazole amide derivatives using PreADMET Server

Comp code	Log p	$LogS_b$ (mg/L)	HIA (%)	HB-donors	HB-acceptors	*In-vitro* PPB (%)
A02	4.9	100.01	99.80	0	5	90.12
A04	4.1	18.62	94.11	0	4	95.24
A07	3.9	71.16	92.90	0	4	99.15
A08	3.5	25.12	87.36	2	3	97.53
A10	2.8	34.18	85.19	0	3	89.92

5.2.5. *IN-VITRO* ANTICANCER ACTIVITY

The benzothiazole bearing amide moiety (**A01-A10**) were evaluated for cytotoxic effects against two human cervical cancer cell lines (SiHa and C33-A). For each compound, cell viability curves for individual cell lines have been measured at a minimum of five concentrations. The 3-(4,5-dimethylthiazol-2-yl)-2,5-diphenyltetrazolium bromide (MTT) assay protocol of 48 h continuous drug exposure has been used, to estimate cell viability or growth. A total of ten benzothiazole derivatives (A01-A10) exhibited variable degrees of growth inhibitory activity towards both the cell lines studied, with IC_{50} values ranging between 5-50 μM. The 50% minimum inhibitory concentrations (IC_{50}) are summarized in Table 5.15.

5.2.5.1. Cytotoxicity study against cervical cancer cell lines

The data of cytotoxicity assay against cervical cancer cell lines revealed the compound **A07** with methoxy and chloro substitution on the second and fifth position of the aryl ring respectively, showed selective and potent growth inhibition against SiHa cells (IC_{50} = 6.13 μM) but exhibited moderate cytotoxicity on C33-A cells (IC_{50} = 34.28 μM). The other lead compounds, **A01, A03** and **A08**, displayed good inhibitory activity (IC_{50} less than 20 μM) on the SiHa cells and modest inhibitory activity (IC_{50} less than 40 μM) on the C33-A cells as compared to standard drug cisplatin (Fig. 5.25). Cisplatin showed an IC_{50} of 15.01 μM and 20.10 μM in SiHa and C33-A cells, respectively [Das *et al.,* 2015]. The remaining compounds have also shown significant anticancer activity in the micromolar range against both the cell lines tested. Interestingly, we observe that the entire amide derivatives demonstrated comparatively good activity on SiHa cells than the C33-A cells (Fig. 5.26). The results suggest that our designed compounds are significantly more effective on HPV-positive cells (SiHa) in comparison to HPV-negative cells (C33-A) - a key remarkable feature of this study. Further, exposure to the compounds was associated with cell shrinkage, membrane blebbing, chromatin condensation, apoptotic nuclei and DNA fragmentation as detected in inverted micrographs (Figs. 5.27 and 5.28).

On the basis of cytotoxicity screening, the preliminary structure activity relationship study suggested that compounds with electron donating groups on phenyl ring were generally more potent than compounds having phenyl ring with electron withdrawing substituents. The pharmacological data indicated that 2-methoxy-5-chloro phenyl analogue (**A07**) showed approximate 5–6 fold improvement in cytotoxicity against the SiHa cell line (IC_{50} 6.14 μM) compared with phenyl analogue having electron withdrawing nitro group at 3,5-position (**A02**, IC_{50} 35.74 μM). However, inspection of cytotoxicity data of compounds

A03 and **A08** showed that conversion of 2-hydroxyl group (**A03**, IC_{50} 18.61 μM, SiHa; IC_{50} 34.86 μM, C33-A) to 2,4-dihydroxyl group of phenyl ring (**A08**, IC_{50} 18.38 μM, SiHa; IC_{50} 39.01μM, C33-A) retained the activity. In nitro-substituted analogues, presence of electron withdrawing group on the 3rd and 5th position (**A02**, IC_{50} 35.74 μM, SiHa; IC_{50} 36.22 μM, C33-A) led to decreased activity as compared to nitro group at 3rd position (**A04**, IC_{50} 21.02 μM, SiHa; IC_{50} 26.18 μM, C33-A) in both cell lines. The cytotoxic activity further gets reduced by the replacement of phenyl ring with styrene ring (**A10**, IC_{50} 27.41μM, SiHa; IC_{50} 28.68μM, C33-A).

Table 5.15 IC_{50} (μM) of compounds A01–A10 in SiHa and C33-A cell lines

Compound Name	SiHa***	C-33A***
A01	17.26±0.02	25.92±0.02
A02	35.74±0.02	36.22±0.01
A03	18.61±0.02	34.86±0.02
A04	21.02±0.03	26.18±0.03
A05	38.44±0.02	47.25±0.02
A06	22.5±0.05	23.14±0.02
A07	6.13±0.01	34.28±0.01
A08	18.38±0.02	39.01±0.02
A09	26.59±0.02	46.74±0.01
A10	27.41±0.02	28.68±0.01
Cisplatin	15.01±0.02	20.10±0.01

*** All the means are significantly different at $P < 0.001$. Activity results are represented as IC_{50}±SEM.

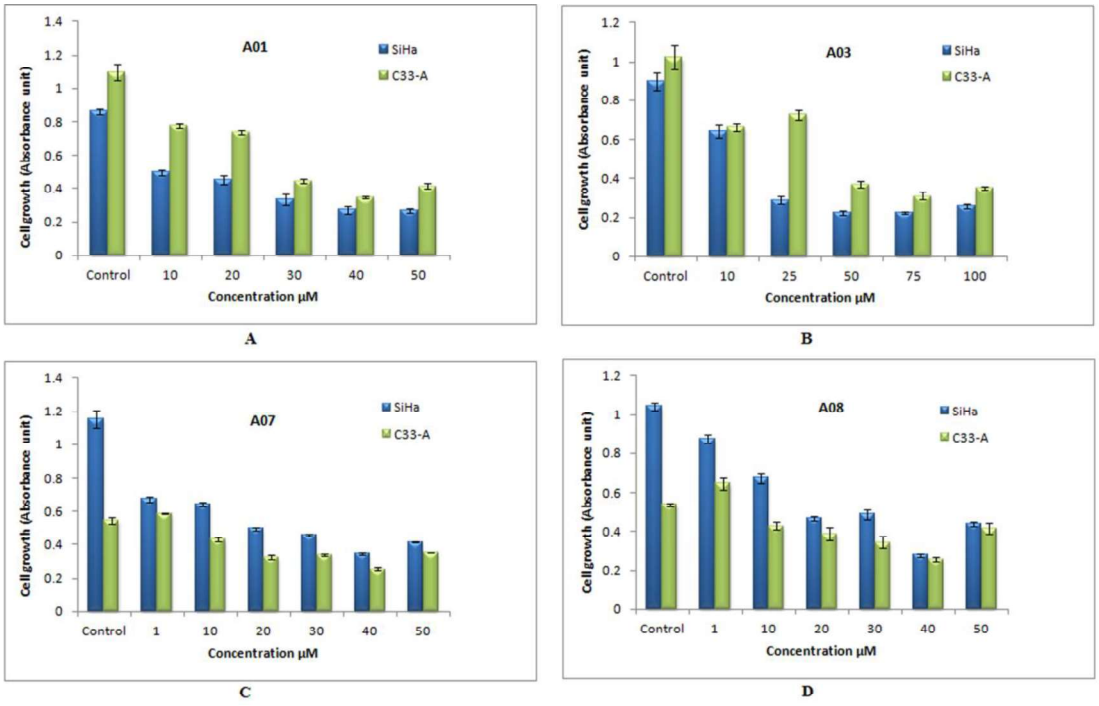

Fig. 5.25 Effect of the lead compounds (A) **A01** (B) **A03** (C) **A07** and (D) **A08** on SiHa and C33-A cell growth. Results are represented as mean±SEM of three assays.

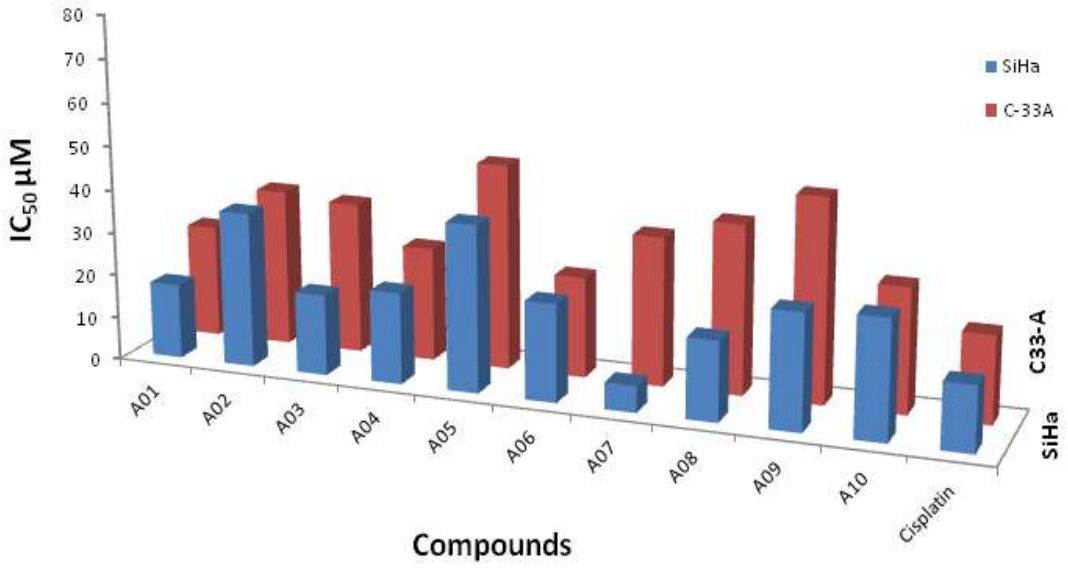

Fig. 5.26 Comparative IC_{50} values of compounds **A01-A10** against SiHa and C33-A cell lines

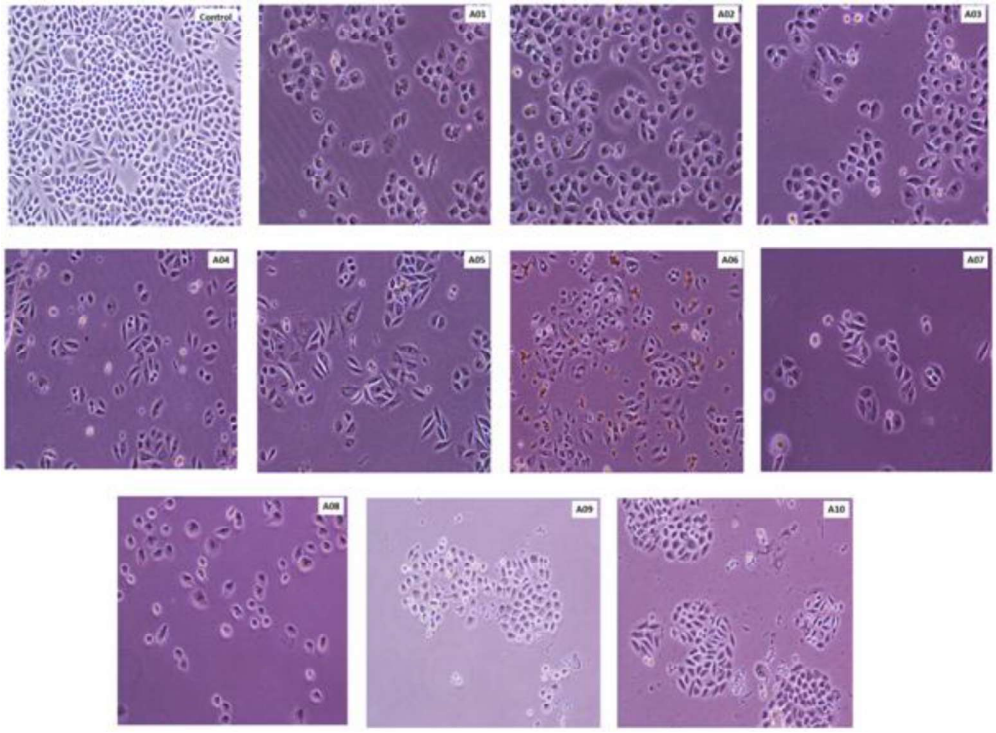

Fig. 5.27 Micrographs of the control and compounds (**A01-A10**) treated SiHa cells. Cells were treated with their respective IC_{50} of the compounds for 48 h. Typical results from three independent experiments are shown.

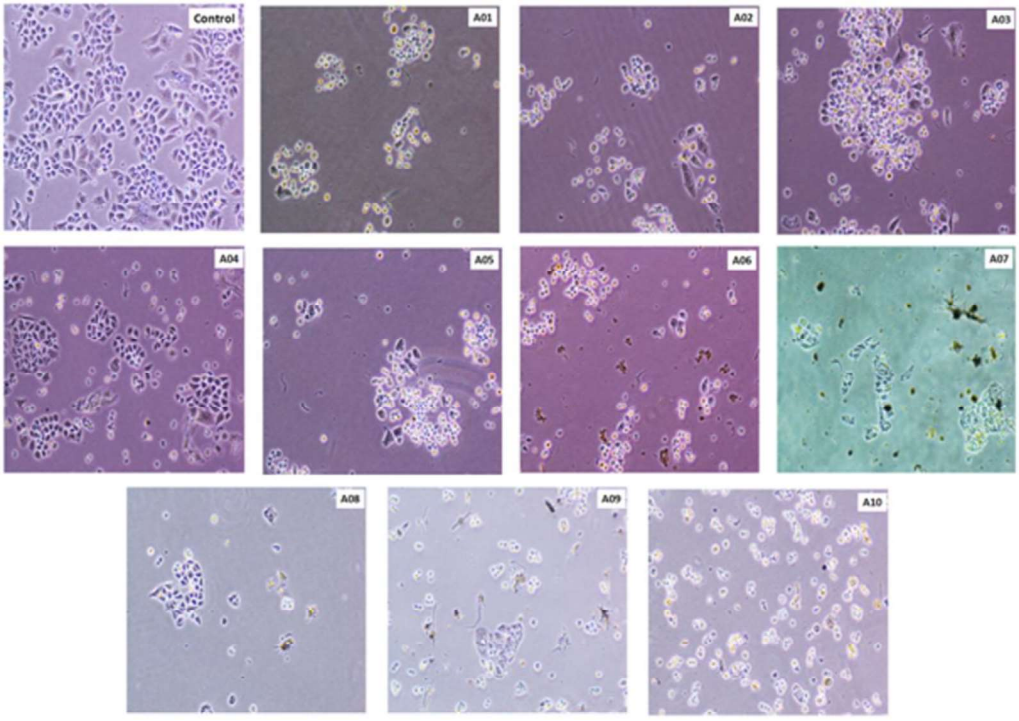

Fig. 5.28 Micrographs of the control and compounds (**A01-A10**) treated C33-A cells. Cells were treated with their respective IC_{50} of the compounds for 48 h. Typical results from three independent experiments are shown.

5.2.5.2. Cytotoxicity assessment on the basis of selectivity index

The major challenging aspect of synthesizing new chemotherapeutic agents is selectivity towards cancerous cells compared to the normal cells. Therefore, we have studied the cytotoxic efficacy of some of the potent compounds **A01, A03, A07** and **A08** on HEK-293, a normal epithelial cell line. The above compounds showed only 25–30% cell death in the HEK-293 cell line (Fig. 5.29), thus are selective toward cancerous cells with high margin of safety.

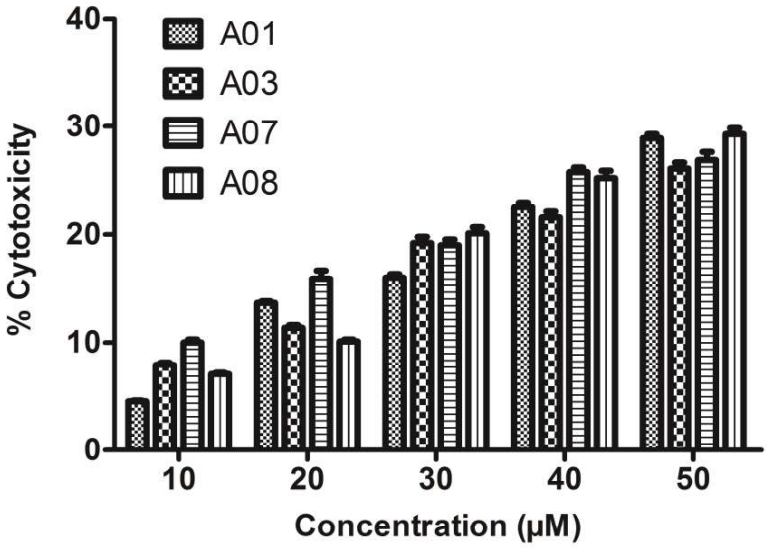

Fig. 5.29 Percentage cytotoxicity of HEK-293, a normal epithelial cell line at various concentrations (10–50 µM) of compounds **A01, A03, A07** and **A08**.

5.2.5.3 Cell cycle study

One of the most common mechanisms in anticancer drug treatment is cell cycle arrest, which can be measured by DNA content. The two set of chromosomes, 2N DNA present in the G0 and G1 phases of each cell cycle, replicates in the S-phase and are represented by 4N DNA in the G2 and M phases in the cell cycle. The anticancer activity data has revealed that the compounds **A01, A03, A07** and **A08** exhibit pronounced and efficient cytotoxicity against both cancer cell lines, specifically compound **A07** was found to be highly effective in causing cytotoxicity in SiHa cells. These results prompted us to investigate the effect of these compounds on cell cycle progression against both human cervical cancer cell lines SiHa and C33-A.

A significant accumulation of SiHa population in the sub-G1 phase of the cell cycle was observed which indicated that the cells have undergone programmed cell death (apoptosis)

for all of the compounds **A01-A10**, tested at their IC_{50} concentrations (Fig. 5.30). However, maximum increase in the percentage of cells in the sub-G1 phase was seen in compounds **A05, A06, A08, A09** and **A10.** Compound **A09** was found to be the most effective with respect to sub-G1 cell cycle arrest. Furthermore, in C33-A we noted that all the compounds **A01-A10** tested at their IC_{50} concentrations caused S-phase arrest except compound **A09** which showed G2/M cell cycle arrest and compounds **A07** and **A10** exhibited apoptosis as evidenced by increase in sub G1 population (Fig. 5.31). The different phases of cell cycle of lead compounds **A01, A03, A07** and **A08** were analyzed and the percentage of sub G1, G1, S, G2/M phase cells were presented graphically in Fig. 5.31 for both the cell lines.

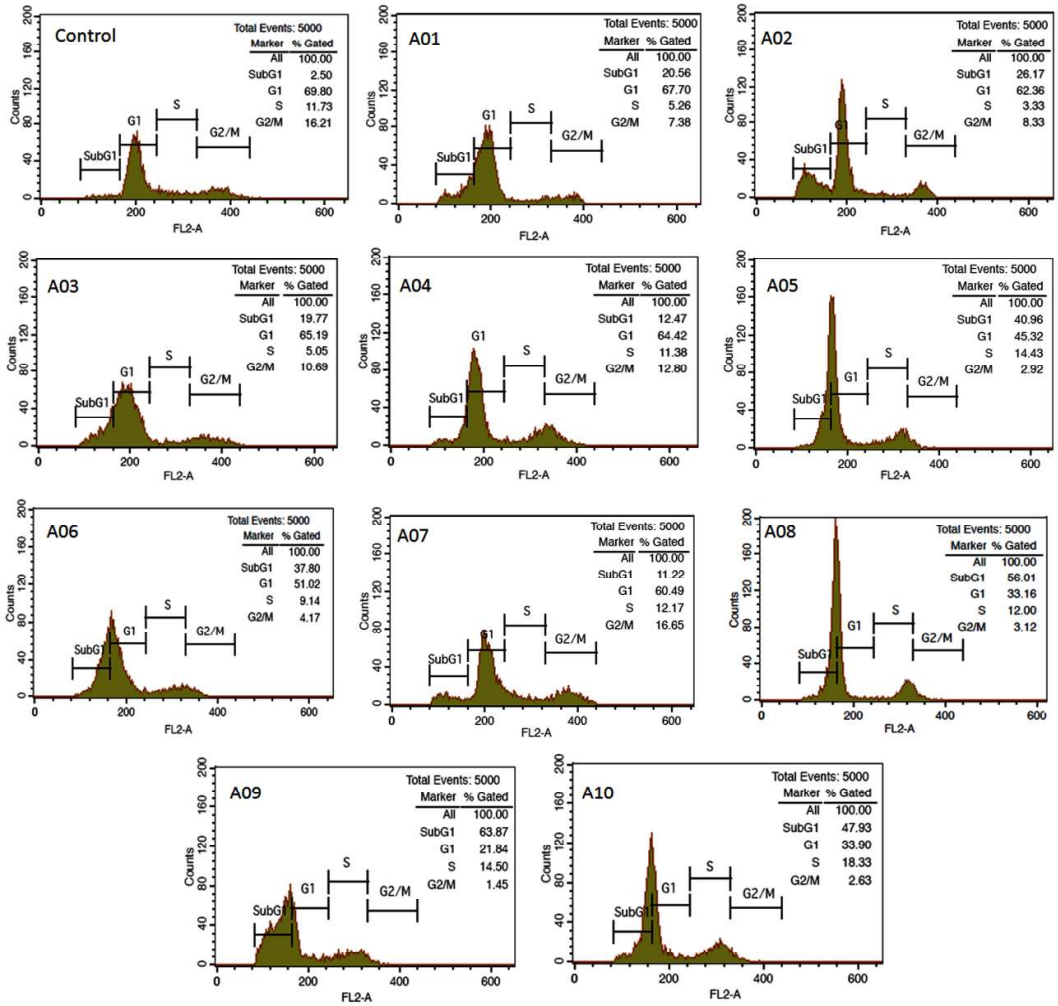

Fig. 5.30 Flow cytometric analysis of the effect of the compounds **A01-A10** on the cellular DNA content of SiHa cells. Cells were grown in the absence (control) or presence of the compounds at their respective IC_{50} for 48 h, stained with propidium iodide, and analyzed by flow cytometry for DNA content.

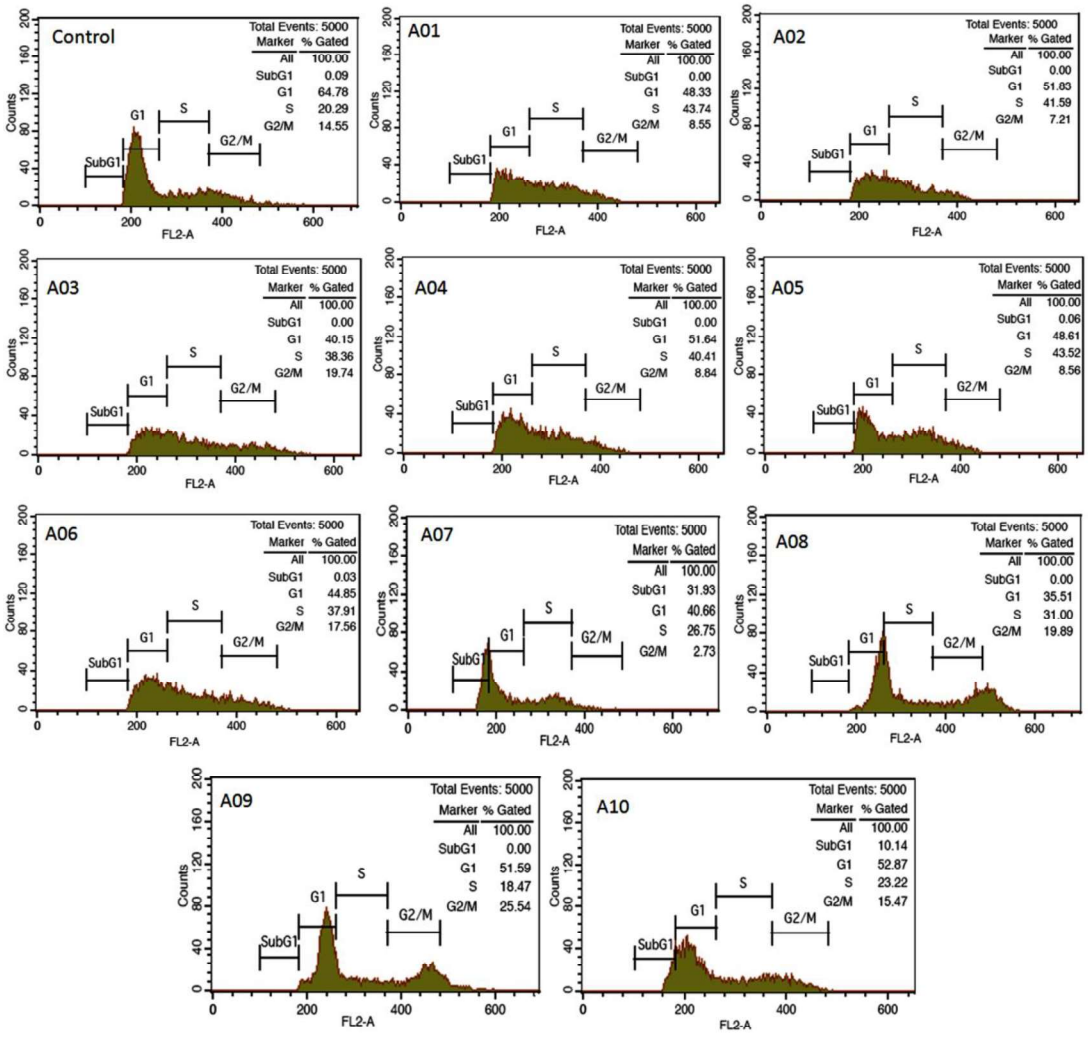

Fig. 5.31 Flow cytometric analysis of the effect of the compounds **A01-A10** on the cellular DNA content of C33-A cells. Cells were grown in the absence (control) or presence of the compounds at their respective IC_{50} for 48 h, stained with propidium iodide, and analyzed by flow cytometry for DNA content.

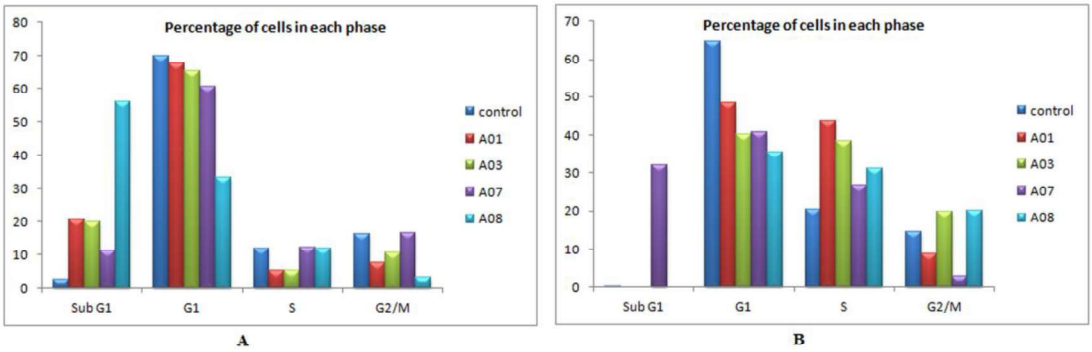

Fig. 5.32. Flow cytometric analysis for the cell cycle distribution of (A) SiHa and (B) C33-A cells after exposure to compounds **A01, A03, A07** and **A08** for 48 h.

5.2.5.4. Apoptosis assay

Deregulation of apoptosis is implicated in cancer. Apoptosis provides a number of clues with respect to effective anticancer therapy, and many chemotherapeutic agents reportedly exert their antitumor effects by inducing apoptosis in cancer cells [Kamesaki *et al.,* 1998]. In the process of apoptosis, phosphatidylserine (PS) located on the cytoplasmic surface, is translocated from the inner to the outer leaflet of the plasma membrane. The extracellular exposed PS has high affinity for binding to the human vascular anticoagulant, annexin V, a 35–36 kDa, Ca^{2+}-dependent, phospholipid-binding protein. This principle is used to determine the binding of annexin V, labeled with a fluorophore or biotin, to exposed PS on the outer leaflet and thereby to identify apoptotic cells [Koopman *et al.,* 1994].

In our study, we found that treatment of cervix cancer-derived SiHa cells with benzothiazole bearing amide moiety (**A01-A10**) resulted in apoptosis by all the compounds except **A09** indicating that this compound might be acting by different mechanism(s) (Fig. 5.33). Similar effects were observed in C33-A cells i.e., all the compounds (**A01-A10**) induce apoptosis except compound **A09** which showed minimum apoptosis as evidenced by apoptosis assay. Interestingly, C33-A cells treated with compounds **A07**, **A08** and **A10** underwent early and late apoptosis (Fig. 5.34). However, it was noticed that compound **A09** which was more active towards SiHa than C33-A cells, caused sub-G1 and G2/M cell cycle arrest, respectively. Further, this compound did not induce apoptosis in SiHa cells and thus exhibited cytotoxicity by different mechanisms. The most potent compound **A07** was found to be highly effective in causing cytotoxicity in SiHa cells with an increase in the percentage of sub G1 population. This was further corroborated by the apoptosis assay.

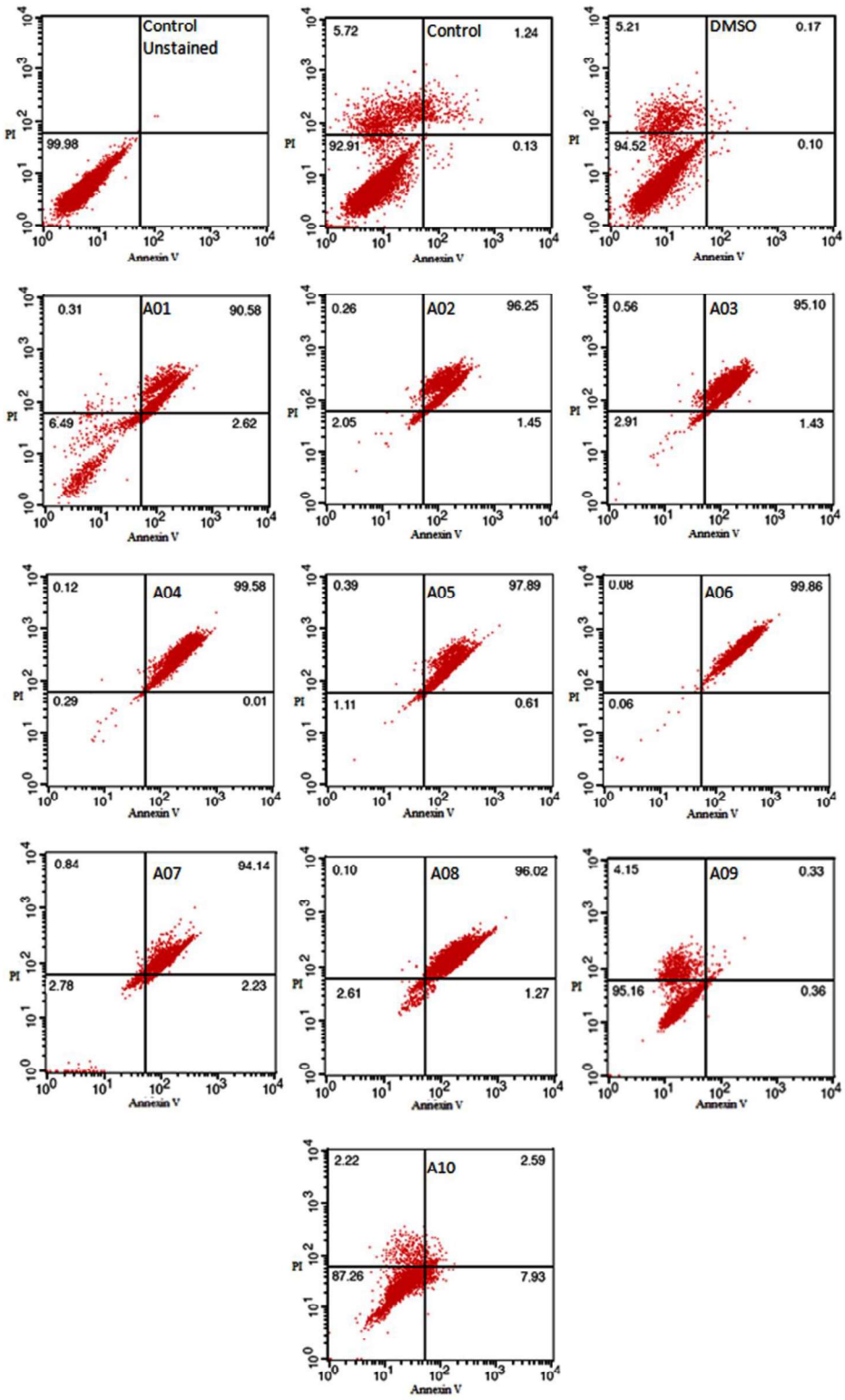

Fig. 5.33 SiHa cells treated with compounds **(A01-10)** at their respective IC_{50}s for 48 h were analyzed using AnnexinV-AlexaFlour488/PI flow cytometry. Quadrant 1 (LL) represents live cells, quadrant 2 (UL) represents dead cells, quadrant 4 (LR) represents AnnexinV positive early apoptotic cells, and quadrant 3 (UR) represents late apoptotic cells. Each sample was analyzed at 20,000 cells per counts.

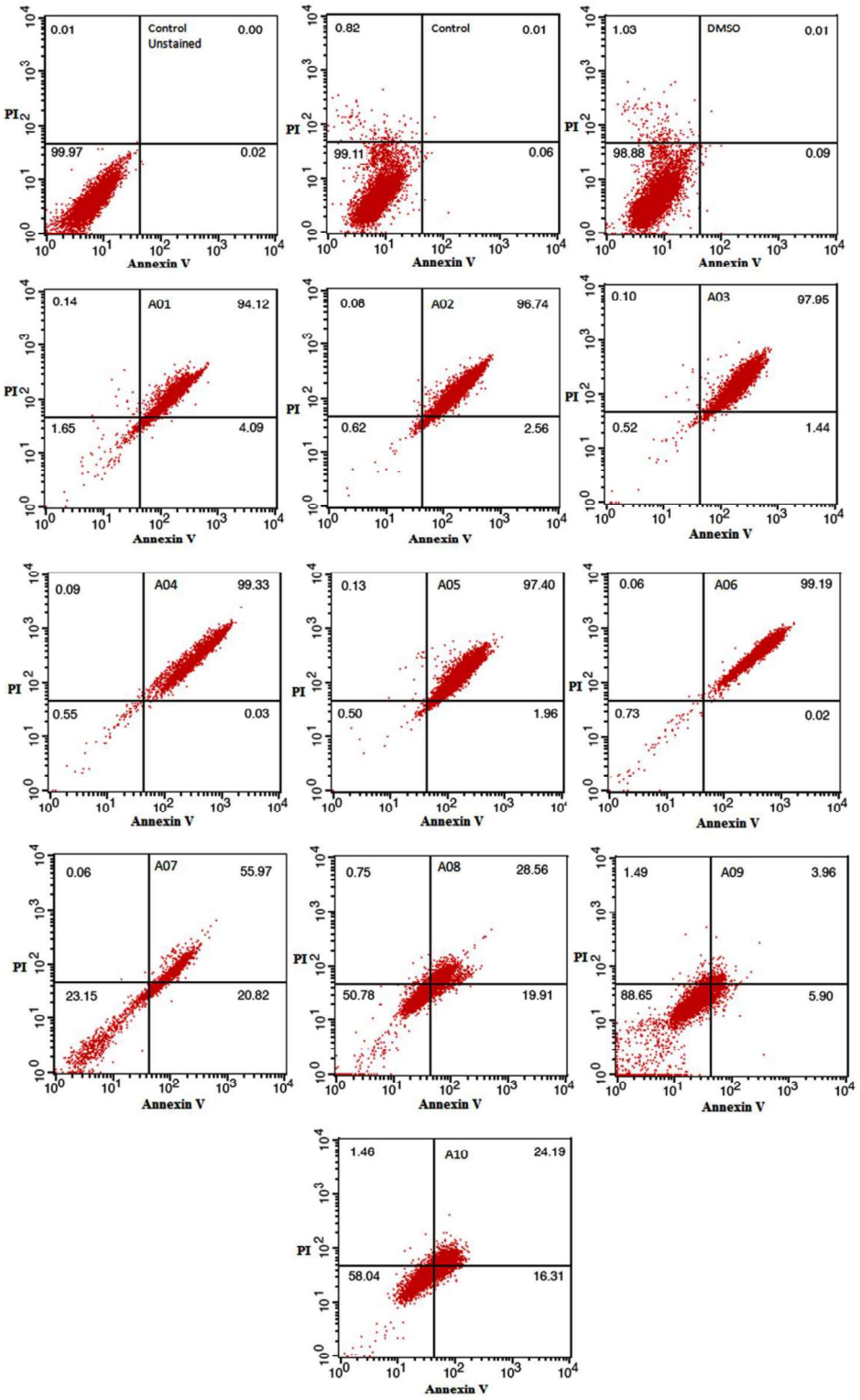

Fig. 5.34 C33-A cells treated with compounds **(A01-10)** at their respective IC_{50}'s for 48 h were analyzed using AnnexinV-AlexaFlour488/PI flow cytometry. Quadrant 1 (LL) represents live cells, quadrant 2 (UL) represents dead cells, quadrant 4 (LR) represents Annexin V positive early apoptotic cells, and quadrant 3 (LR) represents late apoptotic cells. Each sample was analyzed at 20,000 cells per counts.

5.2.5.5. DNA fragmentation

In order to further define the mechanism involved in apoptosis induction after drug treatment, we performed DNA fragmentation assay. The extent of benzothiazole bearing amide moiety (**A01-A10**) induced DNA damage in SiHa and C33-A cervical cancer cells, was assessed in the study as reported earlier [Karthikeyan *et al.* 2015; Kumar *et al.* 2008]. Treatment with the compounds **(A01-A10)** for 48 hr led to fragmentation of chromosomal DNA of SiHa and C33-A cells (Fig. 5.35 and 5.36). In contrast, chromosomal DNA of untreated cells was intact. These results indicated that all the compounds except **A09** in SiHa cells, induced DNA breakage at multiple positions across chromosomal DNA, leading to apoptosis. Subsequently, accumulation of the sub-G1 population by flow cytometric analyses and absence of apoptosis by PI/Annexin V staining in SiHa cells confirmed that compound **A09** displayed cytotoxicity by different signalling pathway(s) apart from DNA fragmentation assay. Thus, all the potent compounds **A01, A03, A07** and **A08** induced DNA fragmentation in both cell lines with their respective apoptotic behaviour.

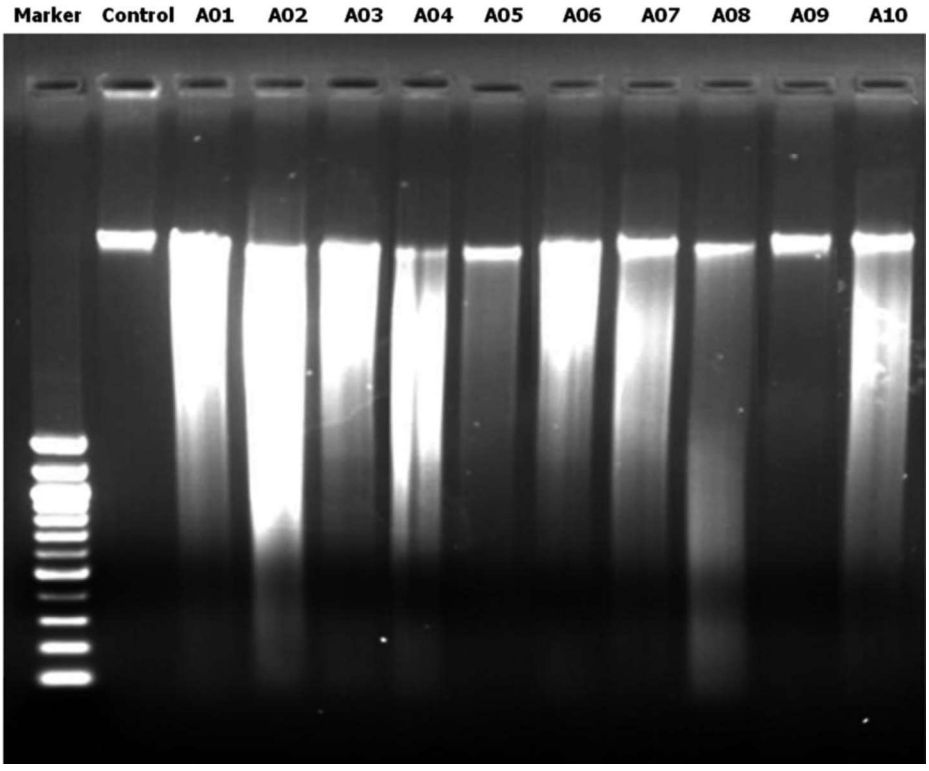

Fig. 5.35 DNA fragmentation of SiHa cells exposed to the compounds **A01-A10**. Cells were incubated with the different compounds at their respective concentrations for 48 h. Each lane reflecting the presence of DNA fragments, were viewed on ethidium bromide stained gel. Typical result from three independent experiments is shown.

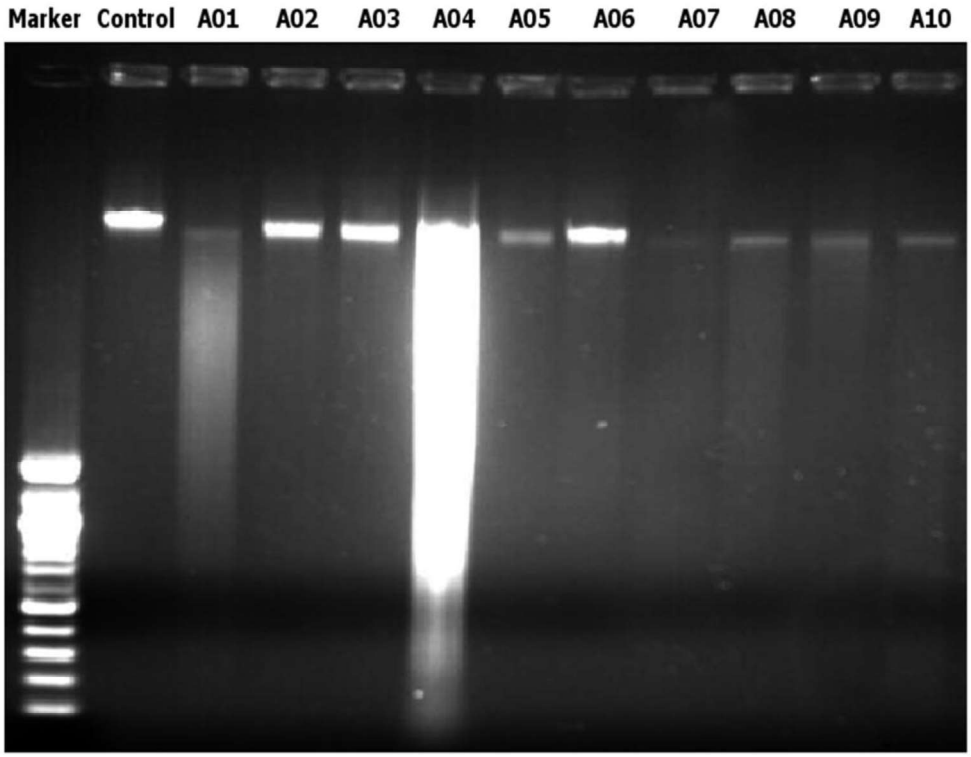

Fig. 5.36 DNA fragmentation of C33-A cells exposed to the compounds **A01-10**. Cells were incubated with the different compounds at their respective concentrations for 48 h. Each lane reflecting the presence of DNA fragments, were viewed on ethidium bromide stained gel. Typical result from three independent experiments is shown.

5. 3. SERIES-3: 4-Thiazolidinone derivatives of 4-arylidine-benzenamine benzothiazole

5.3.1. BACKGROUND

Benzothiazole and its derivatives are widely distributed in nature and are well known to exhibit broad spectrum of antimicrobial activity. Small ring heterocycles, particularly 4-thiazolidinones have also shown important antimicrobial activitiy [Lokhandwala *et al.,* 2008]. Therefore, it was envisaged that chemical entities with benzothiazole and 4-thiazolidinone moieties would result in compounds of interesting biological activities. In view of these, an attempt was made to incorporate these biologically active components together to give a confined structure new 4-thiazolidinone benzothiazole derivatives **(TB01-10)** from Schiff bases of benzothiazoles and evaluated their antimicrobial activity.

5.3.2. CHEMISTRY

The 4-thiazolidinones-benzothiazole conjugates (**TB01-10**) were obtained by refluxing the equimolar quantities of Schiff bases of benzothiazole hybrids and thioglycolic acid in suitable solvent (DMF) in presence of anhyd. $ZnCl_2$ as catalyst. The IR, ^{1}H-NMR, ^{13}C-NMR spectral data of compounds (**TB01-10**) was in accordance with the proposed molecular structures. The structures of 4-thiazolidinones-benzothiazole conjugates (**TB01-10**) were confirmed by their spectral analysis. The FT-IR spectra showed absorption bands at 3,083–3,284 cm^{-1} for aromatic C–H and at 1,624-1,683 for C=O str. of carbonyl group. The ^{1}H NMR showed sharp singlet peak in the range of δ 4.11–4.81 ppm indicating the presence of -CH of thiazolidindione ring. The singlet peak in the range of δ 3.10-3.61 ppm indicated the presence -CH_2 of thiazolidindione ring. The multiplet at δ 6.91–7.99 ppm was due to aromatic protons. Moreover, ^{13}C NMR spectra revealed all the corresponding peaks in the range of δ 61.70–67.71 ppm and δ 31.81–38.40 ppm which were due to -CH of thiazolidindione ring and -CH_2 of thiazolidindione ring respectively. The peaks appearing in the range of δ 174.14–185.40 ppm corresponds to C=O of the thiazolidinone ring and of δ 120.67–155.25 ppm corresponds to aryl carbon. The physicochemical properties of 4-thiazolidinones-benzothiazole conjugates (**TB01-10**) are given in Table 5.16.

5.3.3. PHYSICOCHEMICAL AND SPECTRAL CHARACTERIZATION DATA

Table 5.16 Physicochemical data of 4-thiazolidinones-benzothiazole conjugates (**TB01-10**)

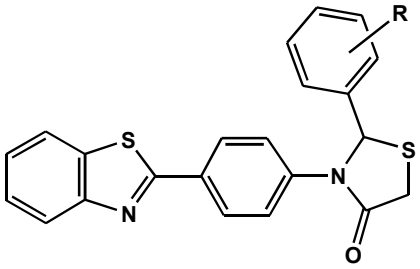

4-Thiazolidinones-Benzothiazole conjugates (TB01-TB10)

Compound code	R	MW	Melting point (℃)	Yield (%)	R_f (solvent system)	Solubility
TB01	4-OCH_3	418.53	245-247	54	0.75 (A)	MeOH, EtAc
TB02	4-Cl	422.95	261-263	62	0.57 (A)	EtAc
TB03	2,4-diCl	457.40	255-257	56	0.71 (A)	MeOH, EtAc
TB04	2,4-diOH	420.50	224-226	68	0.64 (B)	MeOH, EtAc
TB05	3-Br	467.40	205-207	53	0.56 (A)	MeOH, EtAc
TB06	4-OH	404.50	199-201	65	0.61 (B)	MeOH
TB07	3-CH_3	402.53	238-240	75	0.78 (A)	MeOH
TB08	3-NO_2	433.50	196-198	41	0.66 (A)	EtAc
TB09	3-F	406.50	229-231	50	0.69 (A)	MeOH, EtAc
TB10	-H	388.51	194-196	71	0.69 (B)	EtAc

Solvent system: (A) Methanol: Chloroform, 2:8, (B) Ethylacetate: Hexane, 7:3

Spectral data for 4-thiazolidinones-benzothiazole derivatives

Compound TB01: *3-(4-(benzo[d]thiazol-2-yl)phenyl)-2-(4-methoxyphenyl)thiazolidin-4-one*

IR (KBr, υmax cm^{-1}): 1658.84 (C=O str. of carbonyl group), 2850 (C–H str., O–CH_3 group) 3221.23 (Aromatic –C–H str.)

^{1}H NMR (DMSO-d_6, 300 MHz) δ (ppm): 3.72 (s, 3H, OCH_3), 4.81 (s, -CH of Thiazolidindione ring), 3.1 (s, 2H, -CH_2 of Thiazolidindione ring), 7.60–7.89 (m, 12H, Ar–H)

^{13}C NMR (DMSO-d_6) δ (ppm): 55.69 (OCH_3) , 65.70 (-CH of Thiazolidindione ring), 33.11 (-CH_2 of Thiazolidindione ring), 183.34 (C=O), 126.67–140.05 (Aromatic–C, C_2–C_9 $C_{1'}$–$C_{6'}$ $C_{1''}$–$C_{6''}$)

MS (m/z, %): 420 (M + 1, 100).

Anal $C_{23}H_{18}N_2O_2S_2$. Calc. for: C, 66.00; H, 4.33; N, 6.69. Found: C, 66.01; H, 4.28; N, 6.65%.

Compound TB02: *3-(4-(benzo[d]thiazol-2-yl)phenyl)-2-(4-chlorophenyl)thiazolidin-4-one*

IR (KBr, υmax cm^{-1}): 1683.91 (C=O str. of carbonyl group), 1065 (C–Cl str.), 3131.23(Aromatic –C–H str.)

^{1}H NMR (DMSO-d_6, 300 MHz) δ (ppm): 4.51 (s, -CH of Thiazolidindione ring), 3.20 (s, 2H, -CH_2 of Thiazolidindione ring), 7.69–7.90 (m, 12H, Ar–H)

^{13}C NMR (DMSO-d_6) δ (ppm): 67.71 (-CH of Thiazolidindione ring), 32.40 (-CH_2 of Thiazolidindione ring), 181.14 (C=O), 123.07–145.05 (Aromatic–C, C2–C9 C1'–C6' C1"–C6")

MS (m/z, %): 424 (M + 1, 100).

Anal $C_{22}H_{15}ClN_2OS_2$. Calc. for: C, 62.47; H, 3.57; N, 6.62. Found: C, 62.45; H, 3.54; N, 6.62%.

Compound TB03: *3-(4-(benzo[d]thiazol-2-yl)phenyl)-2-(2,4-dichlorophenyl)thiazolidin-4-one*

IR (KBr, υmax cm^{-1}): 1632.54 (C=O str. of carbonyl group) 1108, 1065 (C–Cl str.), 3118, 3083 (Aromatic C–H str.)

^{1}H NMR (DMSO-d_6, 300 MHz) δ (ppm): 4.11 (s, -CH of Thiazolidindione ring), 3.20 (s, 2H, -CH_2 of Thiazolidindione ring), 7.42–7.91 (m, 11H, Ar–H)

^{13}C NMR (DMSO-d_6) δ (ppm): 63.51 (-CH of Thiazolidindione ring), 38.40 (-CH_2 of Thiazolidindione ring), 178.14 (C=O), 121.07–142.05 (Aromatic–C, C2–C9 C1'–C6' C1"–C6")

MS (m/z, %): 458 (M + 1, 100).

Anal $C_{22}H_{14}Cl_2N_2OS_2$. Calc. for: C, 57.77; H, 3.09; N, 6.12. Found: C, 57.75; H, 3.06; N, 6.10%.

Compound TB04: *3-(4-(benzo[d]thiazol-2-yl)phenyl)-2-(2,4-dihydroxyphenyl) thiazolidin-4-one*

IR (KBr, υmax cm^{-1}): 1628.34 (C=O str. of carbonyl group), 3126 (O–H str., br.), 3121.03(Aromatic –C–H str.)

^{1}H NMR (DMSO-d_6, 300 MHz) δ (ppm): 10.69 (br, s, 1H, o–OH group), 9.92 (s, 1H, p–OH group), 4.30 (s, -CH of Thiazolidindione ring), 3.61 (s, 2H, -CH_2 of Thiazolidindione ring), 6.91–7.54 (m, 11H, Ar–H)

^{13}C NMR (DMSO-d_6) δ (ppm): 64.01 (-CH of Thiazolidindione ring), 35.31 (-CH_2 of Thiazolidindione ring), 174.14 (C=O), 122.07–146.05 (Aromatic–C, C2–C9 C1'–C6' C1"–C6")

MS (m/z, %): 421 (M + 1, 100).

Anal $C_{22}H_{16}N_2O_3S_2$. Calc. for: C, 62.84; H, 3.84; N, 6.66. Found: C, 62.83; H, 3.82; N, 6.63%.

Compound TB05: *3-(4-(benzo[d]thiazol-2-yl)phenyl)-2-(3-bromophenyl)thiazolidin-4-one*

IR (KBr, υmax cm^{-1}): 1641.13 (C=O str. of carbonyl group), 765 (C–Br str.), 3221.73(Aromatic –C–H str.)

^{1}H NMR (DMSO-d_6, 300 MHz) δ (ppm): 4.21 (s, -CH of Thiazolidindione ring), 3.30 (s, 2H, -CH_2 of Thiazolidindione ring), 7.01–7.84 (m, 12H, Ar–H)

^{13}C NMR (DMSO-d_6) δ (ppm): 67.62 (-CH of Thiazolidindione ring), 32.11 (-CH_2 of Thiazolidindione ring), 179.24 (C=O), 125.07–149.15 (Aromatic–C, C2–C9 C1'–C6' C1"–C6")

MS (m/z, %): 468 (M + 1, 100).

Anal $C_{22}H_{15}BrN_2OS_2$. Calc. for: C, 56.53; H, 3.23; N, 5.99. Found: C, 56.53; H, 3.20; N, 5.97%.

Compound TB06: *3-(4-(benzo[d]thiazol-2-yl)phenyl)-2-(4-hydroxyphenyl)thiazolidin-4-one*

IR (KBr, υmax cm^{-1}): 1644.21 (C=O str. of carbonyl group), 3426 (O–H str.), 3271.61(Aromatic –C–H str.)

^{1}H NMR (DMSO-d_6, 300 MHz) δ (ppm): 9.72 (s, 1H, –OH), 4.41 (s, -CH of Thiazolidindione ring), 3.40 (s, 2H, -CH_2 of Thiazolidindione ring), 7.11–7.94 (m, 12H, Ar–H)

^{13}C NMR (DMSO-d_6) δ (ppm): 65.21 (-CH of Thiazolidindione ring), 34.50 (-CH_2 of Thiazolidindione ring), 182.84 (C=O), 122.37–150.15 (Aromatic–C, C2–C9 C1'–C6'

C1"–C6")

MS (m/z, %): 405 (M + 1, 100).

Anal $C_{22}H_{16}N_2O_2S_2$. Calc. for: C, 65.32; H, 3.99; N, 6.93. Found: C, 65.33; H, 3.98; N, 6.90%.

Compound TB07: *3-(4-(benzo[d]thiazol-2-yl)phenyl)-2-(3-methylphenyl)thiazolidin-4-one*

IR (KBr, υmax cm^{-1}): 1638.13 (C=O str.of carbonyl group), 2892 (C–H str., $–CH_3$ group), 3171.61(Aromatic –C–H str.)

^{1}H NMR (DMSO-d_6, 300 MHz) δ (ppm): 2.82 (s, 3H, $–CH_3$), 4.12 (s, -CH of Thiazolidindione ring), 3.4 (s, 2H, $-CH_2$ of Thiazolidindione ring), 7.10–7.89 (m, 12H, Ar–H)

^{13}C NMR (DMSO-d_6) δ (ppm): 62.21 (-CH of Thiazolidindione ring), 31.81 ($-CH_2$ of Thiazolidindione ring), 180.14 (C=O), 124.37–152.15 (Aromatic–C, C2–C9 C1'–C6' C1"–C6")

MS (m/z, %): 403 (M + 1, 100).

Anal $C_{23}H_{18}N_2OS_2$. Calc. for: C, 68.63; H, 4.51; N, 6.96. Found: C, 68.62; H, 4.50; N, 6.96%.

Compound TB08: *3-(4-(benzo[d]thiazol-2-yl)phenyl)-2-(3-nitrophenyl)thiazolidin-4-one*

IR (KBr, υmax cm^{-1}): 1624.22 (C=O str. of carbonyl group), 1351 (N=O str.), 3154.03(Aromatic –C–H str.)

^{1}H NMR (DMSO-d_6, 300 MHz) δ (ppm): 4.61 (s, -CH of Thiazolidindione ring), 3.30 (s, 2H, $-CH_2$ of Thiazolidindione ring), 7.06–7.90 (m, 12H, Ar–H)

^{13}C NMR (DMSO-d_6) δ (ppm): 64.30 (-CH of Thiazolidindione ring), 34.51 ($-CH_2$ of Thiazolidindione ring), 182.44 (C=O), 121.47–155.25 (Aromatic–C, C2–C9 C1'–C6' C1"–C6")

MS (m/z, %): 434 (M + 1, 100).

Anal $C_{22}H_{15}N_3O_3S_2$. Calc. for: C, 60.95; H, 3.49; N, 9.69. Found: C, 60.95; H, 3.47; N, 9.67%.

Compound TB09: *3-(4-(benzo[d]thiazol-2-yl)phenyl)-2-(3-fluorophenyl)thiazolidin-4-one*

IR (KBr, υmax cm^{-1}): 1638.23 (C=O str. of carbonyl group), 3254.87 (Aromatic –C–H str.)

^{1}H NMR (DMSO-d_6, 300 MHz) δ (ppm): 4.50 (s, -CH of Thiazolidindione ring), 3.60 (s, 2H, -CH_2 of Thiazolidindione ring), 7.10–7.68 (m, 12H, Ar–H)

^{13}C NMR (DMSO-d_6) δ (ppm): 62.31 (-CH of Thiazolidindione ring), 36.90 (-CH_2 of Thiazolidindione ring), 185.40 (C=O), 123.07–153.85 (Aromatic–C, C2–C9 C1'–C6' C1"–C6")

MS (m/z, %): 407 (M + 1, 100).

Anal $C_{22}H_{15}FN_2OS_2$. Calc. for: C, 65.00; H, 3.72; N, 6.89. Found: C, 65.01; H, 3.70; N, 6.88%.

Compound TB10: *3-(4-(benzo[d]thiazol-2-yl)phenyl)-2-(phenyl)thiazolidin-4-one*

IR (KBr, υmax cm^{-1}): 1640.53 (C=O str. of carbonyl group), 3284.03(Aromatic –C–H str.)

^{1}H NMR (DMSO-d_6, 300 MHz) δ (ppm): 4.11 (s, -CH of Thiazolidindione ring), 3.30 (s, 2H, -CH_2 of Thiazolidindione ring), 7.12–7.99 (m, 13H, Ar–H)

^{13}C NMR (DMSO-d_6) δ (ppm): 61.70 (-CH of Thiazolidindione ring), 34.91 (-CH_2 of Thiazolidindione ring), 178.54 (C=O), 120.67–145.05 (Aromatic–C, C2–C9 C1'–C6' C1"–C6")

MS (m/z, %): 389 (M + 1, 100).

Anal $C_{22}H_{16}N_2OS_2$. Calc. for: C, 68.01; H, 4.15; N, 7.21. Found: C, 68.00; H, 4.13; N, 7.20%.

5.3.4. *IN-VITRO* ANTIMICROBIAL ACTIVITY

The results of anti-microbial studies (inhibition zone of diameter and MIC) of all the novel compounds are presented in Table 5.17 and Table 5.18. Significant antimicrobial activity was observed for some of the members of the series with moderate to good MIC values ranging between 15.6–125 µg/mL. The results of antimicrobial screening revealed that among the compounds screened, compounds **TB02, TB03**, **TB04** and **TB07** showed moderate activity while compounds **TB01** and **TB06** displayed good antimicrobial activity. Particularly, compounds such as 3-(4-(benzo[d]thiazol-2-yl)phenyl)-2-(4-methoxyphenyl)thiazolidin-4-one (**TB01**) and 3-(4-(benzo[d]thiazol-2-yl)phenyl)-2-(4-hydroxyphenyl) thiazolidin-4-one (**TB06**) were found to be the most active candidate against *E. coli* (zone of inhibition up to 22–26 mm at concentration of 15.6 µg/mL) and against *C. albicans* (zone of inhibition up to 16–19 mm at concentration of 15.6 µg/mL). Compounds **TB01** and **TB06** were carrying electron donating group (methoxy, hydroxy) on aryl ring and showed significant increase in antimicrobial activity against *E. coli* and

C. albicans. A significant number of drugs and drug candidates in clinical development are halogenated structures. The formation of halogen bonds in ligand-target complexes is recognized as a kind of intermolecular interaction that favourably contributes to the stability of protein-ligand complexes. The insertion of halogen atoms has been used in innumerous cases of hit-to-lead or lead-to-drug conversions [Bonnefous *et al.,* 2009; Leite *et al.,* 2009]. Derivatization of **TB02** with chloro substitution on phenyl ring exhibited moderate potency (zone of inhibition = 10-18 mm) indicating that substitutions may result in restoration of potency. Whereas, compounds containing other halogen atoms viz., fluoro (**TB09**), bromo (**TB05**) substitutions exhibited least potency. Compounds **TB08** bearing electron withdrawing group (nitro) and of without derivatization **TB10,** also exhibited least potency.

Table 5.17 Antibacterial activity (MIC µg/mL) of 4-thiazolidinone benzothiazole derivatives (**TB01-10**)

Comp code	Bacteria					
	Gram positive bacteria		Gram negative bacteria			
	S. aureus **(ATCC 25323)**	***E. faecalis*** **(Clinical isolate)**	***E. coli*** **(ATCC 35218)**	***S. typhi*** **(MTCC 3216)**	***K. pneumonia*** **(ATCC 31488)**	***P. aeruginosa*** **(ATCC 27893)**
TB01	-	12-14(62.5)	22-26(15.6)	<10(125)	-	-
TB02	14-18(31.2)	15-17(31.2)	12-15(62.5)	12-14(62.5)	-	-
TB03	13-15(62.5)	11-13(62.5)	16-19(31.2)	11-14(62.5)	-	<10(125)
TB04	15-17(31.2)	-	13-17(62.5)	12-15(62.5)	-	-
TB05	-	-	<10(125)	<10(125)	-	11-13(62.5)
TB06	-	<10(125)	24-26(15.6)	<10(125)	-	-
TB07	14-18(31.2)	-	15-18(31.2)	11-14(62.5)	-	-
TB08	-	<10(125)	<10(125)	<10(125)	-	10-12(62.5)
TB09	<10(125)	<10(125)	-	-	-	-
TB10	<10(125)	<10(125)	<10(125)	-	-	14-17(31.2)
CIP	30-32(≥6.25)	28-30(≥6.25)	33-35(≥6.25)	34-35(≥6.25)	30(≥6.25)	33-35(≥3.12)

Structure–activity relationship (SAR) studies from the results of the antimicrobial activity revealed that conversion of Schiff bases via formation of 4-thiazolidinones-benzothiazole Conjugates may contribute for good activity. The greater antimicrobial activity of **TB01, TB02, TB03**, **TB04, TB06** and **TB07** may be attributed to the presence of electron donating substituents such as methoxy, hydroxyl and also of chloro substituents on phenyl ring.

Table 5.18 Antifungal activity (MIC µg/mL) of the 4-thiazolidinone benzothiazole derivatives (**TB01-10**)

Compound code	*C. albicans* (ATCC 90028)	*C. tropicalis* (ATCC 750)	*C. krusei* (ATCC 6268)
TB01	16-18(15.6)	<10(125)	-
TB02	10-12(62.5)	14-16(31.2)	-
TB03	<10(125)	13-15(31.2)	-
TB04	12-15(31.2)	<10(125)	-
TB05	12-15(31.2)	-	-
TB06	17-19(15.6)	12-15(31.2)	-
TB07	<10(125)	10-12(62.5)	-
TB08	<10(125)	-	-
TB09	-	11-13(62.5)	-
TB10	<10(125)	-	-
Fluconazole	22-25(6.25)	24-27 (6.25)	24-27 (6.25)

The value of each compound consisted of 'zone of inhibition range (MIC)' of 03 replicates. Level of significance $p < 0.05$.

5.3.4.1. Mechanism of action study

Bactericidal kinetics

The bactericidal activity of designed compounds **TB03** and **TB07** was determined on *S. aureus* and *E. coli* at 37°C. The results showed a proportionate reduction in numbers of gram positive bacteria (90 to 99%) within initial contact after addition of the compound **TB07** at 4 × MIC (Fig. 5.37). Compound **TB03** was found to be less effective as compared to compound **TB07** in *E.coli* and *S.aureus* even up to 5 h. At 4 × MIC both compounds inhibited bacterial growth from 2 h onwards keeping growth arrested till 5 h. However, complete eradication of bacterial growth was not observed even up to 5 h. At 4 × MIC compound **TB07** exhibited the most potent inhibition of growth compared to compound **TB10** in both the strains. Thus the designed compounds are capable of inhibiting bacterial growth within hours of initial interactions.

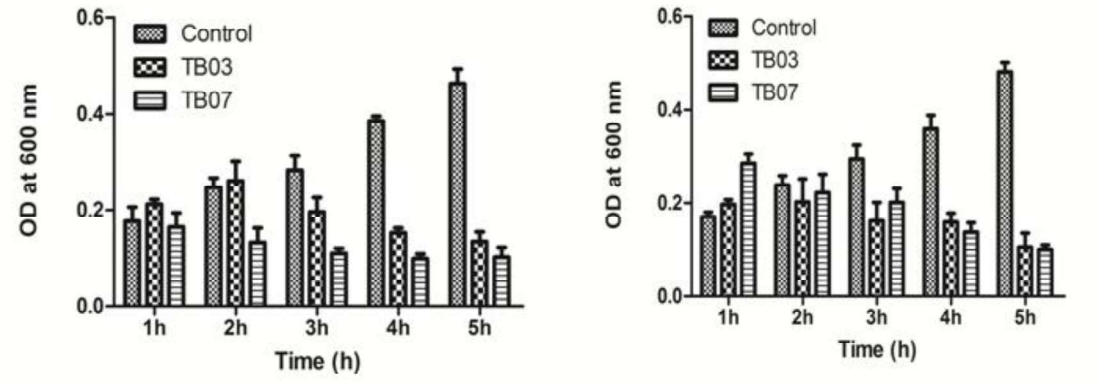

(A) (B)

Fig. 5.37 Time dependent killing of (A) *S. aureus* (B) *E.coli* upon treatment with compounds **TB03** and **TB07** at 4 × MIC.

Cytoplasmic Membrane depolarization assay

Cytoplasmic Membrane depolarization assay was used to determine the membrane destabilization/pore formation of the designed analogues. Compounds **TB03** and **TB07** showed similar profile with respect to positive control triton 2%. At the highest concentration of **TB03** and **TB07** (i.e., 4 x MIC), the level of depolarization appeared to reach a maximum at times from about 2 to 5 min. Compound **TB03** caused maximum depolarization in *E. coli* whereas **TB07** in *S.aureus* (Fig. 5.38). All the designed analogs studied here had the ability to depolarize the cytoplasmic membrane of *S.aureus* and

E.coli; however, compounds with different structures had different concentration-activity profiles.

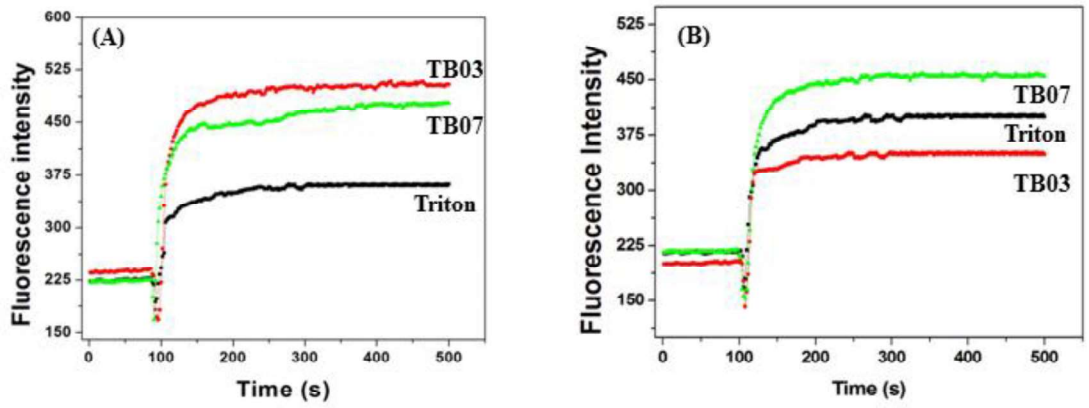

Fig. 5.38 Membrane depolarization ability of designed compounds **TB03** and **TB07** on (A) *E.coli* and (B) *S.aureus*. Cultures were grown to log phase (OD_{600} = 0.05) and treated with 4xMIC concentration of compounds.

Flow Cytometry analysis

Consistent with the permeabilization of bacteria, designed analogs **TB03** and **TB07** induced damages to the membrane organization of *S.aureus* but induced significantly lesser damage to the membrane organization of *E. coli* as indicated by PI staining of the cells following the treatments of these compounds (Fig. 5.39). However, the number of PI-stained cells decreased significantly in **TB03** in *S.aureus* and **TB07** in *E.coli*. Overall this suggests that the mode of action of designed analogs **TB03** and **TB07** and related compounds might result from disruption of the membrane potential that is utilized for cellular energy production. However, this is unlikely to be the sole mechanism, since compound **TB03** was slightly less active than **TB07**. Thus the results showed that the **both the** analogs exhibited contrasting lytic activity towards the bacterial cells.

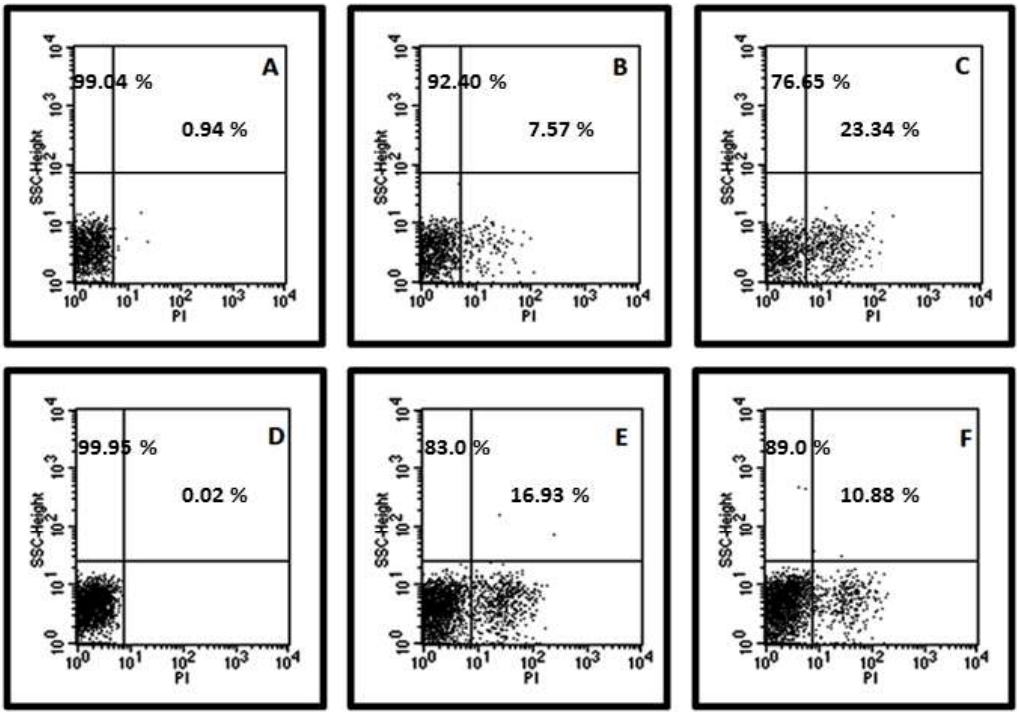

Fig. 5.39 Determination of compound-induced membrane damage of *S.aureus* and *E. coli* cells. (A–F) PI staining of *S.aureus* (A) control without PI treatment (B) **TB03** (C) **TB07** and on *E. coli* (D) control without PI treatment (E) **TB03** (F) **TB07** respectively.

DNA binding

Compound **TB03** showed excellent binding with DNA (200 ng) causing retardation at 3.91μg/mL whereas for **TB07** no retardation was observed at all the concentrations (Fig. 5.40). However it was intriguing that DNA binding was influenced by overall structure of the compounds as dichloro containing compound **TB03** showed the most potent DNA retardation ability as compared to methyl group containing analogue **TB07**. Thus, in the present study upon comparing DNA binding and antimicrobial potency (compound **TB07** showed no DNA binding though was equipotent as **TB03**) it was evident that there were no direct correlations between DNA retardation and antimicrobial mode of action.

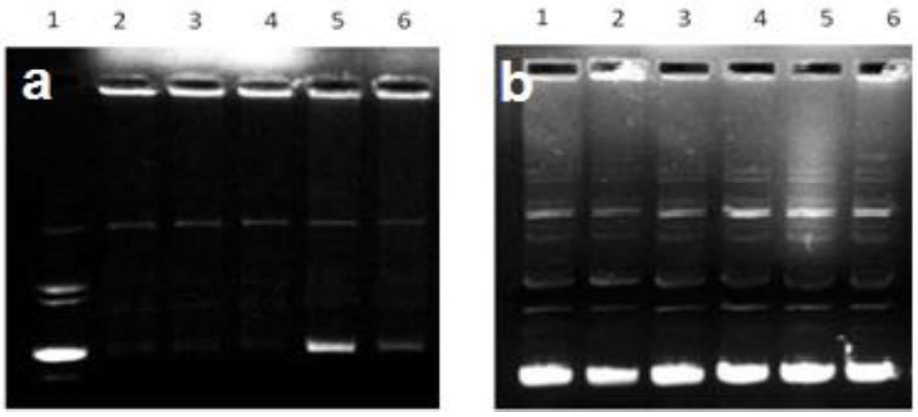

(A) (B)

Fig. 5.40 Agarose gel electrophoresis patterns of plasmid DNA (200 ng) cleaved by (A) **TB03** and (B) **TB07;** in a concentration range (62.5-3.91 µg/mL), after 1h incubation time

5.3.4.2. Docking study against Glc-6-PS

Molecular docking study was carried out to determine the binding interactions of the synthesized 4-Thiazolidindione benzothiazole derivatives, utilizing the active site of glucosamine-6-phosphate synthase (GlcN-6-P synthase), and by using the Surflex dock program incorporated in Sybyl-X1.2. All the molecules showed very good binding energy ranging from 4-6 dock score which was comparable with the standard drugs used. Compounds **TB01, TB04, TB06, TB07** and **TB08** showed good docking score with receptor as shown in Table 5.19. Compound **TB06** was found to have a score of 6.78 forming strong H-bond with Glu488, Cys300, Lys485 and Val605. The ligand receptor interactions of compound **TB01 and TB06** is shown in Fig. 5.41. From the results, it was evident that the *in-silico* findings were in accordance with *in-vitro* antimicrobial assay.

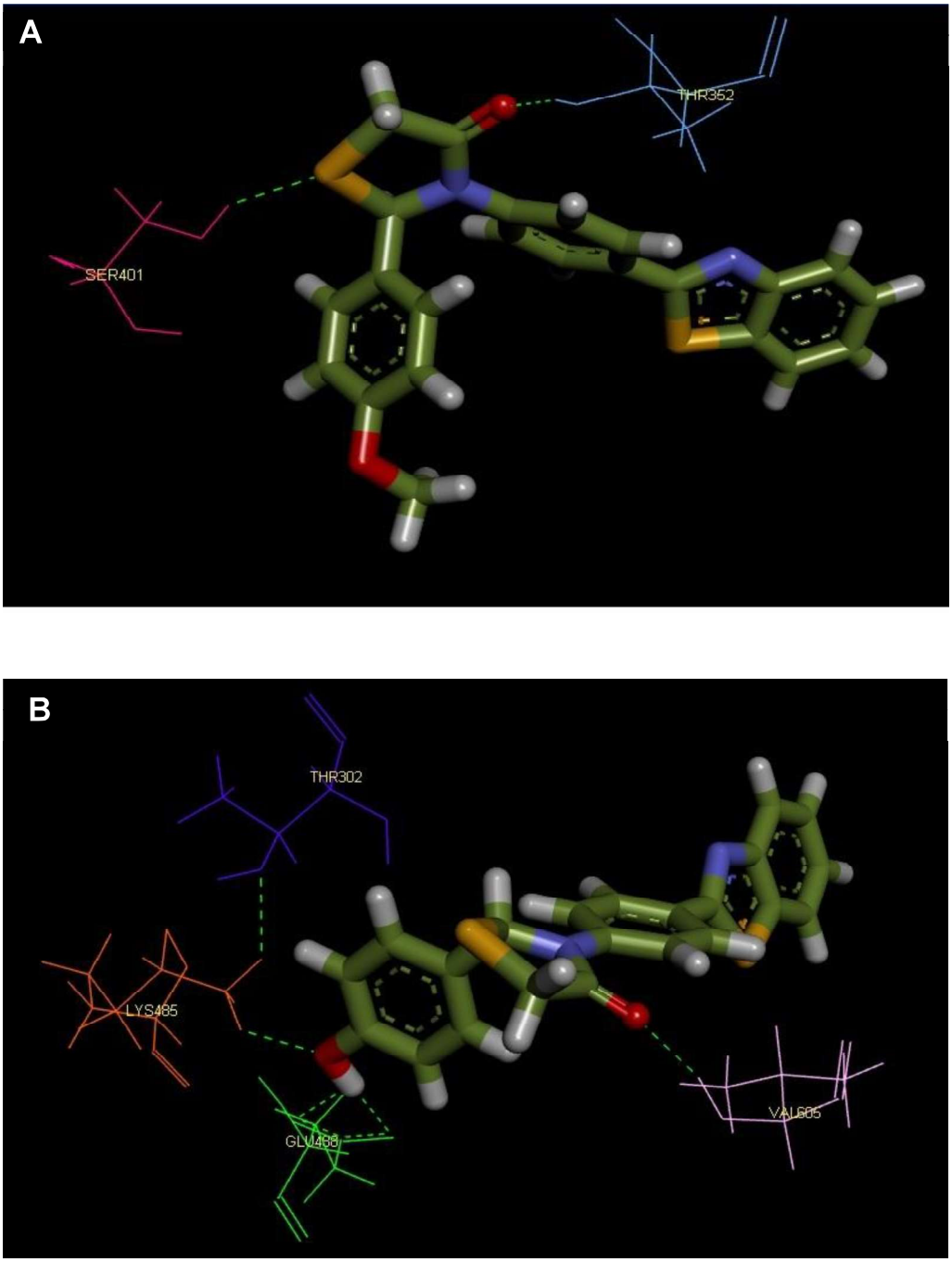

Fig. 5.41 Binding pose of compound (A) **TB01** and (B) **TB06** with glucosamine-6-phosphate synthase. Hydrogen bonding interactions are displayed by green dotted lines.

Table 5.19. Molecular docking scores of 4-thiazolidinone benzothiazole derivatives with GlcN-6-P synthase.

Sr. No	Compound code	Docking Score	Crash Value	Interacting amino acids
1	TB01	5.9597	-1.984	Thr352, Ser401
2	TB02	4.4663	-1.5689	Thr352,Ala602
3	TB03	4.8842	-1.1362	Thr352, Ser401, Ala602
4	TB04	6.083	-0.9182	Thr302, Thr352, Ser401
5	TB05	4.3174	-1.1594	Thr352,Ser401
6	TB06	6.7893	-1.1562	Glu488, Cys300, Lys485, Val605
7	TB07	5.1992	-0.7392	Thr352, Ser401
8	TB08	5.383	-1.5148	Lys485, Ser401, Lys485, Val605
9	TB09	4.2731	-1.6237	Thr352, Val605
10	TB10	4.4363	-0.5955	Thr352
21	Ciprofloxacin	6.0614	2.0428	Ser347, Gln348, Ser349, Ser401, Lys485
22	Fluconazole	6.4092	-1.4344	Val399, Gln348, Ser349, Lys485, Ser604

5.3.4.3. *In-Silico* Pharmacokinetic Predictions

In-silico pharmacokinetic properties prediction was carried out for the compounds **TB01, TB03, TB04, TB06** and **TB07** having significant antimicrobial activity and good docking score by using preADMET server. The predicted drug likelinesss of the all synthesized compounds follows the Lipinski ‘‘Rule of Five’’. The results are summarized in Table 5.20.

Table 5.20. Theoretical prediction of different properties of 4-thiazolidinone benzothiazole derivatives using PreADMET Server

Comp No.	Log p	$LogS_b$ (mg/L)	HIA (%)	HB-donors	HB-acceptors	*In-vitro* PPB (%)
TB01	3.9	103.01	99.80	0	4	99.58
TB03	4.1	10.62	91.24	0	5	97.34
TB04	3.0	67.36	95.29	2	3	92.68
TB06	3.5	65.12	97.16	1	3	93.51
TB07	2.8	15.08	98.76	0	3	91.21

5. 4. SERIES-4: Oxime and Hydrazone derivatives of Benzamide analogues

5.4.1. BACKGROUND

Development in biological evaluation of heterocyclic has undergone manifold changes and the advancement in molecular biology has eased the design of new molecules based on their mechanism of action. In this regard, application of heterocyclic benzothiazole derivatives as efficient and potential agent has been focus of recent research for antibacterial drug discovery. Oximes represent versatile group of organic compounds that were extensively used as excellent ligands in pharmaceutical and synthetic applications, as important precursor in some antibiotics [Fukuoka *et al.,* 1993]. Besides, oximes, hydrazones have also been reported as compounds with great potential in cure of various diseases such as tuberculosis, leprosy and bacterial infections [Donde *et al.,* 2002]. Hydrazones are, in fact, the azomethines having triatomic group, >C=N-N<. Hydrazone function is an important part in compounds with antibacterial activity [Osorio *et al.,* 2012] and with activity against methicillin-resistant *S. aureus* [Pieczonka *et al.,* 2013].

From the view point of molecular design, joining two or more biologically active groups together in a single molecular framework will lead to development of more efficacious compounds. Herein, we synthesized some 2-(4'-aminophenyl) benzothiazole derivatives bearing oxime and hydrazone groups (**A07a, A07b, A10a** and **A10b**) of two potent benzothiazole bearing amide derivatives (A07 and A10) and evaluated their antimicrobial activity and its mode of action.

5.4.2. CHEMISTRY

The Oxime and Hydrazone derivatives of Benzothiazole (**A07a, A07b, A10a** and **A10b**) were obtained by refluxing the benzothiazole bearing amides derivatives and oximes and hydrazones in suitable solvent (ethanol) in presence of glacial HOAc as catalyst. The IR, ^{1}H-NMR, ^{13}C-NMR spectral data of synthesized compounds was in accordance with the proposed molecular structures. The FT-IR spectra showed absorption bands at 3,082–3,047 cm^{-1} for aromatic C–H, at 3,328–3,310 cm^{-1} for –NH str. group, at 3,257– 3,249 cm^{-1} for O–H str. of =N–OH group and at 3,389–3,382 cm^{-1} for N–H str. of NH_2 group. The ^{1}H NMR showed sharp singlet peak in the range of δ 3.75–3.49 ppm of –C–NH– group. A singlet at δ 12.1 ppm corresponds of =NOH group and two singlet peak at δ 10.37, 9.42 ppm corresponds to $–NH_2$ group. Multiplet at δ 7.11–7.94 ppm indicates the presence of aromatic protons. ^{13}C NMR spectra revealed the corresponding peaks in the range of δ 158.78-154.31 ppm of C=N. The peaks appearing in the range of δ 154.51–

156.94 ppm corresponds to benzothiazole–C–2 ring and of δ 119.45–141.75 ppm corresponds to aryl carbon. The physicochemical data of Oxime and Hydrazone derivatives of Benzothiazole are given in Table 5.21.

5.4.3. PHYSICOCHEMICAL AND SPECTRAL CHARACTERIZATION DATA

Table 5.21 Physicochemical data of Oxime and Hydrazone derivatives of Benzothiazole

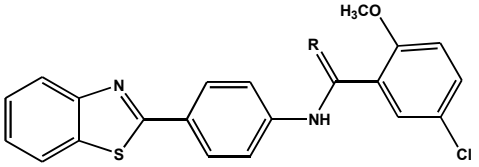

A07a, A07b

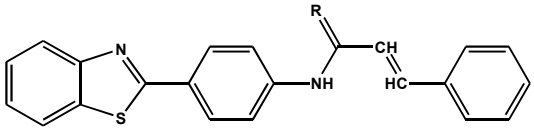

A10a, A10b

Compound code	R	MW	Melting point (℃)	Yield (%)	R_f (solvent system)	Solubility
A07a	=NOH	410.12	170–172	77	0.70 (B)	$CHCl_3$
A07b	$=NNH_2$	409.42	190–192	65	0.59 (B)	$CHCl_3$
A10a	=NOH	371.10	177–179	71	0.67 (B)	$CHCl_3$
A10b	$=NNH_2$	370.98	182–184	74	0.73 (A)	$CHCl_3$

Solvent system: (A) Methanol: Chloroform, 2:8, (B) Ethylacetate: Hexane, 7:3

Spectral data for Oxime and Hydrazone derivatives of benzothiazole

Compound A07a: *N-(4-(benzo[d]thiazol-2-yl)phenyl)-(1'-oxime)-2-methoxy-5-chloro-benzamides*

IR (KBr, υmax cm^{-1}): 3310.34 (–NH str.), 3257.45 (O–H str. of =N–OH group), 991.12 (=N–O str. of oxime group) 1385.34 (C=N str.), 3068.33 (Ar–C–H str.), 2846.11 (C–H str., OCH_3 group)

^{1}H NMR ($CDCl_3$, 300 MHz) δ (ppm): 7.12-7.80 (m, 11H, Ar–H), 12.15 (s, 1H, =NOH), 3.49 (s, 1H, –C–NH– group), 3.91 (s, 3H, OCH_3)

^{13}C NMR (DMSO-d6) δ (ppm): 158.78 (C=N), 58.43 (OCH_3), 154.51 (benzothiazole–C–2), 121.30-138.39 (Aromatic–C, C4–C9 C1'–C6' C1"–C6")

MS (m/z, %): 411 ($C_{21}H_{16}ClN_3O_2S$, $[M + H]^+$)

Anal $C_{21}H_{16}ClN_3O_2S$. Calc. for: C, 61.53; H, 3.93; N, 10.25. Found: C, 61.51; H, 3.90; N, 10.23%.

Compound A07b: *N-(4-(benzo[d]thiazol-2-yl)phenyl)-(1'-hydrazone)-2-methoxy-5-chloro-benzamides*

IR (KBr, υmax cm^{-1}): 3323.60 (–NH str.), 3382.21(N–H str. of NH_2 group), 3047.33 (Ar–C–H str.), 2867.31 (C–H str., OCH_3 group)

^1H NMR ($CDCl_3$, 300 MHz) δ (ppm): 7.11-7.78 (m, 11H, Ar–H), 10.37, 9.42 (2 s, 2H, NH_2), 3.57 (s, 1H, –C–NH– group), 3.89 (s, 3H, OCH_3)

^{13}C NMR (DMSO-d6) δ (ppm): 154.21 (C=N), 58.18 (OCH_3), 156.71 (benzothiazole–C–2), 121.86-138.35 (Aromatic–C, C4–C9 C1'–C6' C1"–C6")

MS (m/z, %): 410 ($C_{21}H_{17}ClN_4OS$, $[M + H]^+$)

Anal $C_{21}H_{17}ClN_4OS$. Calc. for: C, 61.68; H, 4.19; N, 13.70. Found: C, 61.65; H, 4.17; N, 13.68%.

Compound A10a: *N-(4-(benzo[d]thiazol-2-yl)phenyl)-(1'-oxime)-styrene-amides*

IR (KBr, υmax cm^{-1}): 3325.20 (–NH str.), 3249.54 (O–H str. of =N–OH group), 987.42 (=N–O str. of oxime group) 1388.34 (C=N str.), 3082.90 (Ar–C–H str.)

^1H NMR ($CDCl_3$, 300 MHz) δ (ppm): 7.16-7.84 (m, 13H, Ar–H), 12.10 (s, 1H, =NOH), 6.70, 6.76 (dd, –CH=CH), 3.65 (s, 1H, –C–NH– group)

^{13}C NMR (DMSO-d6) δ (ppm): 157.18 (C=N), 155.20 (benzothiazole–C–2), 120.61, 143.86 (–CH=CH), 123.26-139.75 (Aromatic–C, C4–C9 C1'–C6' C1"–C6")

MS (m/z, %): 372 ($C_{22}H_{17}N_3OS$, $[M + H]^+$)

Anal $C_{22}H_{17}N_3OS$. Calc. for: C, 71.14; H, 4.61; N, 11.31. Found: C, 71.12; H, 4.60; N, 11.30%.

Compound A10b: *N-(4-(benzo[d]thiazol-2-yl)phenyl)-(1'-hydrazone)-styrene-amides*

IR (KBr, υmax cm^{-1}): 3328.03 (–NH str.), 3389.31(N–H str. of NH_2 group), 3073.42 (Ar–C–H str.)

^1H NMR ($CDCl_3$, 300 MHz) δ (ppm): 7.28-7.96 (m, 13H, Ar–H), 10.17, 9.45 (2 s, 2H, NH_2), 6.71, 6.78 (dd, –CH=CH), 3.75 (s, 1H, –C–NH– group)

^{13}C NMR (DMSO-d6) δ (ppm): 154.31 (C=N), 156.94 (benzothiazole–C–2), 116.67, 142.90 (–CH=CH), 119.45-141.75 (Aromatic–C, C4–C9 C1'–C6' C1"–C6")

MS (m/z, %): 371 ($C_{22}H_{18}N_4S$, $[M + H]^+$)

Anal $C_{22}H_{18}N_4S$. Calc. for: C, 71.32; H, 4.90; N, 15.12. Found: C, 71.30; H, 4.88; N, 15.10%.

5.4.4. *IN-VITRO* ANTIMICROBIAL ACTIVITY

The results of antibacterial screening revealed that, compounds **A10a** and **A10b** showed moderate antibacterial activity. However, compounds **A07a and A07b** showed good antibacterial activity when compared with ciprofloxacin. Particularly, compound **A07a** showed maximum antibacterial activity (Zone of inhibition up to 31mm) against *E.coli* and *S.aureus*. Compound N-(4-(benzo[d]thiazol-2-yl)phenyl)(1'-hydrazone)-2-methoxy-5-chloro-benzamides (**A07a)** carrying chloro and methoxy groups on phenyl ring and oxime moiety on carbonyl carbon showed broad-spectrum antimicrobial activity with MIC values in the range of 3.91–31.2 µg/mL (Table 5.22 and 5.23). Among the four potent compounds, **A07a** and **A07b** displayed higher activity against *S. aureus* and *E. coli* due to optimum lipophilicity. In context to antifungal screening compound **A07a** showed good activity against *C. albicans* with a MIC of 15.6 µg/mL while the rest of the compounds showed moderate activity. None of the compounds exhibit activity against *C. krusei* strains. Thus, it was inferred that derivatives bearing chloro and methoxy substituents are the most suitable compounds for attaining the best antimicrobial spectrum.

Table 5.22 Antibacterial activity (MIC µg/mL) of Oxime and Hydrazone derivatives of benzothiazole (**A07a, A07b, A10a** and **A10b**)

Comp code	Bacteria					
	Gram positive bacteria		Gram negative bacteria			
	S. aureus **(ATCC 25323)**	***E. faecalis*** **(Clinical isolate)**	***E. coli*** **(ATCC 35218)**	***S. typhi*** **(MTCC 3216)**	***K. pneumonia*** **(ATCC 31488)**	***P. aeruginosa*** **(ATCC 27893)**
A07 a	28-31(3.91)	12-15(31.2)	24-25(7.81)	16-18(15.6)	13-15(31.2)	14-16(31.2)
A07 b	16-19(15.6)	11-13(62.5)	16-19(15.6)	13-15(31.2)	13-15(31.2)	16-19(15.6)
A10 a	<10(125)	11-13(62.5)	10-13(62.5)	<10(125)	12-15(31.2)	14-16(31.2)
A10 b	11-13(62.5)	12-13(62.5)	14-16(31.2)	<10(125)	12-15(31.2)	16-19(15.6)
CIP	30-32(≥6.25)	28-30(≥6.25)	33-35(≥6.25)	34-35(≥6.25)	29-30(≥6.25)	33-35(≥3.12)

Table 5.23 Antifungal activity (MIC µg/mL) of the Oxime and Hydrazone derivatives of benzothiazole (**A07a, A07b, A10a** and **A10b**)

Compound code	*C. albicans* (ATCC 90028)	*C. tropicalis* (ATCC 750)	*C. krusei* (ATCC 6268)
A07 a	16-18(15.6)	<10(125)	-
A07 b	10-12(62.5)	14-16(31.2)	-
A10 a	<10(125)	13-15(31.2)	-
A10 b	12-15(31.2)	<10(125)	-
Fluconazole	22-25(6.25)	24-27 (6.25)	20-24(6.25)

The value of each compound consisted of 'zone of inhibition range (MIC)' of 03 replicates. Level of significance $p < 0.05$.

5.4.4.1. Mechanism of action study

Bactericidal kinetics

The bactericidal activity of lead compounds **A07a** and **A07b** were directed in confirming its potency toward the specific *S.aureus* and *E.coli* strains. Time-kill studies demonstrated that compounds **A07a** and **A07b** were rapid with 90 to 99% lethality within 2 to 5 h (Fig. 5.42).The inhibition kinetics in *E.coli* and *S.aureus* showed compound **A07b** to be less effective than **A07a** even up to 5 h. At concentration of 4 × MIC, both the compounds inhibited bacterial growth 2 h onwards until 5 h.

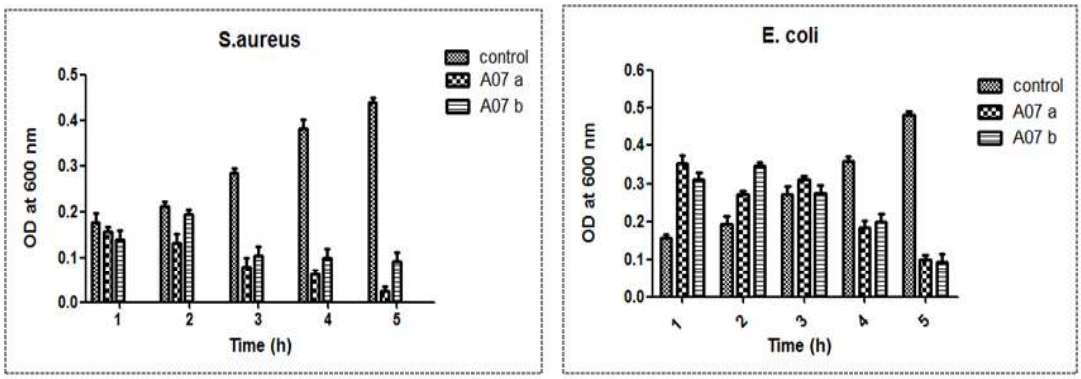

A B

Fig. 5.42 Bactericidal kinetics of (A) *S.aureus* (B) *E.coli* after treatment with test compounds **A07a** and **A07b** at 4 × MIC.

Membrane depolarization

At the maximum concentration of designed analogues **A07a, b** and **A10a, b** tested (i.e., 4 x MIC), the level of depolarization reached to saturation from about 2 to 5 mins of time. All the novel analogues studied here were found to have the ability to depolarize the cytoplasmic membrane of *S.aureus* and *E.coli*; however, the compounds with different structures have different concentration-activity profiles (data not shown here). Compounds **A07a** and **A07b** have completely depolarized the membrane at concentrations lower than those other compounds used in study. All compounds showed similar profile with respect to positive control triton (Fig. 5.43).

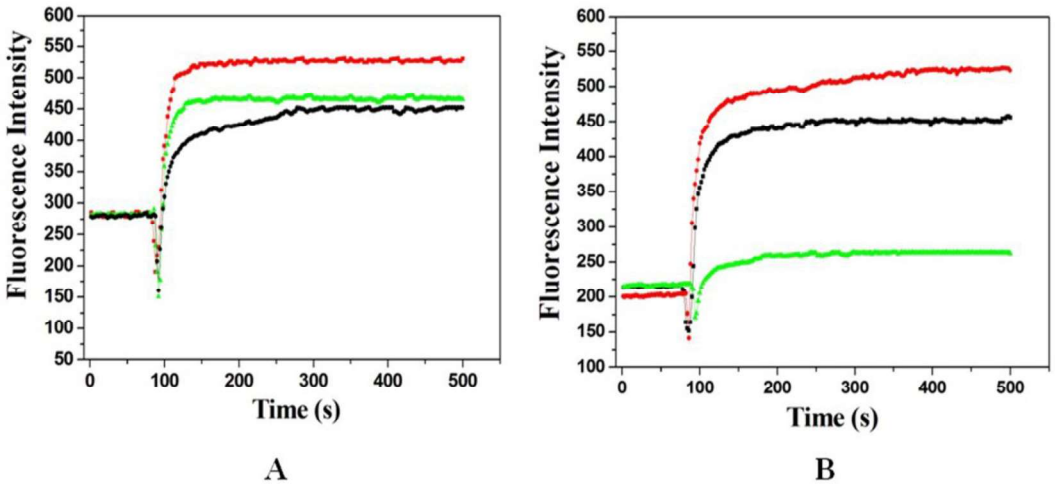

Fig. 5.43. Membrane depolarization aptitude of test compounds **A07a** and **A07b** at 4 × MIC on (A) *S.aureus* and (B) *E.coli*. Compounds represented as red curve for **A07a**, green curve for **A07b** and black curve for Triton 2% (positive control).

Membrane permeability of viable bacteria

Consistent with the outer membrane depolarization assay of bacteria, designed analogues **A07a** and **A07b** induced damages to the membrane organization of *S. aureus* and leads to more pore formation as compared to *E. coli* as indicated by PI staining of the cells (Fig. 5.44). However, maximum damage of bacterial membrane of both strains was observed in compound **A07a** with a value of 44% in *E. coli* and 77% in *S. aureus* as compared to compound **A07b** causing damage with a range of 25-30%.

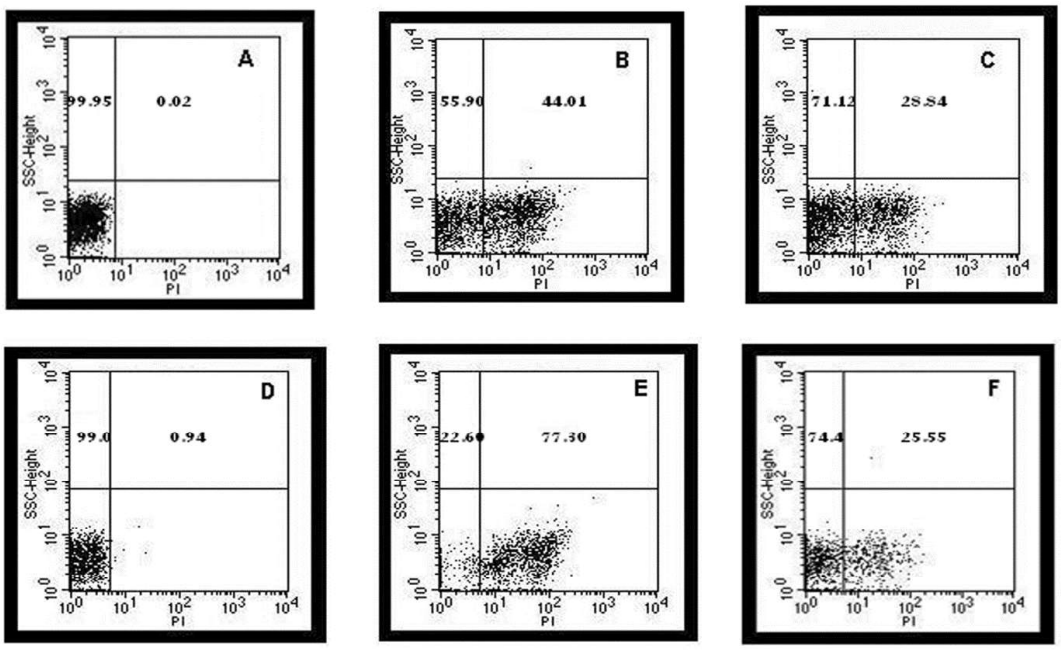

Fig. 5.44 Fluorescence assisted cell sorting (FACS) data of *E. coli* and *S.aureus* (A–F). On *E. coli* (A) control without PI treatment (B) **A07a** (C) **A07b** and, on *S.aureus* (D) control without PI treatment (E) **A07a** (F) **A07b** respectively.

DNA binding activity

In conjunction with the results of membrane permeabilization assay and FACS analysis, we conclude that series of benzothiazole bearing oxime and hydrazone moiety could dislodge the integrity of membrane, leading to bacterial cell contents leakage. Simultaneously, during the interaction process with membrane, test compounds unavoidably come into cytoplasm, but the outcome of test compounds in the cytoplasm is absolutely unknown. Thus, we determined the DNA-binding propensity of test compounds **A07a, A07b, A10a** and **A10b** to determine the mode of action. Results signifies compound **A07a** exhibit prominent binding with DNA (200ng) causing retardation at 7.81 µg/mL, whereas for **A07b** retardation was found at 31.2 µg/mL concentration (Fig. 5.45) and leads to cleavage of plasmid DNA also, at higher concentration of the lead compounds. However it was fascinating that DNA binding/retardation was predisposed with the whole structure of the compounds, i.e. chloro and methoxy containing compound **A07a,b** showed most potent DNA retardation ability in comparison with styrene analog **A10a,b**.

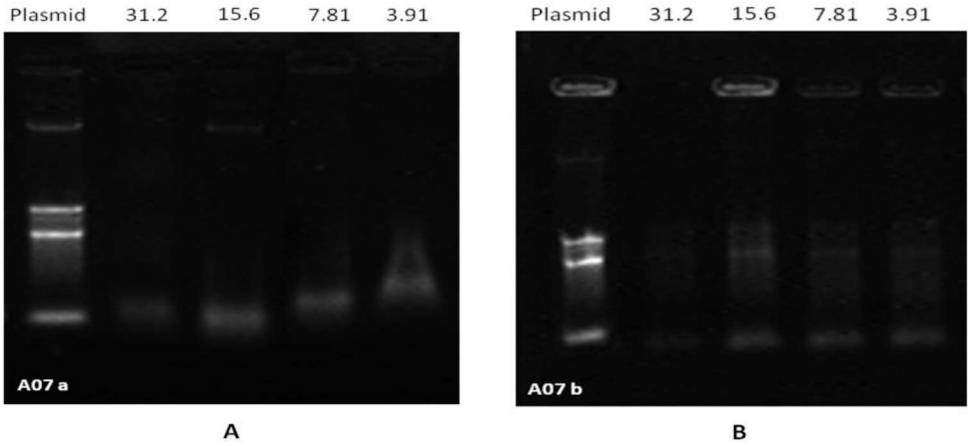

Fig. 5.45 DNA binding Agarose gel electrophoresis represents (A) **A07a** and (B) **A07b,** in concentration range: 31.2–3.91 µg/mL, after 1 h incubation time using pUC19 (200 ng).

5.4.4.2. Docking study against Glc-6-PS

Molecular docking study of Oxime and Hydrazone derivatives of benzothiazole revealed all the compounds showed good binding interactions with energy ranging from 4-6 dock score except compound **A07b** with a poor dock score of 2.68, and were comparable with the standard drugs ciprofloxacin and fluconazole. Compounds **A07a, A10a** and **A10b** showed good docking score with receptor as shown in Table 5.24. Compound **A07a** was found to have a score of 6.12 forming strong H-bond with Val399, Gly301, Thr302 and Ser604. The ligand receptor interactions of compound **A07a** and **A07b** is shown in Fig. 5.46. Finally results revealed that the wet lab findings are in agreement with dry lab findings.

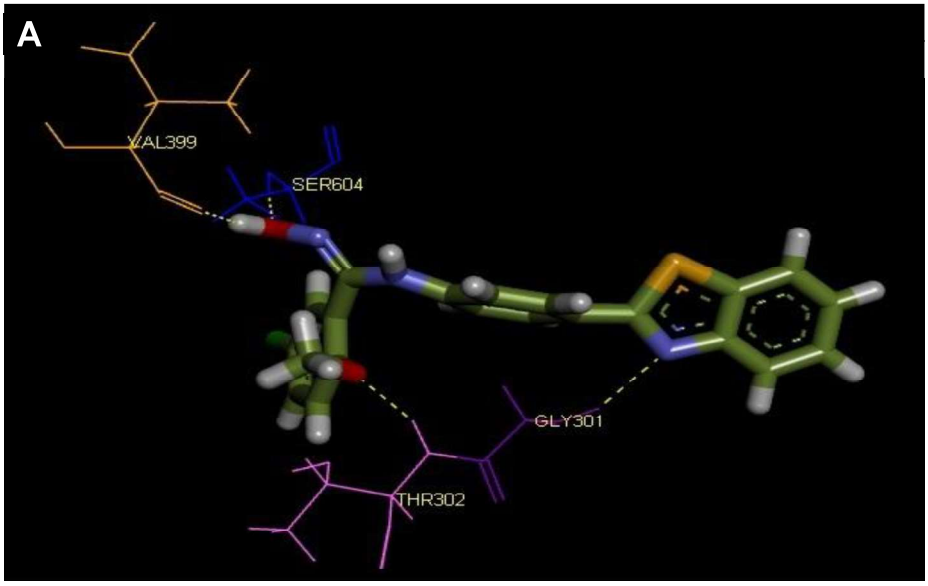

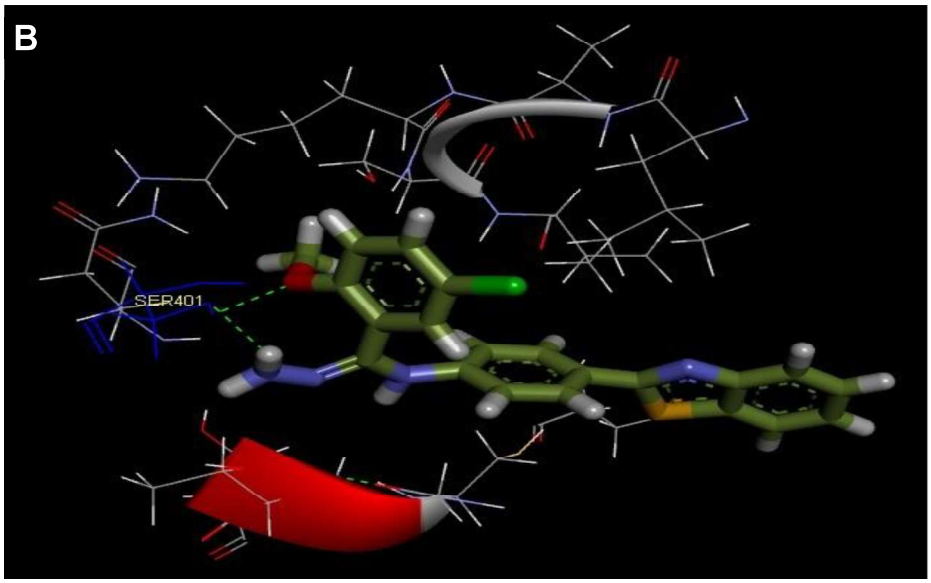

Fig. 5.46 Binding pose of compound (A) **A07a** and (B) **A07b** with glucosamine-6-phosphate synthase. Hydrogen bonding interactions are displayed by green dotted lines.

Table 5.24 Molecular docking scores of Oxime and Hydrazone derivatives of benzothiazole with GlcN-6-P synthase.

Sr. No	Compound Id	Docking Score	Crash Value	Interacting amino acids
1	A07a	6.1623	-0.8253	Val399, Gly301, Thr302, Ser604
2	A07b	2.6832	-1.1011	Ser401,
3	A10a	5.3829	-0.9665	Ser401, Lys485, Glu488,
4	A10b	4.5518	-0.9995	Thr302,Lys485,Ser401, Glu488
5	Ciprofloxacin	6.0614	2.0428	Ser347, Gln348, Ser349, Ser401, Lys485
6	Fluconazole	6.4092	-1.4344	Val399, Gln348, Ser349, Lys485, Ser604

5.4.4.3. *In-Silico* Pharmacokinetic Predictions

In-silico pharmacokinetic properties prediction was carried out for the Oxime and Hydrazone derivatives of benzothiazole **A07a** and **A10a** having significant antimicrobial activity and good docking score and checked for their ADME properties by using preADMET server. The predicted drug likelinesss of the all synthesized compounds follows the Lipinski''Rule of Five''. Both the compounds showed prominent human intestinal absorption and plasma protein binding with a good lipophilicity thus, suggested pronounced interactions with the receptor GlcN-6-P synthase. The results are summarized in Table 5.25.

Table 5.25 Theoretical prediction of different properties of Oxime and Hydrazone derivatives of benzothiazole using PreADMET Server

Comp No.	Log p	$LogS_b$ (mg/L)	HIA (%)	HB-donors	HB-acceptors	*In-vitro* PPB (%)
A07a	4.6	78.6	85.25	1	5	98.45
A10a	3.5	25.12	87.36	1	4	99.13

5. 5. SERIES-5: Semicarbazone and Thiosemicarbazone derivatives of Benzamide analogues

5.5.1. BACKGROUND

Treating infectious diseases, caused by bacteria or fungi, remains an important and challenging public health problem. The exploration of new heterocycles that can accommodate potency to multiple biological targets remains an intriguing scientific endeavour. 2-(4-aminophenyl) benzothiazole moiety is present in various bioactive molecules such as orexin receptor antagonist [Bergman *et al*., 2006] and the Gram-positive selective antibacterial [Ali *et al*., 2001]. Structure-activity relationship (SAR) carried out on these heterocycles have shown that positions 2 and 6 are crucial for antibacterial activity against Gram-positive and Gram-negative bacterial strains [Yildiz-Oren *et al*., 2004].

The chemistry of thiosemicarbazone and semicarbazone has received considerable attention because of their variable bonding modes, promising biological implications, structural diversity, and ion–sensing ability [Mishra *et al*., 2006]. Semicarbazones and thiosemicarbazones have been known to show significant pharmacological profiles against important pathogens. In addition to these, there has been a growing attention towards thiosemicarbazones and semicarbazones related to their wide range of biological properties, specifically as antifungal, antibacterial [Pandeya *et al*., 2012], antitubercular [Cocco *et al*., 2002] agents etc. Keeping this in view, we have developed newer analogs of the nucleus-benzothiazole i.e., semicarbazone and thiosemicarbazone derivatives (**SC01–10** and **TS01-10)** and carried out its biological activity against different Gram-positive (*S. aureus*, *E. faecalis*) and Gram-negative (*E. coli, S. typhi, K. pneumoniae, P. aeruginosa*) bacterial and three fungal strains.

5.5.2. CHEMISTRY

The Semicarbazone and Thiosemicarbazone derivatives of Benzothiazole (**SC01–10** and **TS01-10**) were obtained by refluxing the equimolar quantities of benzothiazole bearing amides derivatives and Semicarbazide/ Thiosemicarbazide hydrochloride in suitable solvent (ethanol) in presence of glacial NaOAc as catalyst. The IR, ^{1}H-NMR, ^{13}C-NMR spectral data of synthesized compounds was in accordance with the proposed molecular structures. The FT-IR spectra showed absorption bands at 3,107–3,0343 cm^{-1} for aromatic C–H. Band at 3,298–3,112 cm^{-1} and at 3,506– 3,184 cm^{-1} confirms the presence

of –NH str. and $–NH_2$ str. group respectively. Band at 1,678–1,624 cm^{-1} corresponds to C=O str. of semicarbazone group and at 1,273–1,242 cm^{-1} corresponds to C=S str. of thiosemicarbazone group. The ^1H NMR showed sharp singlet peak in the range of δ 13.97–13.11 ppm of –NH group. Two sharp singlet peaks in the range at δ 9.83–8.31 ppm corresponds to $–NH_2$ group. Multiplet at δ 7.00–8.23 ppm indicates the presence of aromatic protons. ^{13}C NMR spectra revealed the corresponding peaks in the range of δ 157.78-145.11 ppm of –C=N. The peak appearing in the range of δ 167.51–162.94 ppm corresponds to carbonyl carbon of C=O group and δ 184.27–181.14 ppm of thiol carbon of C=S group. A peak at δ 159.73–155.13 ppm signifies of benzothiazole–C–2 ring and of δ 111.54–148.10 ppm corresponds to aryl carbon.

Depending upon the polarity of compounds, eluents used for TLC analysis included (A) Methanol: Chloroform-2:8; (B) Methanol: Chloroform-1:9; (C) Ethyl acetate: Hexane-7:3. For each reaction, a single distinct spot of product was observed in TLC analysis which confirmed the completion of reaction and purity of synthesized compounds. Most of the compounds were obtained in satisfactory yield (52 to 91%) except SC04 (46%). Results of Log P value analysis indicated that incorporation of semicarbazone and thiosemicarbazone group imparted the hydrophilicity and for each compound Log P value is less than 3, indicating their suitability for passive transcellular absorption across intestinal epithelia. All compounds showed sharp melting point with the narrow melting range, indicating the purity of compounds (Table 5.26).

5.5.3. PHYSICOCHEMICAL AND SPECTRAL CHARACTERIZATION DATA

Table 5.26 Physicochemical properties of Semicarbazone and Thiosemicarbazone derivatives of Benzothiazole (**SC01-10**) and (**TS01-10**)

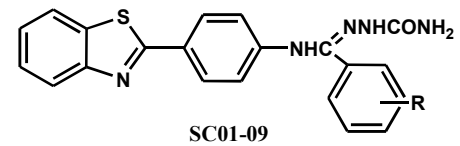

SC01-09

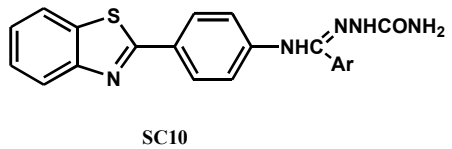

SC10

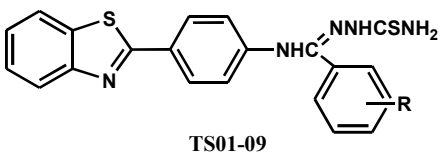

TS01-09

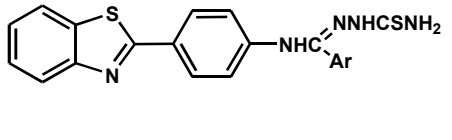

TS10

Compound code	R, Ar	MW	Melting point (℃)	Yield (%)	R_f (solvent system)	Solubility
SC01	H	387.46	198-200	76	0.73 (A)	$CHCl_3$, MeOH, EtAc
SC02	3,5-di NO_2	477.45	222-224	56	0.68 (B)	$CHCl_3$, EtAc
SC03	2-OH	403.46	218-220	78	0.71 (A)	$CHCl_3$, MeOH, EtAc
SC04	3-NO_2	432.46	192-194	46	0.65 (B)	$CHCl_3$, MeOH
SC05	2-Cl	421.92	248-250	81	0.55 (B)	$CHCl_3$, MeOH, EtAc
SC06	2-F	405.45	240-242	67	0.60 (A)	$CHCl_3$, MeOH
SC07	5-Cl, 2-OCH_3	451.93	259-260	84	0.63 (A)	MeOH, EtAc
SC08	2,4-diOH	419.46	210-212	72	0.69 (B)	$CHCl_3$, EtAc
SC09	2-OCH_3	417.48	227-229	66	0.72 (A)	$CHCl_3$, MeOH, EtAc
SC10	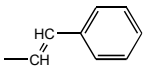	413.49	201-203	52	0.69 (A)	$CHCl_3$, MeOH, EtAc
TS01	H	403.52	189-190	70	0.58 (A)	$CHCl_3$, MeOH
TS02	3,5-di NO_2	493.52	187-189	59	0.69 (C)	$CHCl_3$, MeOH
TS03	2-OH	419.52	211-213	84	0.62 (C)	$CHCl_3$, MeOH
TS04	3-NO_2	448.52	224-225	68	0.55 (A)	$CHCl_3$, MeOH
TS05	2-Cl	437.97	261-263	85	0.73 (B)	$CHCl_3$, MeOH
TS06	2-F	421.51	236-238	79	0.70 (C)	$CHCl_3$, MeOH
TS07	5-Cl, 2-OCH_3	467.99	239-240	91	0.68 (B)	$CHCl_3$, MeOH
TS08	2,4-diOH	435.52	227-229	86	0.52 (B)	$CHCl_3$, MeOH
TS09	2-OCH_3	433.55	206-208	72	0.65 (C)	$CHCl_3$, MeOH
TS10	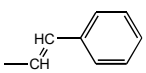	429.56	215-218	82	0.57 (B)	$CHCl_3$, MeOH

Solvent system: (A) Methanol: Chloroform, 2:8, (B) Methanol: Chloroform, 1:9, (C) Ethylacetate: Hexane, 7:3

Spectral data for Semicarbazone and Thiosemicarbazone derivatives of Benzothiazole

Compound SC01: *N-(4-(benzo[d]thiazol-2-yl)phenyl)-(1'-semicarbazone)benzamides*

IR (KBr, υmax cm^{-1}): 3248.06 (–NH str.), 3367.04, 3343.63 (–NH_2 str.), 1673.50 (C=O str. of semicarbazone), 1572.57 (C=N str.), 3078.12 (Ar–C–H str.)

^{1}H NMR ($CDCl_3$, 300 MHz, δ ppm): 7.21–7.88 (m, 13H, Ar–H), 13.56 (s, 1H, NH), 9.35 (s, 1H, –CNH), 8.95, 8.93 (2s, 2H, NH_2)

^{13}C NMR (*DMSO–d6*, 300 MHz, δ ppm): 165.28 (C=O of semicarbazone), 151.32 (–C=N), 156.23 (benzothiazole–C–2), 118.16–141.67 (Aromatic–C, C4–C9 C1′–C6′ C1″–C6″)

MS (*m/z*, %): 388 (M + 1, 100).

Anal $C_{21}H_{17}N_5OS$. Calc. for: C, 65.10; H, 4.42; N, 18.08. Found: C, 65.10; H, 4.40; N, 18.06%.

Compound SC02: *N-(4-(benzo[d]thiazol-2-yl)phenyl)-(1'-semicarbazone)-3,5-dinitro-benzamides*

IR (KBr, υmax cm^{-1}): 3143.81 (–NH str.), 3214.09, 3358.10 (–NH_2 str.), 1631.42 (C=O str. of semicarbazone), 1565.38 (C=N str.), 1320.31, 1555.28 (NO_2 str.), 3079.23 (Ar–C–H str.)

^{1}H NMR ($CDCl_3$, 300 MHz, δ ppm): 7.12–7.78 (m, 11H, Ar–H), 13.11 (s, 1H, NH), 9.41 (s, 1H, –CNH), 8.42, 8.36 (2s, 2H, NH_2)

^{13}C NMR (*DMSO–d6*, 300 MHz, δ ppm): 162.97 (C=O of semicarbazone), 152.64 (–C=N), 157.06 (benzothiazole–C–2), 121.36–138.42 (Aromatic–C, C4–C9 C1′–C6′ C1″–C6″)

MS (*m/z*, %): 478 (M + 1, 100).

Anal $C_{21}H_{15}N_7O_5S$. Calc. for: C, 52.83; H, 3.17; N, 20.54. Found: C, 52.81; H, 3.15; N, 20.54%.

Compound SC03: *N-(4-(benzo[d]thiazol-2-yl)phenyl)-(1'-semicarbazone)-2-hydroxy-benzamides*

IR (KBr, υmax cm^{-1}): 3231.06 (–NH str.), 3359.21, 3375.03 (–NH_2 str.), 1655.85 (C=O str. of semicarbazone), 1571.18 (C=N str.), 3491.83 (–OH str.), 3047.33 (Ar–C–H str.)

^{1}H NMR ($CDCl_3$, 300 MHz, δ ppm): 7.18–7.80 (m, 12H, Ar–H), 13.42 (s, 1H, NH), 9.33 (s, 1H, –CNH), 8.85, 8.78 (2s, 2H, NH_2), 10.46 (br, s, 1H, –OH)

^{13}C NMR (*DMSO–d6*, 300 MHz, δ ppm): 166.08 (C=O of semicarbazone), 152.54 (–C=N), 155.13 (benzothiazole–C–2), 113.10–142.52 (Aromatic–C, C4–C9 C1′–C6′ C1″–C6″); MS (*m/z*, %): 404 (M + 1, 100).

Anal $C_{21}H_{17}N_5O_2S$. Calc. for: C, 62.52; H, 4.25; N, 17.36. Found: C, 62.51; H, 4.23; N, 17.35%.

Compound SC04: *N-(4-(benzo[d]thiazol-2-yl)phenyl)-(1'-semicarbazone)-3-nitro-benzamides*

IR (KBr, υmax cm^{-1}): 3180.72 (–NH str.), 3267.52, 3327.32 (–NH_2 str.), 1624.12 (C=O str. of semicarbazone), 1577.82 (C=N str.), 1313.57, 1533.46 (NO_2 str.), 3037.99 (Ar–C–H str.)

^{1}H NMR ($CDCl_3$, 300 MHz, δ ppm): 7.00–7.91 (m, 12H, Ar–H), 13.17 (s, 1H, NH), 9.36 (s, 1H, –CNH), 8.43, 8.31 (2s, 2H, NH_2)

^{13}C NMR (*DMSO–d6*, 300 MHz, δ ppm): 163.27 (C=O of semicarbazone), 153.00 (–C=N), 156.56 (benzothiazole–C–2), 124.56–133.94 (Aromatic–C, C4–C9 C1′–C6′ C1″–C6″)

MS (*m/z*, %): 433 (M + 1, 100).

Anal $C_{21}H_{16}N_6O_3S$. Calc. for: C, 58.32; H, 3.73; N, 19.43. Found: C, 58.30; H, 3.72; N, 19.43%.

Compound SC05: *N-(4-(benzo[d]thiazol-2-yl)phenyl)-(1'-semicarbazone)-2-chloro-benzamides*

IR (KBr, υmax cm^{-1}): 3226.81 (–NH str.), 3315.94, 3365.03 (–NH_2 str.), 1678.30 (C=O str. of semicarbazone), 1566.32 (C=N str.), 1052.67 (–C–Cl str.), 3082.92 (Ar–C–H str.);

^{1}H NMR ($CDCl_3$, 300 MHz, δ ppm): 7.01–7.75 (m, 12H, Ar–H), 13.46 (s, 1H, NH), 9.43 (s, 1H, –CNH), 8.76, 8.85 (2s, 2H, NH_2)

^{13}C NMR (*DMSO–d6*, 300 MHz, δ ppm): 163.88 (C=O of semicarbazone), 152.12 (–C=N), 156.06 (benzothiazole–C–2), 121.15–144.21 (Aromatic–C, C4–C9 C1′–C6′ C1″–C6″MS (*m/z*, %): 422 (M + 1, 100).

Anal $C_{21}H_{16}ClN_5OS$. Calc. for: C, 59.78; H, 3.82; N, 16.60. Found: C, 59.76; H, 3.80; N, 16.60%.

Compound SC06: *N-(4-(benzo[d]thiazol-2-yl)phenyl)-(1'-semicarbazone)-2-fluoro-benzamides*

IR (KBr, υmax cm^{-1}): 3298.38 (–NH str.), 3421.83, 3506.70 (–NH_2 str.), 1647.26 (C=O str. of semicarbazone), 1543.10 (C=N str.), 3107.43 (Ar–C–H str.)

^{1}H NMR ($CDCl_3$, 300 MHz, δ ppm): 7.07–7.88 (m, 12H, Ar–H), 13.32 (s, 1H, NH), 9.56 (s, 1H, –CNH), 8.53, 8.51 (2s, 2H, NH_2)

^{13}C NMR (*DMSO–d6*, 300 MHz, δ ppm): 167.31 (C=O of semicarbazone), 153.17 (–C=N), 159.73 (benzothiazole–C–2), 115.79–139.17 (Aromatic–C, C4–C9 C1′–C6′ C1″–C6″)

MS (*m/z*, %): 406 (M + 1, 100).

Anal $C_{21}H_{16}FN_5OS$ Calc. for: C, 62.21; H, 3.98; N, 17.27. Found: C, 62.20; H, 3.96; N, 17.26%.

Compound SC07: *N-(4-(benzo[d]thiazol-2-yl)phenyl)-(1'-semicarbazone)-2-methoxy-5-chloro-benzamides*

IR (KBr, υmax cm^{-1}): 3253.12 (–NH str.), 3365.31, 3387.73 (–NH_2 str.), 1673.30 (C=O str. of semicarbazone), 1532.92 (C=N str.), 1062.17 (–C–Cl str.), 2917.66 (–C–H str. of OCH_3), 3069.92 (Ar–C–H str.)

^{1}H NMR ($CDCl_3$, 300 MHz, δ ppm): 7.27–7.98 (m, 11H, Ar–H), 13.31 (s, 1H, NH), 9.54 (s, 1H, –CNH), 8.37, 8.74 (2s, 2H, NH_2), 3.81 (s, 3H, OCH_3)

^{13}C NMR (*DMSO–d6*, 300 MHz, δ ppm): 55.60 (OCH_3), 162.38 (C=O of semicarbazone), 154.26 (–C=N), 156.49 (benzothiazole–C–2), 122.62–140.61 (Aromatic–C, C4–C9 C1′–C6′ C1″–C6″)

MS (*m/z*, %): 452 (M + 1, 100).

Anal $C_{22}H_{18}ClN_5O_2S$ Calc. for: C, 58.47; H, 4.01; N, 15.50. Found: C, 58.45; H, 4.00; N, 15.50%.

Compound SC08: *N-(4-(benzo[d]thiazol-2-yl)phenyl)-(1'-semicarbazone)-2,4-dihydroxy-benzamides*

IR (KBr, υmax cm^{-1}): 3242.16 (–NH str.), 3374.13, 3379.03 (–NH_2 str.), 1645.08 (C=O str. of semicarbazone), 1562.78 (C=N str.), 3361.83 (–OH str.), 3054.63 (Ar–C–H str.)

^{1}H NMR ($CDCl_3$, 300 MHz, δ ppm): 7.16–7.70 (m, 11H, Ar–H), 13.23 (s, 1H, NH), 9.26 (s, 1H, –CNH), 8.71, 8.79 (2s, 2H, NH_2), 10.21, 10.34 (s, 2H, –OH)

^{13}C NMR (*DMSO–d6*, 300 MHz, δ ppm): 162.15 (C=O of semicarbazone), 153.64 (–C=N), 156.38 (benzothiazole–C–2), 111.54–138.02 (Aromatic–C, C4–C9 C1′–C6′ C1″–C6″)

MS (*m/z*, %): 420 (M + 1, 100).

Anal $C_{21}H_{17}N_5O_3S$ Calc. for: C, 60.13; H, 4.09; N, 16.70. Found: C, 60.12; H, 4.07; N, 16.70%.

Compound SC09: *N-(4-(benzo[d]thiazol-2-yl)phenyl)-(1'-semicarbazone)-2-methoxy-benzamides*

IR (KBr, υmax cm^{-1}): 3206.41 (–NH str.), 3295.14, 3342.83 (–NH_2 str.), 1666.13 (C=O str. of semicarbazone), 1573.72 (C=N str.), 2948.30 (–C–H str. of OCH_3), 3074.22 (Ar–C–H str.)

^{1}H NMR ($CDCl_3$, 300 MHz, δ ppm): 7.13–7.69 (m, 12H, Ar–H), 13.28 (s, 1H, NH), 9.48 (s, 1H, –CNH), 8.64, 8.82 (2s, 2H, NH_2), 3.80 (s, 3H, OCH_3)

^{13}C NMR (*DMSO–d6*, 300 MHz, δ ppm): 55.62 (OCH_3), 162.14 (C=O of semicarbazone), 153.23 (–C=N), 155.10 (benzothiazole–C–2), 118.35–148.10 (Aromatic–C, C4–C9 C1′–C6′ C1″–C6″)

MS (*m/z*, %): 418 (M + 1, 100).

Anal $C_{22}H_{19}N_5O_2S$. Calc. for: C, 63.29; H, 4.59; N, 16.78. Found: C, 63.27; H, 4.57; N, 16.76%.

Compound SC10: *N-(4-(benzo[d]thiazol-2-yl)phenyl)-(1'-semicarbazone)-styrene-amides*

IR (KBr, υmax cm^{-1}): 3237.47 (–NH str.), 3335.14, 3371.39 (–NH_2 str.), 1652.92 (C=O str. of semicarbazone), 1563.12 (C=N str.), 3083.02 (Ar–C–H str.)

^{1}H NMR ($CDCl_3$, 300 MHz, δ ppm): 7.19–7.75 (m, 13H, Ar–H), 9.51 (s, 1H, –CNH), 6.70, 6.73 (dd, –CH=CH)

^{13}C NMR (*DMSO–d6*, 300 MHz, δ ppm): 165.28 (C=O of amide), 153.13 (–C=N), 156.00 (benzothiazole–C–2), 117.32–138.75 (Aromatic–C, C4–C9 C1′–C6′ C1″–C6″)

MS (*m/z*, %): 414 (M + 1, 100).

Anal $C_{23}H_{19}N_5OS$. Calc. for: C, 66.81; H, 4.63; N, 16.94. Found: C, 66.80; H, 4.61; N, 16.92%.

Compound TS01: *N-(4-(benzo[d]thiazol-2-yl)phenyl)-(1'-thiosemicarbazone)benzamides*

IR (KBr, υmax cm^{-1}): 3176.56 (–NH str.), 3326.12, 3210.73 (–NH_2 str.), 1271.60 (C=S str.), 1542.17 (C=N str.), 3048.15 (Ar–C–H str.)

^{1}H NMR ($CDCl_3$, 300 MHz, δ ppm): 7.32–7.98 (m, 13H, Ar–H), 13.61 (s, 1H, NH), 9.28 (s, 1H, –CNH), 9.15, 8.92 (2s, 2H, NH_2)

^{13}C NMR (*DMSO–d6*, 300 MHz, δ ppm): 181.08 (C=S), 149.02 (–C=N), 157.13 (benzothiazole–C–2), 121.16–141.63 (Aromatic–C, C4–C9 C1′–C6′ C1″–C6″)

MS (*m/z*, %): 404 (M + 1, 100).

Anal $C_{21}H_{17}N_5S_2$. Calc. for: C, 62.51; H, 4.25; N, 17.36. Found: C, 62.49; H, 4.24; N, 17.34%.

Compound TS02: *N-(4-(benzo[d]thiazol-2-yl)phenyl)-(1'-thiosemicarbazone)-3,5-dinitro-benzamides*

IR (KBr, υmax cm^{-1}): 3122.86 (–NH str.), 3321.53, 3184.58 (–NH_2 str.), 1242.20 (C=S str.), 1575.89 (C=N str.), 3036.06 (Ar–C–H str.), 1311.64, 1348.29, 1533.46 (NO_2 str.)

^{1}H NMR ($CDCl_3$, 300 MHz, δ ppm): 7.26–8.23 (m, 11H, Ar–H), 13.68 (s, 1H, NH), 9.72 (s, 1H, –CNH), 9.21, 8.91 (2s, 2H, NH_2)

^{13}C NMR (*DMSO–d6*, 300 MHz, δ ppm): 182.49 (C=S), 149.53 (–C=N), 158.11 (benzothiazole–C–2), 124.07–139.42 (Aromatic–C, C4–C9 C1′–C6′ C1″–C6″)

MS (*m/z*, %): 494 (M + 1, 100).

Anal $C_{21}H_{15}N_7O_4S_2$. Calc. for: C, 51.11; H, 3.06; N, 19.87. Found: C, 51.10; H, 3.04; N, 19.88%.

Compound TS03: *N-(4-(benzo[d]thiazol-2-yl)phenyl)-(1'-thiosemicarbazone)-2-hydroxy-benzamides*

IR (KBr, υmax cm^{-1}): 3183.15 (–NH str.), 3363.13, 3217.80 (–NH_2 str.), 1239.10 (C=S str.), 1562.19 (C=N str.), 3079.16 (Ar–C–H str.)

^{1}H NMR ($CDCl_3$, 300 MHz, δ ppm): 7.12–8.02 (m, 12H, Ar–H), 13.93 (s, 1H, NH), 9.67 (s, 1H, –CNH), 9.10, 8.89 (2s, 2H, NH_2)

^{13}C NMR (*DMSO–d6*, 300 MHz, δ ppm): 183.45 (C=S), 145.72 (–C=N), 156.14 (benzothiazole–C–2), 121.37–138.83 (Aromatic–C, C4–C9 C1′–C6′ C1″–C6″)

MS (*m/z*, %): 420 (M + 1, 100).

Anal $C_{21}H_{17}N_5OS_2$. Calc. for: C, 60.12; H, 4.08; N, 16.69. Found: C, 60.12; H, 4.06; N, 16.68%.

Compound TS04: *N-(4-(benzo[d]thiazol-2-yl)phenyl)-(1'-thiosemicarbazone)-3-nitro-benzamides*

IR (KBr, υmax cm^{-1}): 3212.95 (–NH str.), 3381.15 (–NH_2 str.), 1246.90 (C=S str.), 1573.29 (C=N str.), 3099.26 (Ar–C–H str.)

^{1}H NMR ($CDCl_3$, 300 MHz, δ ppm): 7.14–7.87 (m, 12H, Ar–H), 13.72 (s, 1H, NH), 9.84 (s, 1H, –CNH), 9.21, 8.76 (2s, 2H, NH_2)

^{13}C NMR (*DMSO–d6*, 300 MHz, δ ppm): 181.44 (C=S), 147.84 (–C=N), 156.39 (benzothiazole–C–2), 122.46–139.03 (Aromatic–C, C4–C9 C1′–C6′ C1″–C6″)

MS (*m/z*, %): 449 (M + 1, 100).

Anal $C_{21}H_{16}N_6O_2S_2$. Calc. for: C, 56.23; H, 3.60; N, 18.74. Found: C, 56.22; H, 3.60; N, 18.72%.

Compound TS05: *N-(4-(benzo[d]thiazol-2-yl)phenyl)-(1'-thiosemicarbazone)-2-chloro-benzamides*

IR (KBr, υmax cm^{-1}): 3122.86 (–NH str.), 3329.25 (–NH_2 str.), 1244.13 (C=S str.), 1575.89 (C=N str.), 3034.13 (Ar–C–H str.) 1087.89 (C–Cl); ^{1}H NMR ($CDCl_3$, 300 MHz, δ ppm): 7.31–7.88 (m, 12H, Ar–H), 13.87 (s, 1H, NH), 9.66 (s, 1H, –CNH), 8.93, 8.81 (2s, 2H, NH_2); ^{13}C NMR (*DMSO–d6*, 300 MHz, δ ppm): 181.30 (C=S), 157.42 (–C=N), 164.24 (benzothiazole–C–2), 124.56–139.90 (Aromatic–C, C4–C9 C1′–C6′ C1″–C6″); MS (*m/z*, %): 438 (M + 1, 100).

Anal $C_{21}H_{16}ClN_5S_2$. Calc. for: C, 57.59; H, 3.68; N, 15.99. Found: C, 57.57; H, 3.67; N, 15.97%.

Compound TS06: *N-(4-(benzo[d]thiazol-2-yl)phenyl)-(1'-thiosemicarbazone)-2-fluoro-benzamides*

IR (KBr, υmax cm^{-1}): 3168.13 (–NH str.), 3336.25, 3214.65 (–NH_2 str.), 1258.12 (C=S str.), 1566.39 (C=N str.), 3078.54 (Ar–C–H str.); ^{1}H NMR ($CDCl_3$, 300 MHz, δ ppm): 7.19–7.79 (m, 12H, Ar–H), 13.97 (s, 1H, NH), 9.42 (s, 1H, –CNH), 9.83, 8.78 (2s, 2H, NH_2); ^{13}C NMR (*DMSO–d6*, 300 MHz, δ ppm): 182.10 (C=S), 154.76 (–C=N), 158.14 (benzothiazole–C–2), 123.66–141.78 (Aromatic–C, C4–C9 C1′–C6′ C1″–C6″)

MS (*m/z*, %): 422 (M + 1, 100).

Anal $C_{21}H_{16}FN_5S_2$. Calc. for: C, 59.84; H, 3.83; N, 16.61. Found: C, 59.84; H, 3.81; N, 16.60%.

Compound TS07: *N-(4-(benzo[d]thiazol-2-yl)phenyl)-(1'-thiosemicarbazone)-2-methoxy-5-chloro-benzamides*

IR (KBr, υmax cm^{-1}): 3223.12 (–NH str.), 3358.41, 3327.73 (–NH_2 str.), 1273.30 (C=S str.), 1562.02 (C=N str.), 1065.15 (–C–Cl str.), 2932.56 (–C–H str. of OCH_3), 3071.62 (Ar–C–H str.)

^{1}H NMR ($CDCl_3$, 300 MHz, δ ppm): 7.15–7.90 (m, 11H, Ar–H), 13.63 (s, 1H, NH), 9.47 (s, 1H, –CNH), 9.32, 8.90 (2s, 2H, NH_2), 3.82 (s, 3H, OCH_3)

^{13}C NMR (*DMSO–d6*, 300 MHz, δ ppm): 56.43 (OCH_3), 182.08 (C=S), 153.06 (–C=N), 156.37 (benzothiazole–C–2), 118.62–140.01 (Aromatic–C, C4–C9 C1′–C6′ C1″–C6″); MS (*m/z*, %): 469 (M + 1, 100)

Anal $C_{22}H_{18}ClN_5OS_2$. Calc. for: C, 56.46; H, 3.88; N, 14.96. Found: C, 56.43; H, 3.86; N, 14.95%.

Compound TS08: *N-(4-(benzo[d]thiazol-2-yl)phenyl)-(1'-thiosemicarbazone)-2,4-dihydroxy-benzamides*

IR (KBr, υmax cm^{-1}): 3147.46 (–NH str.), 3338.52, 3312.63 (–NH_2 str.), 1245.75 (C=S str.), 1568.64 (C=N str.), 3376.53 (–OH str.), 3085.63 (Ar–C–H str.)

^{1}H NMR ($CDCl_3$, 300 MHz, δ ppm): 7.26–7.87 (m, 11H, Ar–H), 13.46 (s, 1H, NH), 9.62 (s, 1H, –CNH), 8.91, 8.73 (2s, 2H, NH_2), 10.33, 10.13 (s, 2H, –OH)

^{13}C NMR (*DMSO–d6*, 300 MHz, δ ppm): 182.55 (C=S), 154.09 (–C=N), 156.68 (benzothiazole–C–2), 113.80–141.62 (Aromatic–C, C4–C9 C1′–C6′ C1″–C6″)

MS (*m/z*, %): 436 (M + 1, 100).

Anal $C_{21}H_{17}N_5O_2S_2$. Calc. for: C, 57.91; H, 3.93; N, 16.08. Found: C, 57.91; H, 3.90; N, 16.06%.

Compound TS09: *N-(4-(benzo[d]thiazol-2-yl)phenyl)-(1'-thiosemicarbazone)-2-methoxy-benzamides*

IR (KBr, υmax cm^{-1}): 3134.96 (–NH str.), 3395.14, 3238.03 (–NH_2 str.), 1256.13 (C=S str.), 1558.42 (C=N str.), 2936.13 (–C–H str. of OCH_3), 3075.32 (Ar–C–H str.)

^{1}H NMR ($CDCl_3$, 300 MHz, δ ppm): 7.24–7.88 (m, 12H, Ar–H), 13.58 (s, 1H, NH), 9.42 (s, 1H, –CNH), 8.97, 8.84 (2s, 2H, NH_2), 3.83 (s, 3H, OCH_3)

^{13}C NMR (*DMSO–d6*, 300 MHz, δ ppm): 55.48 (OCH_3), 182.54 (C=S), 151.23 (–C=N), 155.78 (benzothiazole–C–2), 121.65–144.32 (Aromatic–C, C4–C9 C1′–C6′ C1″–C6″);

MS (*m/z*, %): 434 (M + 1, 100).

Anal $C_{22}H_{19}N_5OS_2$. Calc. for: C, 60.95; H, 4.42; N, 16.15. Found: C, 60.93; H, 4.40; N, 16.14%.

Compound TS10: *N-(4-(benzo[d]thiazol-2-yl)phenyl)-(1'-thiosemicarbazone)-styrene-amides*

IR (KBr, υmax cm^{-1}): 3175.87 (–NH str.), 3373.74, 3277.39 (–NH_2 str.), 1252.64 (C=S str.), 1558.49 (C=N str.), 3068.32 (Ar–C–H str.)

^{1}H NMR ($CDCl_3$, 300 MHz, δ ppm): 7.14–7.65 (m, 13H, Ar–H), 9.70 (s, 1H, –CNH), 6.71, 6.69 (dd, –CH=CH)

^{13}C NMR (*DMSO–d6*, 300 MHz, δ ppm): 184.27 (C=S), 154.16 (–C=N), 156.95 (benzothiazole–C–2), 119.13–135.67 (Aromatic–C, C4–C9 C1′–C6′ C1″–C6″)

MS (*m/z*, %): 430 (M + 1, 100).

Anal $C_{23}H_{19}N_5S_2$. Calc. for: C, 64.31; H, 4.46; N, 16.30. Found: C, 64.30; H, 4.44; N, 16.29%.

5.5.4. *IN-VITRO* ANTIMICROBIAL ACTIVITY

The results revealed that most of the semicarbazone and thiosemicarbazone derivatives of benzothiazole exhibited good to moderate MIC values ranging between 1.56 and 125 µg/mL in DMSO. Compound N-(4-(benzo[d]thiazol-2-yl)phenyl)-(1′-semicarbazone)-2-floro-benzamides (**SC06)** exhibited maximum antibacterial activity against *E.coli* and *K. pneumoniae* (zone of inhibition up to 18–19 mm at concentration of 15.6 µg/mL). Similarly, compound N-(4-(benzo[d]thiazol-2-yl)phenyl)-(1′-semicarbazone)-2-methoxy-benzamides (**SC09)** showed maximum activity against *S. aureus* (zone of inhibition up to 24–26 mm at concentration of 7.81 µg/mL) and *P. aeruginosa* (zone of inhibition up to 17-19 mm at concentration of 15.6 µg/mL). Compound N-(4-(benzo[d]thiazol-2-yl)phenyl)-(1′-thiosemicarbazone)-2-chloro-benzamides (**TS05)** and N-(4-(benzo[d]thiazol-2-yl)phenyl)-(1′-thiosemicarbazone)-5-chloro-2-methoxy-benzamides (**TS07**) displayed broad-spectrum antimicrobial activity against all tested bacterial strains with MIC values in the range of 1.56 – 31.2 µg/mL. Compound **TS05** displayed the most potent activity with MIC values of 3.91, 15.6, 7.81, 1.56 µg/mL against *S. aureus*, *E. faecalis, E. coli* and *P. aeruginosa* respectively and compound **TS07** displayed MIC values of 7.81, 15.6, 15.6, 15.6 µg/mL against *S. aureus*, *E. faecalis*, *E. coli* and *K. pneumoniae* respectively, which was comparable to ciprofloxacin with corresponding MIC values of 6.25, 6.25, 6.25, 6.25 µg/mL. Some of the compounds **SC02**, **SC04**, **SC07** and **SC10** exhibited good activity against few bacterial strains having MIC value of 15.6 µg/mL while rest of the compounds showed moderate activity. In addition, it was observed that the potent compounds (**SC06, SC09, TS05** and **TS07**) displayed greater activity against *S. aureus* and *E. coli* (Table 5.27). In context to antifungal activity, compound **TS07** exhibit pronounced activity MIC 7.81 and 3.91 µg/mL against *C. albicans* and *C. krusei*, respectively (Table 5.28).

Structure activity relationship (SAR) demonstrated the effect of substituent's on the antimicrobial activity. Compounds **SC06, SC09, TS05** and **TS07** with electronegative groups (F, Cl) and electron releasing (OCH_3) groups were found to be more active than the compounds with electron withdrawing (NO_2) groups. However, compounds **SC03, TS03, SC08** and **TS08** bearing electron releasing OH group were moderately active. Hence, it can be contingent that chloro, fluoro and methoxy substituents bearing derivatives offer the most suitable compounds for achieving the best antibacterial spectrum. The antibacterial activity data of compounds (**SC05**, **SC07**; MIC: 15.6–62.5 µg/mL) and (**TS05**, **TS07**; MIC: 1.56–31.2 µg/mL) showed that thiosemicarbazone derivatives exhibited more pronounced

activity than semicarbazones. However, both semicarbazones and thiosemicarbazones exhibited much better activity in comparison to benzothiazole amide derivatives.

Table 5.27 Antibacterial activity (MIC µg/mL) of the synthesized semicarbazone and thiosemicarbazone derivatives of benzothiazole (**SC01-10** and **TS01-10**)

	Bacteria					
	Gram positive bacteria		**Gram negative bacteria**			
Comp code	***S. aureus* (ATCC 25323)**	***E. faecalis* (Clinical isolate)**	***E. coli* (ATCC 35218)**	***S. typhi* (MTCC 3216)**	***K. pneumonia* (ATCC 31488)**	***P. aeruginosa* (ATCC 27893)**
SC01	-	12-14(62.5)	11-13(62.5)	-	-	10-12(62.5)
SC02	18-20-(15.6)	10-13(62.5)	13-16(31.2)	-	13-15(31.2)	-
SC03	12-14(62.5)	-	11-13(62.5)	-	-	13-15(31.2)
SC04	10-12(62.5)	-	11-14(31.2)	-	16-19(15.6)	-
SC05	13-15(31.2)	10-12(62.5)	13-15(31.2)	14-16(31.2)	-	10-12(62.5)
SC06	13-16(31.2)	-	17-19(15.6)	10-12(62.5)	16-19(15.6)	-
SC07	10-12(62.5)	-	14-16(31.2)	-	16-18(15.6)	13-14(31.2)
SC08	-	<10(125)	10-12(62.5)	-	10-12(62.5)	-
SC09	23-26(7.81)	10-13(62.5)	13-15(31.2)	-	13-15(31.2)	16-19(15.6)
SC10	10-13(62.5)	<10(125)	10-12(62.5)	-	<10(125)	-
TS01	-	12-14(62.5)	11-13(62.5)	-	13-14(31.2)	10-12(62.5)
TS02	13-16(31.2)	13-15(31.2)	13-16(31.2)	-	13-15(31.2)	-
TS03	13-15(31.2)	-	-	-	-	-
TS04	10-12(62.5)	-	11-14(31.2)	-	-	-
TS05	28-30(3.91)	13-15(31.2)	23-25(7.81)	13-16(31.2)	13-15(31.2)	20-22(15.6)
TS06	10-13(62.5)	-	10-12(62.5)	-	13-15(31.2)	-
TS07	24-25(7.81)	17-19(15.6)	16-19(15.6)	14-16(31.2)	16-18(15.6)	13-14(31.2)
TS08	-	<10(125)	10-12(62.5)	-	-	10-12(62.5)
TS09	13-16(31.2)	11-13(62.5)	10-12(62.5)	-	13-16(31.2)	-
TS10	11-13(62.5)	10-13(62.5)	13-15(31.2)	-	13-15(31.2)	16-19(15.6)
CIP	30-32(≥6.25)	28-30(≥6.25)	33-35(≥6.25)	34-35(≥6.25)	29-30(≥6.25)	33-35(≥3.12)

Table 5.28 Antifungal activity (MIC µg/mL) of the synthesized semicarbazone and thiosemicarbazone derivatives of benzothiazole (**SC01-10** and **TS01-10**)

Compound code	*C. albicans* (ATCC 90028)	*C. tropicalis* (ATCC 750)	*C. krusei* (ATCC 6268)
SC01	-	10-12(62.5)	-
SC02	12-15(31.2)	10-12(62.5)	13-15(31.2)
SC03	-	10-14(62.5)	-
SC04	12-15(31.2)	12-15(31.2)	16-19(15.6)
SC05	<10(125)	16-18(15.6)	-
SC06	15-18(15.6)	10-14(62.5)	12-15(31.2)
SC07	12-15(31.2)	12-15(31.2)	12-15(31.2)
SC08	12-16(31.2)	-	10-13(62.5)
SC09	10-14(62.5)	-	-
SC10	12-15(31.2)	-	<10(125)
TS01	12-16(31.2)	<10(125)	10-12(62.5)
TS02	10-12(62.5)	14-16(31.2)	10-12(62.5)
TS03	<10(125)	17-19(15.6)	12-15(31.2)
TS04	12-15(31.2)	<10(125)	12-15(31.2)
TS05	13-15(31.2)	<10(125)	-
TS06	<10(125)	-	12-15(31.2)
TS07	24-25(7.81)	10-12(62.5)	28-31(3.91)
TS08	12-15(31.2)	-	-
TS09	-	11-13(62.5)	-
TS10	<10(125)	-	-
Fluconazole	22-25(6.25)	24-27 (6.25)	20-24 (6.25)

The value of each compound consisted of 'zone of inhibition range (MIC)' of 03 replicates. Level of signifcance $p < 0.05$.

5.5.4.1. Mechanism of action study

Bactericidal kinetics

The bactericidal activity of lead compounds **SC06, SC09, TS05** and **TS07** were directed in confirming its potency toward the specific *S. aureus* and *E. coli* strains. Time-kill studies demonstrated that compounds **SC06** and **TS05** were rapid with 90 to 99% lethality within 2 to 5 h (Fig. 5.47). Compound **SC09** was found to be less effective as compared to compounds **SC06, TS05** and **TS07** in both strains even up to 5 h. At 4 × MIC compounds inhibited bacterial growth from 2 h onwards keeping growth arrested till 5 h. However, complete eradication of bacterial growth by any of the tested compounds was not observed up to 5 h. Compound **TS05** exhibited the most potent inhibition of growth in both the strains at 4 × MIC.

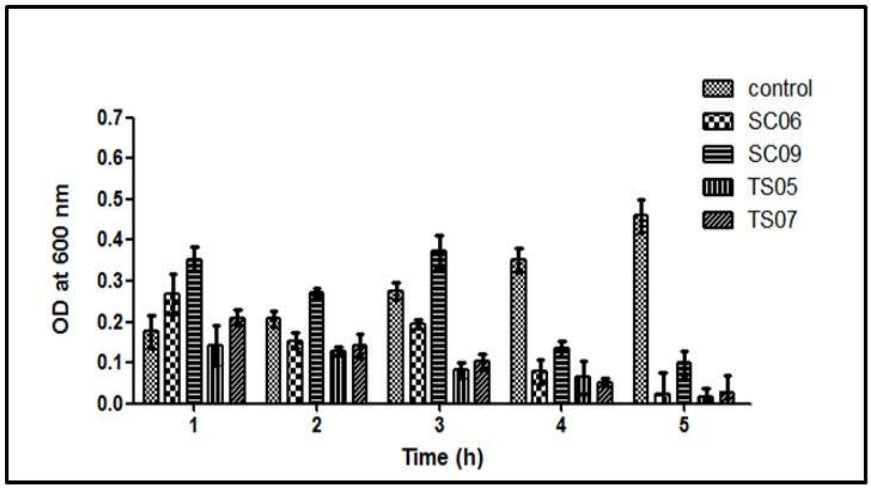

(A)

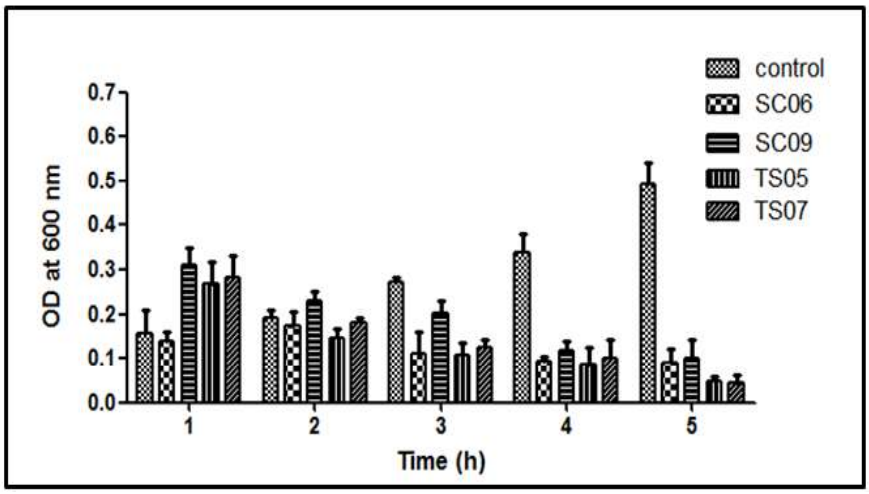

(B)

Fig. 5.47 Time dependent killing of (A) *S. aureus* (B) *E.coli* upon treatment with compounds **SC06, SC09, TS05** and **TS07**at 4 × MIC concentrations.

Outer membrane permeabilization assay

All compounds showed similar profile with respect to positive control proton ionophore valinomycin which was found to hyperpolarize the membrane by specifically binding to potassium ions (K^+ ions) and thereby acts as K^+ ions carrier molecule. However none of the designed compounds shows depolarisation of the bacterial membrane as observed in case of negative control Triton. At the highest concentration of designed analogs **SC06, SC09, TS05** and **TS07** tested (i.e., 4 × MIC), the level of hyper polarization appeared to reach a maximum at times from about 1 min to 5 min (Fig. 5.48). Consistent with their cytotoxic and antimicrobial properties, **SC09** showed the minimum while **TS05** showed maximum relative percentage fluorescence with respect to valinomycin as described in Fig. 5.49. Unusual pattern of emitted fluorescence was observed in the both strains. All the designed analogs studied had the ability to hyperpolarize the cytoplasmic membrane of *S. aureus* and *E. coli*; however, compounds with different structures had different concentration–activity profiles (data not shown here). Compounds **SC06** and **TS05** completely hyperpolarized the membrane at lower concentrations than those of the other compounds studied.

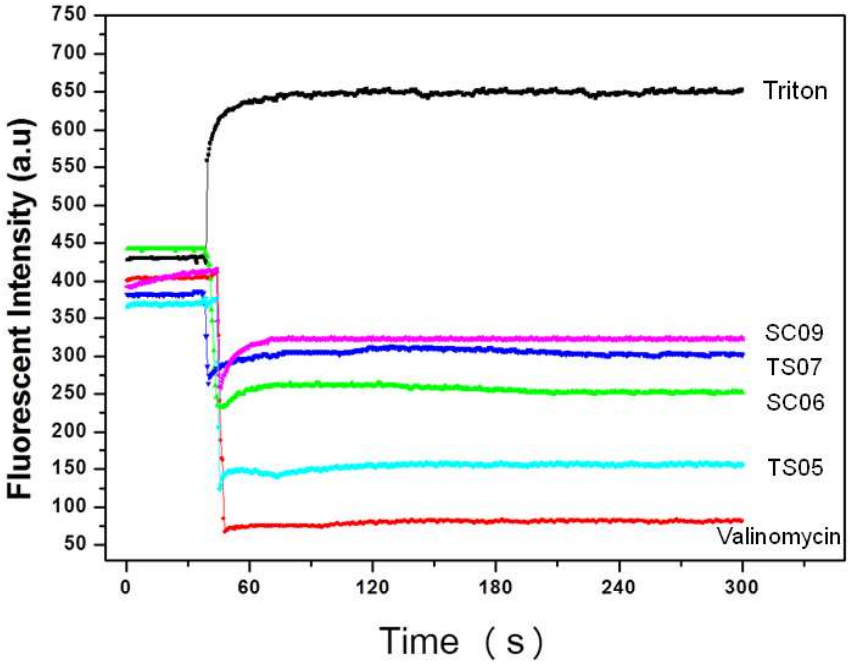

(A)

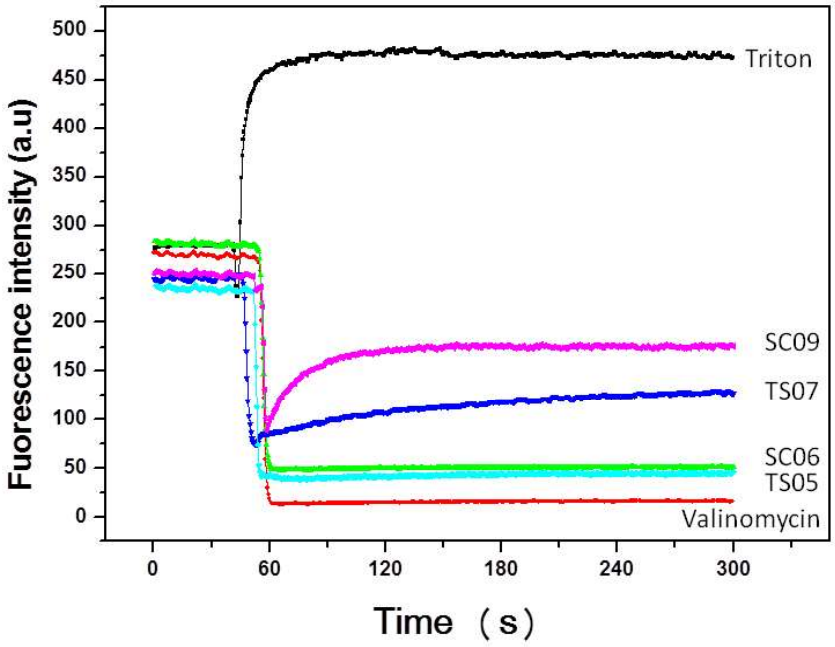

(B)

Fig. 5.48 Membrane depolarization ability of designed compounds on (A) *S.aureus* and (B) *E.coli* treated with 4xMIC concentration of compounds **TS05, SC06, TS07** and **SC09**.

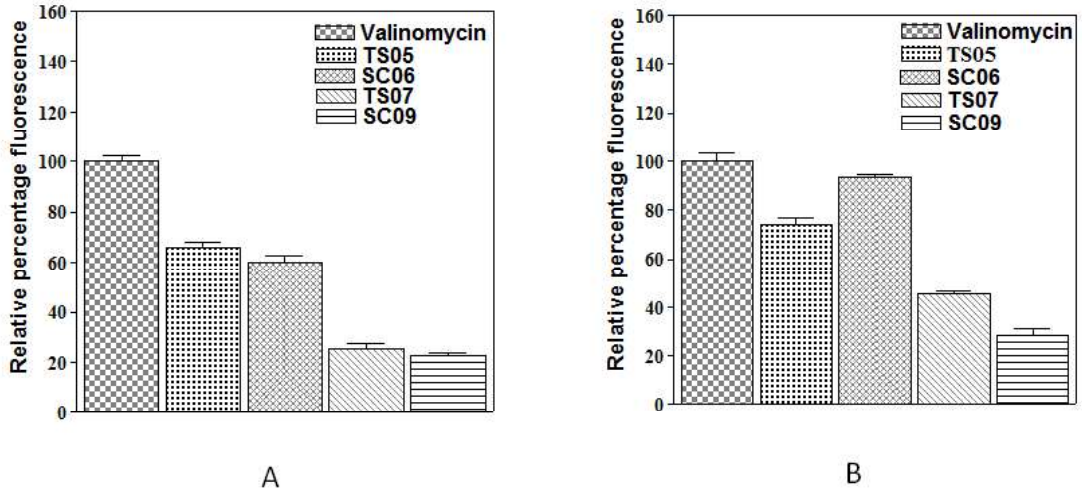

Fig. 5.49 Bar diagram showing relative percentage fluorescence of (A) *S. aureus* and (B) *E.coli* of compounds **TS05, SC06, TS07, SC09** and Valinomycin.

Permeabilization of membrane of viable bacteria

The results revealed that test compounds **SC06, SC09, TS05** and **TS07** induced maximum damages to the membrane organization of *E. coli* as compared to significantly lesser

damage to the membrane of *S. aureus.* Further, the number of PI-stained cells decreased significantly in **SC09** and **TS07** in *S. aureus* (19.09% and15.97% resp.) as compared to *E. coli* (60.61% and 58.29% resp.), implicating lesser membrane damage of *S. aureus.* However, maximum damage of bacterial membrane of both strains was observed in compound **SC06** and **TS05** (Fig. 5.50).

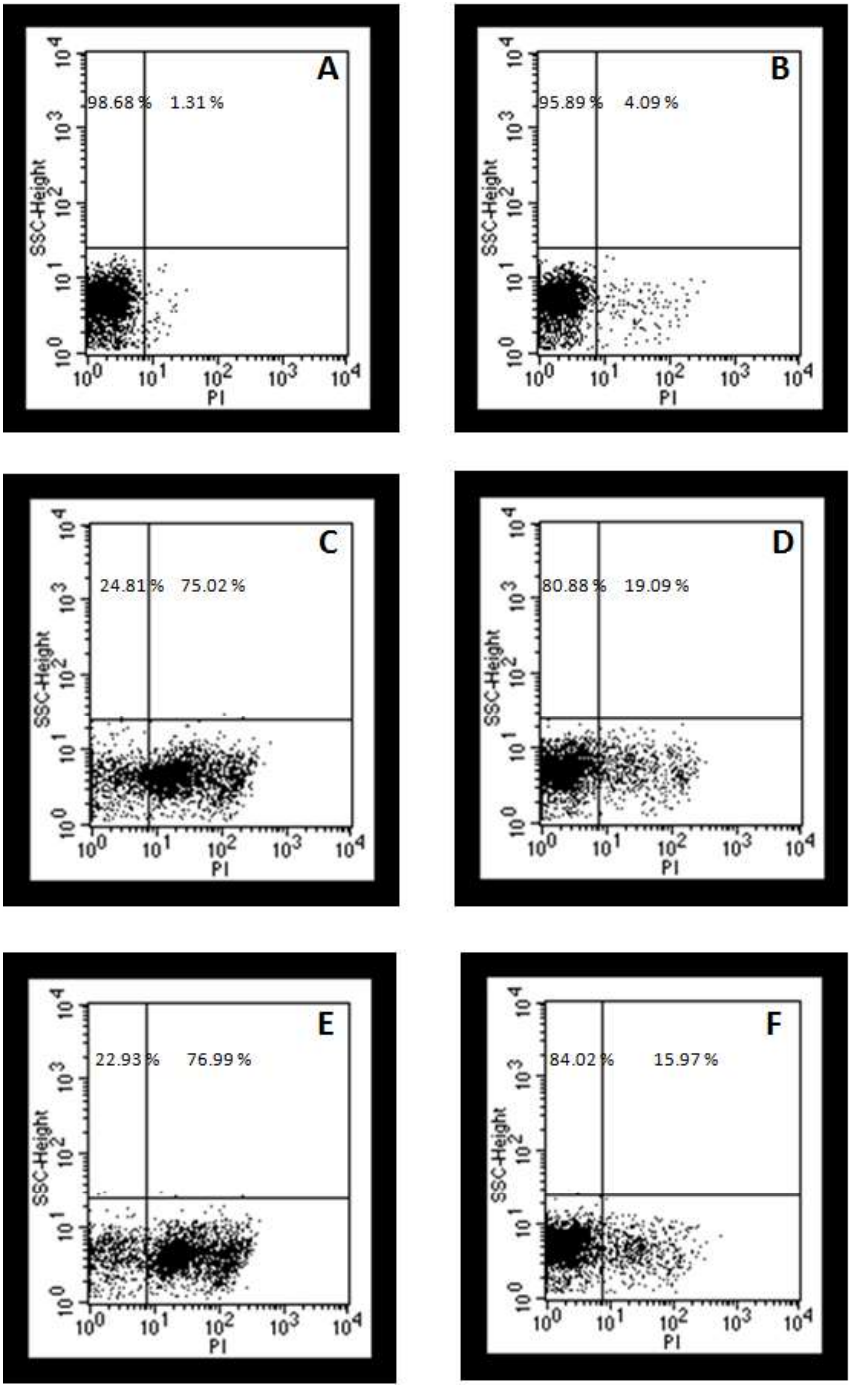

(I)